Aus der

Forschungsgruppe „Proteasome Function in Lung Disease“

Leitung: Prof. Dr. rer. nat. Silke Meiners

Comprehensive Pneumology Center München

Direktor: Prof. Dr. Ali Önder Yildirim


# *Experimental Investigations on the Role of the Immunoproteasome in Lung Fibrogenesis*

Dissertation
zum Erwerb des Doktorgrades der Medizin
an der Medizinischen Fakultät
der Ludwig-Maximilians-Universität zu München

vorgelegt von

Johannes Felix Clemens Peter Nowak
aus Hamburg

2024

Mit Genehmigung der Medizinischen Fakultät
der Universität München

| | |
|---|---|
| Berichterstatterin: | Prof. Dr. Silke Meiners |
| Mitberichterstatter: | Prof. Dr. Rudolf M. Huber |
| | PD Dr. Tobias Veit |
| Mitbetreuung durch promovierte Mitarbeiterin: | Dr. Ilona E. Kammerl |
| Dekan: | Prof. Dr. med. Thomas Gudermann |
| Tag der mündlichen Prüfung: | 21.03.2024 |

## Eidesstattliche Versicherung

Ich, Johannes Felix Clemens Peter Nowak, erkläre hiermit an Eides statt, dass ich die vorliegende Dissertation mit dem Thema

„*Experimental Investigations on the Role of the Immunoproteasome in Lung Fibrogenesis*“

selbstständig verfasst, mich außer der angegebenen keiner weiteren Hilfsmittel bedient und alle Erkenntnisse, die aus dem Schrifttum ganz oder annähernd übernommen sind, als solche kenntlich gemacht und nach ihrer Herkunft unter Bezeichnung der Fundstelle einzeln nachgewiesen habe.

Ich erkläre des Weiteren, dass die hier vorgelegte Dissertation nicht in gleicher oder in ähnlicher Form bei einer anderen Stelle zur Erlangung eines akademischen Grades eingereicht wurde.

| | |
|---|---|
| Zürich, den 21.05.2024 | Johannes Nowak |
| Ort, Datum | Unterschrift |

## Table of contents

## Summary

Correct cellular, and by that organismal, function is unimaginable without proteasomes. The ubiquitously occurring proteasomes are cellular protein complexes that play indispensable roles in eukaryotes, archaea, and even some bacteria. By breaking peptide bonds between misfolded, unnecessary, or damaged proteins, proteasomes digest proteins that no longer add to the well-being of a cell and thereby contribute to proteostasis. The control of protein levels is essential for cellular function, from basal protein turnover to highly complex signalling cascades. This clearing and cleaning up contributes to cellular homeostasis and function by impacting gene expression and cell cycle regulation. An imbalance in proteasomal degradation easily leads to the accumulation of misfolded proteins and thereby contributes to diseases such as neurodegenerative or cardiovascular, autoimmunity, and even malignancies. Therefore, a better understanding of the role of the immunoproteasome is of utmost importance to contribute to the understanding of underlying pathophysiologic mechanisms in the named diseases.

This study investigated the role of a specialised proteasomal sub-type. Inflammatory stimuli lead to the formation of the so-called immunoproteasome, which is characterised by its three catalytically active subunits LMP2, LMP7, and MECL-1. Immunoproteasomes are constitutively expressed in immune cells, but they are inducible in parenchymal cells by inflammatory stimuli like IFNγ or TNFα. Peptides that have been processed by immunoproteasomes show improved binding properties to antigenic pockets of MHC I molecules thereby fostering activation of $CD8^+$ T cells. Besides its important role in antigen presentation and thereby shaping adaptive immune responses, the immunoproteasome is involved in the expansion and survival of T cells, T helper cell differentiation, production of several inflammatory cytokines, and prevention from autoimmunity after infection.

Immunoproteasomes have been shown to be upregulated in lung tissue homogenate of IPF patients compared to donor. Immunohistochemistry staining revealed an overexpression not only in lung immune cells but also in the pulmonary interstitium of IPF patients. This inappropriate expression of the immunoproteasome in parenchymal lung cells suggests a potential pathogenic role of the immunoproteasome for IPF. This study aimed to investigate a potential role of the immunoproteasome in lung fibrosis. Therefore, three aims were set up:

- Firstly, to investigate a putative impact of a pro-fibrotic stimulus on the immunoproteasome, primary human lung fibroblasts (phLF) were subjected to TGF-β1-treatment *in vitro* and immunoproteasomal expression was quantified both on mRNA and protein levels.

- Secondly, it was hypothesised that the immunoproteasome regulates pro-fibrotic marker gene expression. Therefore, immunoproteasome single-subunit-deficient pmLF, murine lung sections and mice were subjected to pro-fibrotic conditions and compared to their specific wildtype counterpart regarding profibrotic marker gene expression as analysed by RT-qPCR.
- Finally, a potential impact of an immunoproteasome inhibitor on fibrogenesis was investigated. For that, phLF, murine tissue sections and mice were subjected to either pro-fibrotic or pro-inflammatory conditions and treated with or without an immunoproteasome-specific inhibitor.

Unexpectedly, the immunoproteasome was downregulated by TGF-β1 treatment on both the mRNA and protein levels. This might indicate that other factors may lead to IP overexpression in lung fibrosis which exceed the inhibitory effects of TGF-β1. The TGF-β1-mediated downregulation might explain existing literature and lines up with previously described suppression of antiviral and proinflammatory responses by TGF-β1 in macrophages (Grunwell, Yeligar et al. 2018).

No alterations in the fibrosis-related marker gene expression profile were observed between LMP2$^{-/-}$ and wildtype pmLFs and mPCLS groups. LMP7$^{-/-}$ mice undergoing a 14-day bleomycin challenge were characterised by significant survival benefit and less bodyweight alterations, when compared to wildtype littermates, whereas no alterations in fibrosis-related mRNA could be observed between LMP7-deficient and wildtype littermates.

Finally, following the single-subunit-knockout experiments, wildtype fibroblasts (*in vitro*), murine tissue sections (*ex vivo*) (data not shown) and mice (*in vivo*) were subjected to pro-fibrotic and pro-inflammatory conditions. However, this time, we applied the specific immunoproteasome pan-inhibitor to investigate anti-fibrotic and anti-inflammatory effects, which have been described in literature several times. Bleomycin challenges were performed on immunoproteasome-pan-inhibited versus un-inhibited mice for three days (data not shown) and seven days. LU-005i and bleomycin co-treatment decreased *Il23a* levels in mice, which is in line with existing literature. In parallel, we observed increased lung-specific expression of *Il17a*, *Il6* and *Tnf*, which is however contradictory to the literature.

The observed significant survival benefit of LMP7$^{-/-}$ mice 14 days after exposure to bleomycin is a new and important finding, as this suggests immunoproteasomes or their subunits respectively as potential druggable targets in the treatment of lung fibrosis.

## Zusammenfassung

Ohne das ubiquitär vorkommende Proteasom wäre eine geregelte Zellfunktion und somit das Leben der Organismen, wie wir sie kennen undenkbar. Diese Zellkomplexe spielen eine unabdingbare Rolle in Eukaryoten, Archaeen und sogar Bakterien. Proteasome bauen Proteine ab, die der Zellhomöostase nicht mehr dienlich sind, so zum Beispiel fehlgefaltete, beschädigte oder gerade auch nicht mehr benötigte Proteine. Die Kontrolle des Proteoms ist essenziell für die Aufrechterhaltung zellulärer Funktionen bis hin zum Ablauf höchst komplexer Signalkaskaden. Eine Störung des empfindlichen Protein-Gleichgewichts kann schnell zur Anhäufung fehlgefalteter Proteine und somit zum Aggravieren von neurodegenerativen und kardiovaskulären Krankheiten, sowie Autoimmunität und sogar Tumoren führen, was die pathophysiologische Bedeutung des Komplexes hervorhebt und weitere Forschung an diesem Zellorganell erforderlich macht.

Diese Arbeit beschäftigte sich mit einer besonderen Unterform des Proteasoms, dem sogenannten Immunoproteasom, welches durch drei enzymatisch aktive Untereinheiten, namens LMP2, LMP7 und MECL-1 charakterisiert ist. Diese Proteasome werden, wie der Name schon nahelegt, in Immunzellen exprimiert, sind jedoch auch in parenchymalen Zellen induzierbar, beispielsweise durch inflammatorische Stimuli, wie IFNγ oder TNFα. Peptide, die von Immunoproteasomen prozessiert werden, zeichnen sich durch eine bessere Präsentierbarkeit durch MHC I Moleküle aus, was die Aktivierung von $CD8^+$ T fördert. Jedoch hat das Immunoproteasom neben der Rolle in der Antigenpräsentation auch noch Einflüsse auf beispielsweise die Expansion und das Überleben von T-Zellen, sowie die Differenzierung von T-Helfer-Zellen, der Produktion inflammatorischer Zytokine. Zudem trägt das Immunoproteasom zum Schutz des Körpers vor autoimmunen Reaktionen im Rahmen einer Infektion bei.

Immunhistochemisch gefärbtes Lungengewebe von an Idiopathischer Lungenfibrose erkrankten Patienten zeigte eine Überexpression des Immunoproteasoms. Dies galt nicht nur in Immunzellen, sondern auch in parenchymständigen Zellen. Diese Arbeit zielte darauf, eine mögliche Rolle des Immunoproteasoms in der Lungenfibrose zu identifizieren und zu beschreiben. Hierfür wurden drei Ziele formuliert:

- Als erstes wurde untersucht, ob der pro-fibrotische Stimulus TGF-β1 für eine Überexpression des Immunoproteasoms in primären humanen Lungenfibroblasten verantwortlich sein kann. Quantifiziert wurde die Expression des Immunoproteasoms auf mRNA und Proteinebene.
- Als Nächstes wurden Experimente mit Zellen, Gewebe oder Tieren durchgeführt, die hinsichtlich einer Untereinheit des Immunoproteasoms defizient waren. Nach dem Aussetzen gegenüber pro-fibrotischen

Konditionen wurden Wildtyp- mit Knockout-Gruppen hinsichtlich ihrer fibrogenen Reaktionen verglichen. Ziel dieser Experimente war die Quantifizierung Fibrose-assoziierter Markergenexpression mittels RT-qPCR.

- Abschließend wurden Untersuchungen mit einem Immunoproteasominhibitor unternommen. Zellen, Gewebe und Tiere wurden pro-fibrotischen und pro-inflammatorischen Konditionen ausgesetzt und nicht-inhibierte mit inhibierten Gruppen bezüglich fibrogener und inflammatorischer Reaktionen verglichen.

Unerwarteterweise wurde die Expression des Immunoproteasoms durch TGF-β1 sowohl auf mRNA- als auch auf Proteinebene herunterreguliert. Das könnte darauf hinweisen, dass möglicherweise andere Mediatoren für die histologisch gezeigte Überexpression des Immunoproteasoms in IPF-typischen Geweben verantwortlich sein könnten. Die Herunterregulierung des Immunoproteasoms scheint kohärent mit der Literatur zu sein, da bereits eine Unterdrückung antiviraler und pro-inflammatorischer Reaktionen in mit TGF-β1 behandelten Makrophagen gezeigt wurde (Grunwell, Yeligar et al. 2018).

Weder in Wildtyp noch in LMP2$^{-/-}$ pmLFs und mPCLS konnte ein Unterschied der Fibrose-assoziierten Markergene gefunden werden. Dennoch zeigte sich in LMP7$^{-/-}$ Mäusen 14 Tage nach Bleomycininstillation ein signifikant geringerer Gewichtsverlust, der mit einem Überlebensvorteil einherging. Hinsichtlich der Fibrose-assoziierten Markergenexpression konnten keine Unterschiede zwischen den überlebenden Wildtyp- und Knockout-Tieren festgestellt werden.

Zu guter Letzt wurden Fibroblasten, Gewebekulturen und Mäuse vom Wildtyp gegenüber pro-fibrotischen und pro-inflammatorischen Konditionen ausgesetzt, dieses Mal jedoch mit einem Immunoproteasominhibitor behandelt. Diesem wurden in der Literatur bereits häufig anti-fibrotische und anti-inflammatorische Effekte zugeschrieben. Die Behandlung mit Bleomycin und dem Inhibitor LU-005i verringerte *Il23a* Level bei den Mäusen, was auch bereits in der Literatur gezeigt wurde. Darüber hinaus beobachteten wir eine erhöhte Expression von *Il17a*, *Il6* and *Tnf*, welches sich aktuell nicht mit der Literatur in Einklang bringen lässt.

Der jedoch signifikant niedrigere Gewichtsverlust und der damit verbundene Überlebensvorteil der LMP7$^{-/-}$ Mäuse 14 Tage nach Bleomycininstillation legt jedoch nahe, dass das Immunoproteasom, beziehungsweise seine Untereinheiten als medikamentöses Ziel zur Behandlung von Lungenfibrose betrachtet werden kann.

# 1 Introduction

## 1.1 Idiopathic pulmonary fibrosis (IPF)

Idiopathic pulmonary fibrosis (IPF) is a chronic interstitial lung disease (ILD). With an incidence of 0.75 to 0.93 per 10.000 in North America, it is the most common form of ILD with men being more frequently affected than women (Raghu, Collard et al. 2011, Maher, Bendstrup et al. 2021). European studies indicate increasing IPF incidence and a median survival of two to three years from diagnosis, of which the latter remained constant over the years (Nalysnyk, Cid-Ruzafa et al. 2012, Hutchinson, Fogarty et al. 2015, Barratt, Creamer et al. 2018). A main feature of IPF is fibrotic remodelling of the lung structure, characterised by extracellular matrix (ECM) deposition. Tissue remodelling and inflammatory cell invasion in the space between the vascular endothelium and alveolar epithelium lead to an impaired gas exchange between alveolar air and erythrocytes which causes organ failure and death due to hypoxemic respiratory insufficiency (Gross and Hunninghake 2001, King, Pardo et al. 2011, Wynn and Ramalingam 2012).

### 1.1.1 Risk factors for pulmonary fibrosis

Several risk factors were identified to contribute to the development of pulmonary fibrosis. For example, bleomycin, commonly used as a chemotherapeutic drug in several cancer therapies due to its induction of deoxyribonucleic acid (DNA) strand breaks resulting in reactive oxygen species (ROS) production and finally, cell apoptosis, causes pulmonary fibrosis in three to five percent of the patients who receive the drug, thus limiting its therapeutic use. Experimental lung scientists use bleomycin's adverse effects to induce experimental lung fibrosis in rodents (Walters and Kleeberger 2008). Additionally, rheumatological treatments like methotrexate and other drug classes such as antibiotics, e.g., nitrofurantoine, or antiarrhythmic drugs like amiodarone may cause pulmonary fibrosis (Schwaiblmair, Behr et al. 2012, Skeoch, Weatherley et al. 2018). Occupational exposures to radiation and metal dust, wood, silica, and asbestos

also contribute to progressive fibrotic remodelling of the lung interstitium (Hubbard, Venn et al. 1998, Wynn 2008, Straub, New et al. 2015). In fact, a significant correlation between IPF and occupation in agriculture and farming has been found (Taskar and Coultas 2008). In addition to inorganic irritants, infectious microbial agents (viral, fungal, and bacterial) also play a role in the fibrotic remodelling of the lung, and studies focusing on antiviral, antifungal and antibiotic agents seem to be promising for anti-fibrotic treatment as well (Wilson, Shulgina et al. 2014, Chioma and Drake 2017). Comorbidities such as hyperlipoproteinemia, myocardial infarction, obesity, hypertension, poorly controlled diabetes, gastroesophageal reflux disease (GERD), micro-aspirations, and collagen vascular diseases such as systemic sclerosis (SSc) represent risk factors for ILD (Raghu, Freudenberger et al. 2006, Wynn 2008, King, Pardo et al. 2011, Juarez, Chan et al. 2015).

Ageing, characterised by impaired proteostasis, telomere attrition, epigenetic and genetic changes, mitochondrial dysfunction, cell senescence, and altered intercellular communication, is the major known risk factor for IPF, and its incidence increases with age (Nalysnyk, Cid-Ruzafa et al. 2012, Selman and Pardo 2014, Lopez-Ramirez, Suarez Valdivia et al. 2018). Smoking is known to contribute to the development of IPF and most patients who suffer from IPF have a history of cigarette consumption. In fact, an increased risk is even associated with ex-smoking (Baumgartner, Samet et al. 1997, Spira, Beane et al. 2004, Behr, Kreuter et al. 2015). Mutations in genes related to alveolar stability, such as Pulmonary Surfactant-Associated Protein C (*SFTPC*) and Pulmonary Surfactant-Associated Protein A2 (*SFTPA2*) (Thomas, Lane et al. 2002, Wang, Kuan et al. 2009) and linked to telomere function, such as Telomerase Reverse Transcriptase (*TERT*) and Telomerase RNA Component (*TERC*) (Armanios, Chen et al. 2007, Tsakiri, Cronkhite et al. 2007) have been associated with IPF. Promotor polymorphisms of mucin 5B (*MUC5B*), a gene that plays a role in the rheological properties of airway mucus, mucociliary transport, and mediating macrophagic response in airway defence have been shown to be present in 37.5 % of IPF patients and may increase the risk of IPF up to 20-fold (Seibold, Wise et al. 2011).

### 1.1.2 Clinical manifestations and diagnostic criteria for IPF

Chronic exertional dyspnoea and coughing are the main symptoms of IPF patients. In addition, bibasilar inspiratory crackles and digital clubbing may be frequently observed. IPF can only be diagnosed if i) known causes of ILD as described above can be excluded AND ii) high resolution computed tomography (HRCT) patterns of usual interstitial pneumonia (UIP) (honeycombing, traction bronchiectasis, traction bronchiolectasis, ground-glass opacification, fine reticulation) are present OR iii) specific HRCT patterns and histopathological patterns (dense fibrosis and scarring with fibroblast foci in subpleural and paraseptal parenchyma, microscopic honeycombing juxtaposed with relatively unaffected lung parenchyma) can be detected (Behr, Gunther et al. 2021), as shown in **Figure 1**.

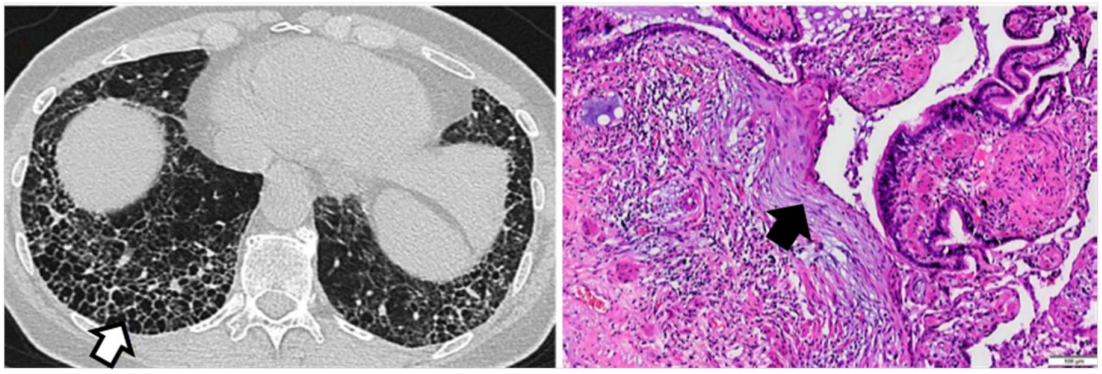

**Figure 1: Radiographic and histopathological lung patterns of usual interstitial pneumonia (UPI), derived from (Behr, Gunther et al. 2021)**

Left: axial high resolution computed tomography (HRCT) image reconstruction of a patient with usual interstitial pneumonia (UIP) pattern, such as honeycombing (white arrow). Right: fibroblastic focus – subepithelial accumulation of myofibroblasts (black arrow, white bar in the right lower corner indicates 100 µm), derived by (Behr, Gunther et al. 2021) (white and black arrows added by the author).

### 1.1.3 Treatment of IPF

The following paragraph gives a brief overview of the two main drugs in IPF treatment, namely *Nintedanib* and *Pirfenidone*. The orally available tyrosine kinase inhibitor *Nintedanib* inhibits vascular endothelial growth factor (VEGF-), platelet-derived growth factor (PDGF-), and fibroblast growth factor (FGF-) receptors and impacts positively the progress of IPF (Behr, Gunther et al. 2020). The anti-inflammatorily and anti-fibrotically acting *Pirfenidone* affects tumour necrosis factor alpha (TNFα) and transforming growth factor beta (TNFβ)'s pathways (Aravena, Labarca et al. 2015). Both drugs protect against the rate of decline in spirometry (Finnerty et al 2021). Further, formerly applied treatment options such as prednisone, azathioprine, and N-acetylcysteine were shown to act unfavourably and are no longer used in IPF treatment (Behr, Gunther et al. 2020). Because IPF cannot yet be cured, symptom control including IPF exacerbation management is crucial in treatment strategies. Several mechanisms are leading to rapid disease progression, characterised by an up to 85 % mortality rate during or after an exacerbation (Song, Hong et al. 2011, Polke, Kondoh et al. 2021). Since an increased prevalence of several comorbidities has been found in IPF patients, IPF therapy also focuses on comorbidity management (Ahmad and Nathan 2018). A large portion of IPF patients dies from comorbidities due to their negative impact on general health (Kreuter, Ehlers-Tenenbaum et al. 2015, King and Nathan 2017), here to mention cardiovascular diseases, GERD, obstructive sleep apnoea (OSA), diabetes, lung cancer, and pulmonary arterial hypertension (PAH) (Oldham and Collard 2017). PAH is present in almost 32 % of IPF patients and is one of the major life-limiting comorbidities (Lettieri, Nathan et al. 2006). The effect of combined drug therapies such as the combination of *Sildenafil* and *Pirfenidone* has been investigated, which so far did not provide beneficial effects on IPF patients when compared to *Pirfenidone* plus placebo (Behr, Nathan et al. 2021). Drugs such as statins, angiotensin-converting enzyme (ACE) inhibitors, and anticoagulants were shown to impact positively on cardiovascular comorbidities, while GERD can be managed with anti-acidic drugs or laparoscopic surgeries (Somogyi, Chaudhuri et al. 2019). Novel approaches to target IPF include

several antibody-based therapies, leukotriene antagonists, protein-kinase-inhibitors, and the gut microbiome (Somogyi, Chaudhuri et al. 2019).

Despite efforts in developing an effective treatment for IPF, the disease has remained incurable until today. For a minority of IPF patients whose symptoms and lung function worsen over time despite ongoing therapy, lung transplantation remains an option. Various factors including IPF severity, the use of extracorporeal membrane oxygenation (ECMO), comorbidity status and age have an impact on post-transplant survival (Brown, Kaya et al. 2016, Bleisch, Schuurmans et al. 2019). Whereas patients undergoing a single lung transplantation benefit from less cardiac manipulation and better perioperative outcomes, increased long-term survival, and reduced chronic lung allograft dysfunction is more likely after bilateral lung transplantation which is therefore an advantageous option for younger patients (Somogyi, Chaudhuri et al. 2019).

### 1.1.4 Pathophysiology of IPF

Organ fibrosis as a hallmark in IPF and SSc can be seen as an imbalance between ECM deposition and degradation. Due to an aberrant healing process upon inflammation or repeated or severe tissue injuries, excessive deposition of ECM occurs, and failure of an appropriate resolution can lead to fibrosis (Bonnans, Chou et al. 2014). In physiological wound repair four well-orchestrated, overlapping steps are observed: 1) initiation of an anti-fibrinolytic-coagulation cascade, 2) an inflammatory phase, 3) a proliferative phase, and finally 4) a tissue remodelling phase as shown in **Figure 2**, derived from (Wynn 2011).

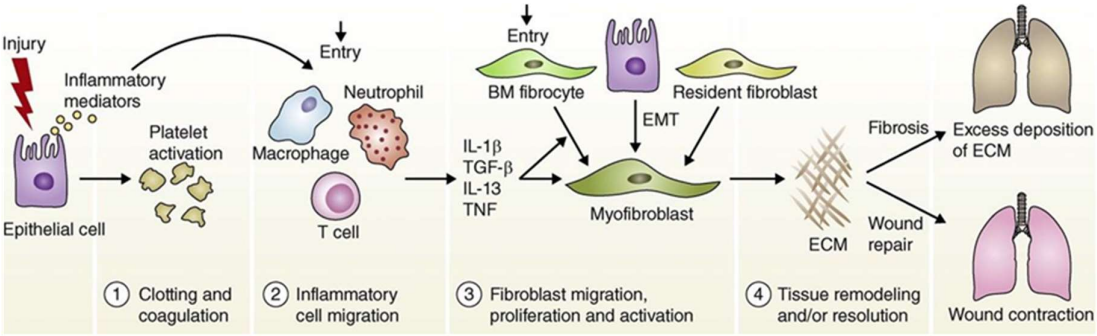


**Figure 2: Stages in alveolar injury, from (Wynn 2011)**

In physiological wound repair four well-orchestrated, overlapping steps are observed: 1) initiation of an anti-fibrinolytic-coagulation cascade, 2) an inflammatory phase, 3) a proliferative phase, and finally 4) a tissue remodelling phase, derived by (Wynn 2011). Upon tissue injury, vasoconstriction occurs and a fibrin containing clot forms out of platelets, that have been activated upon encountering exposed collagen and von Willebrand factor (vWF) in the sub-endothelial layer (Esmon 2005). Both the clot and damaged tissue release pro-inflammatory cytokines and growth factors such as Transforming Growth Factor β (TGF-β), Fibroblast Growth Factor (FGF) and Platelet Derived Growth Factor (PDGF). Next, inflammatory cells are recruited and migrate to the wound, which is facilitated by locally increased vessel permeability. Neutrophils clear cell debris and kill invading microbes. To prevent any bystander tissue damage due to proteases and reactive oxygen species (ROS) produced by neutrophils, a proper clearance of the neutrophils is warranted by macrophages. Macrophages also release cytokines to attract additional leukocytes to stimulate the inflammatory response. TGF-β1 secreted by a variety of inflammatory cells stimulates fibroblasts to contribute to wound closure and ECM management in order to generate a functional scaffold for migration and proliferation of epithelial and endothelial cells to re-epithelialise and reconstitute tissue (Martin 1997, Betensley, Sharif et al. 2016). In the final remodelling phase that can last years, the newly formed vessels undergo a regression and normal vascular constitution is restored. ECM components and effector cells are eliminated, and the wound undergoes a contraction, presumably due to the contractile properties of myofibroblasts that will be described further below (Gosain and DiPietro 2004, Wietecha, Cerny et al. 2013, Rockey, Bell et al. 2015). BM fibrocyte = bone marrow derived fibrocyte; EMT = epithelial to mesenchymal transition; IL1β = interleukin 1 beta; TGF-β1 = transforming growth factor beta 1; IL13 = interleukin 13; TNF = tumour necrosis factor; ECM = extracellular matrix.

Local blood clotting and vasoconstriction follow upon almost every tissue injury. Damaged tissue and blood clots release pro-inflammatory cytokines to recruit inflammatory cells which then clear cell debris and kill invading microbes. Attracted macrophages also release cytokines to stimulate leukocytes augmenting the inflammatory response. TGF-β-stimulated fibroblasts contribute to generating a functional ECM scaffold for migration and proliferation of epithelial and endothelial cells to re-epithelialise and reconstitute tissue and thereby close the wound (Martin 1997, Betensley, Sharif et al. 2016). Finally, it comes to normal vascular reconstitution

and wound contraction (Gosain and DiPietro 2004, Wietecha, Cerny et al. 2013, Rockey, Bell et al. 2015).

The peptidic cytokine TGF-β is a key molecule in fibrotic remodelling. Three main isoforms exist, namely TGF-β1, -β2, and -β3, while TGF-β1 is said to play the major role in tissue fibrosis (Ask, Bonniaud et al. 2008). ECM synthesis is driven by TGF-β1 via stimulation of collagen type I alpha 1 chain (*COL1A1*) and many more ECM-related genes. TGF-β1 also maintains ECM preservation by increasing the number of additional cross-links in the ECM scaffold. Beyond this post-transcriptional modification of collagen, tissue inhibitor of metalloproteinase (*TIMP1*) gene transcription is upregulated while matrix metalloproteinase (*MMP*) activity is attenuated by TGF-β1, as shown in **Figure 3** (Schiller, Javelaud et al. 2004, Mauviel 2005, Verrecchia and Mauviel 2007).

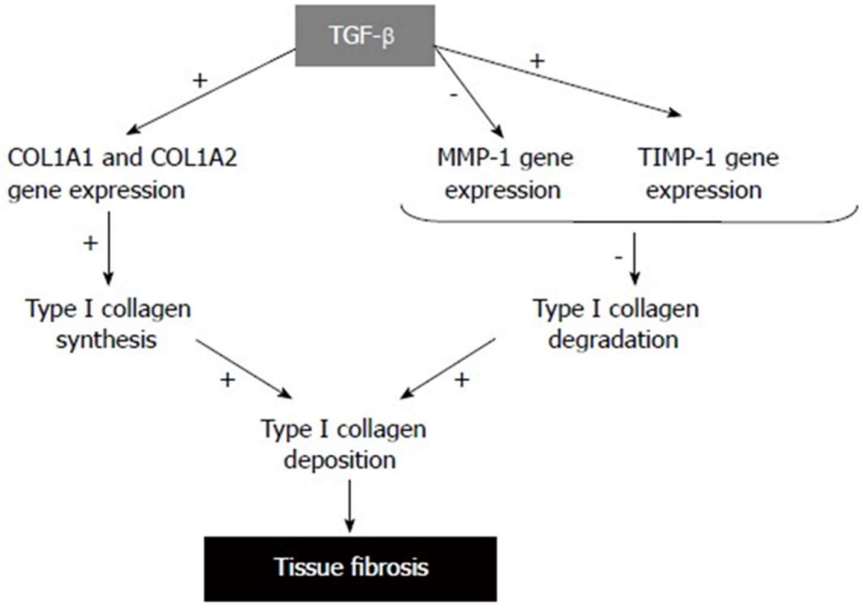


**Figure 3: TGF-β mediates tissue fibrosis, from (Verrecchia and Mauviel 2007).**

Transforming growth factor beta (TGF-β) stimulates (+) collagen type I alpha chain (*COL1A1* and *COL1A2*) gene expression which leads to an increase of type I collagen synthesis. Meanwhile, by lowering (-) matrix metalloproteinase (*MMP-1*) gene expression and promoting tissue inhibitor of metalloproteinase (*TIMP1*) gene expression, the presence of TGF-β hinders type I collagen from being degraded. In total, extracellular matrix (ECM) synthesis is driven by TGF-β by leading to higher amount of type I collagen deposition (Verrecchia and Mauviel 2007). An excess amount of ECM proteins, such as collagens is responsible for the pathological stiffness in IPF lungs (Burgess, Mauad et al. 2016).

ECM is mainly both produced and reabsorbed by fibroblasts, as they not only secrete collagen but also matrix-degrading enzymes like matrix-metalloproteinases (MMPs) (Kendall and Feghali-Bostwick 2014). Beyond forming a scaffold for tissue restoration upon injury, fibroblasts undergo a phenotypic transition into myofibroblasts to contract matrix for wound closure (Gabbiani 2003). Myofibroblast characteristics are contractility, α-smooth-muscle-actin (αSMA) expression, increased ECM synthesis, and resistance to apoptosis (Kendall and Feghali-Bostwick 2014).

Collagens provide the primary structural element of the ECM. Their three pro-α-chains form the triple-stranded procollagen that divides into collagen after secretion (Gordon and Hahn 2010). Besides a well-structured scaffold, stable links between the ECM and the invading cells are required to allow attachment to matrices to warrant functional tissue remodelling. Here, a dimeric glycoprotein comes into play, called fibronectin (Fn) (Singh, Carraher et al. 2010). ECM proteins, such as collagens and proteoglycans like fibronectin or tenascin c (Tnc), produced by myofibroblasts, are responsible for the pathological stiffness in IPF lungs (Burgess, Mauad et al. 2016). Fn has been shown to be essential for collagen deposition in a pulmonary injury model of bleomycin-treated rats (Muro, Moretti et al. 2008) and was found in fibroblastic foci of IPF lungs as well, co-localising with Tnc. Tnc gene and protein expression was significantly increased in IPF lung tissue homogenate when compared to normal lungs, – highest levels correlated with % forced vital capacity (FVC) decline – while Tnc expression was almost undetectable in normal tissue. Histological analyses revealed Tnc to be expressed in subepithelial fibroblastic foci, where also αSMA-positive myofibroblasts were present (Estany, Vicens-Zygmunt et al. 2014).

The large hexameric ECM glycoprotein Tnc was found to be expressed specifically and transiently upon tissue injury. Downregulation occurs after tissue repair or finalisation of the scarring process (Midwood and Orend 2009). Tnc is known to be an essential player in fibroblast migration and cell adhesion and thereby contributes to tissue remodelling (Trebaul, Chan et al. 2007, Snyder, Zemke et al. 2009).

IPF lung-derived fibroblasts were shown to express more Tnc and αSMA gene expression compared to healthy lung-derived fibroblasts. Tnc and αSMA gene

expression was found to be inducible by 24 hours of TGF-β treatment (Estany, Vicens-Zygmunt et al. 2014). The four named proteins – collagen, αSMA, fibronectin and tenascin C – or their corresponding genes serve as disease progression markers in this study.

This brief introduction to the mechanism of well-functioning wound repair shows that it is a brilliantly organised process that is, nevertheless, vulnerable in each phase. Multiple factors may affect the wound-healing process. Besides systemic aspects including age and gender, stress, comorbidities, and lifestyle factors (such as smoking, alcohol, and malnutrition), local factors like oxygenation and foreign bodies, such as silica, also play a role in the physiological process of wound repair (Guo and Dipietro 2010). Likewise, severe or persistent tissue injury can lead to tissue fibrosis (Wynn 2011).

### 1.1.5 Bleomycin-induced pulmonary fibrosis

The antibiotic drug bleomycin is used in cancer therapy, but its use is limited by the fibrogenic side-effects of the drug (Walters and Kleeberger 2008), as already mentioned in **Chapter 1.1.1**. In experimental pneumology, several methods such as the instillation of silica or asbestos and tissue-damaging radiation are used to mimic features of IPF. However, so far, no model can induce "the entire disease" – including irreversibility and progressivity – due to its still unclear aetiology (Moeller, Ask et al. 2008). Bleomycin is the most commonly favoured drug to induce reversible experimental pulmonary fibrosis in rodents (Li, Shi et al. 2021). The inflammatory phase of the bleomycin-induced pulmonary fibrosis lasts approximately until day nine which can be determined by the messenger ribonucleic acid (mRNA) expression level of several inflammatory cytokines, most of which significantly decrease after day 9. Subsequently, a fibrotic phase occurs, which can be monitored by the determination of pro-collagen I gene expression, which peaks at day 14 (Chaudhary, Schnapp et al. 2006). Investigations on cytokine expression after bleomycin administration were tested in a time course, and day 14 after the instillation of bleomycin was shown to be

the most suitable time point for lung fibrosis assessment, as bleomycin-induced pulmonary fibrosis is at least partially reversible without intervention (Izbicki, Segel et al. 2002).

For the followingly presented study, both phases of bleomycin-induced pulmonary fibrosis were analysed, i.e., the inflammatory phase and the fibrotic phase.

## 1.2 Systemic sclerosis

Systemic sclerosis (SSc) – also called scleroderma – is an autoimmune disease affecting multiple organ systems due to connective tissue impairment. Autoimmune processes are considered to lead to epithelial dysfunction, characterised by small-vessel vasculopathy and to modulation of fibroblasts into a pro-inflammatory phenotype, causing fibrosis of multiple internal organs due to excessive collagen production (Chizzolini, Raschi et al. 2002, Solomon, Olson et al. 2013, Schoenfeld and Castelino 2017, Adigun and Bhimji 2018). The main causes of death in SSc patients are the development of ILD and PAH. Clinically relevant pulmonary fibrosis can be found in one quarter of all SSc patients, while pulmonary dysfunction or radiological abnormalities are obvious in a much higher percentage of these patients (Tyndall, Bannert et al. 2010, Schoenfeld and Castelino 2017). With an incidence of 3-21 per one million people, SSc belongs to the rare diseases affecting all racial groups, with a higher reported incidence in Europe than in Asia (Silman 1991, Barnes and Mayes 2012). Apart from environmental factors, positive family history remains the major risk factor for SSc (Rezaei, Aslani et al. 2018). Currently, immunosuppressive therapy is mostly used for treating patients suffering from SSc with ILD (SSc-ILD), whereas lung transplantation remains an option, but is controversial due to the systemic properties of the disease. As SSc-related diseases (including reflux and oesophageal dysmotility) may contradict lung transplantation, the 1- and 5-year-survival rates are comparable to Non-SSc-ILD patients, who neither get transplanted (Sottile, Iturbe et al. 2013).

## 1.3 The proteasome system

### 1.3.1 Proteasomal protein degradation

Proteins are involved in virtually every cellular process. Ribosomes synthesise proteins as a lined-up sequence of amino acids and chaperones subsequently fold them into their specific three-dimensional structures which are directly linked to their individual functions in every cell (Kim, Hipp et al. 2013). Environmental stress, ageing or upregulated ribosomal protein synthesis and a simultaneously lower translational fidelity lead to so-called "protein stress" (Soti and Csermely 2007). For the degradation of most eukaryotic proteins, two pathways have been described: the autophagy-lysosome-system (ALS) which degrades most long-lived proteins, aggregated proteins, and cellular organelles, and secondly, the ubiquitin-proteasome-system (UPS) which degrades 80-90 % of proteins (Rock, Gramm et al. 1994). Since the recycling of amino acids is more energy-effective than *de novo* synthetisation, the two systems contribute to protein homeostasis (Lilienbaum 2013).

Proteasomes are proteases and can be found in all nucleated cells. The so-called 26S proteasome digests most of the cellular proteins to short peptides both in the cytosol and in the nucleus (Finley 2009). This protease of over 2 Megadalton (MDa) has been highly conserved during evolution, and even in archaebacterial and eubacteria simpler forms of it have been found (Coux, Tanaka et al. 1996). Misfolded or damaged proteins that are targeted for degradation are covalently attached to at least four copies of the 8.5 Kilodalton (kDa) protein ubiquitin by ubiquitin ligases and conjugating enzymes (Wickner, Maurizi et al. 1999, Bhattacharyya, Yu et al. 2014). Disturbances in this process can lead to irreversible damage and may hamper cell viability, which is why the ubiquitin marking is a highly controlled procedure (Collins and Goldberg 2017). Ubiquitination begins with the attachment of one ubiquitin to the ubiquitin-activating enzyme E1 and interaction with the ubiquitin-conjugating enzyme E2, where poly-ubiquitination takes place.

The UPS is not only essential for protein homeostasis and quality control but also plays crucial roles in cell cycle control and progression, major histocompatibility complex

(MHC) class I antigen processing, transcriptional regulation, and many other biological processes (Hershko and Ciechanover 1998, Sijts and Kloetzel 2011, Benanti 2012, Geng, Wenzel et al. 2012, Meiners and Eickelberg 2012).

### 1.3.2 26S proteasome complexes

The degradation of ubiquitinated proteins is mediated by the 26S proteasome (Finley 2009). The 26S is built from the 20S catalytic core particle (CP) and the 19S regulatory particle (RP), acting as a proteasome activator. This most abundant regulator consists of at least 19 subunits (Lander, Estrin et al. 2012). The base, which is directly in contact with the CP, consists of six regulatory particles triple A-ATPases (Rpt1-6) and four non-ATPase proteins (Rpn1, Rpn2, Rpn10, and Rpn13), whereas Rpn10 and Rpn13 serve as proteasome intrinsic ubiquitin receptors (Bard, Goodall et al. 2018).

The lid is formed by non-ATPase subunits (Rpn3, Rpn5-9, Rpn11, Rpn12) and plays an essential role in deubiquitinating substrates with deubiquitinases Rpn11 (*PSMD4*). Rpn11 cuts off the ubiquitin chain ATP-dependently. Three different deubiquitinases exist that can work together with the proteasome, UCH37, UBP6, and USP14 (Leggett, Hanna et al. 2002, Lee, Lu et al. 2016, VanderLinden, Hemmis et al. 2016). Rpn6 (*PSMD11*) is known for promoting the assembly of the RP and CP (Finley and Prado 2020). In summary, the 19S RP coordinates substrate recognition, removal of substrate polyubiquitin chains, and substrate unfolding and translocation into the CP for degradation (Tomko and Hochstrasser 2013).

### 1.3.3 Alternative regulatory particles

Besides the 19S RP, other proteasome activators exist, namely PA28αβ, PA28γ, and PA200. PA28αβ consists of PA28α and PA28β which activate the proteasome in an ATP-independent manner and mediate ubiquitin-independent degradation of substrates. PA28αβ is localised in the cytoplasm, while PA28γ can only be found in the nucleus (Stadtmueller and Hill 2011).

The PA200 proteasome activator is mainly localised in the nucleus. It is a 200 kDa large single molecule with a dome-like structure, that associates with most of the α-subunits of the 20S core. Its biological function is still not well understood until today.
Inhibition of the catalytic activities of the proteasome was demonstrated as the only inhibitory regulatory particle that has been described for the 20S proteasome, i.e. PI31, referring to its molecular weight of 31 kDa (Chu-Ping, Slaughter et al. 1992, Zaiss, Bekker et al. 2011) (**Figure 4**).

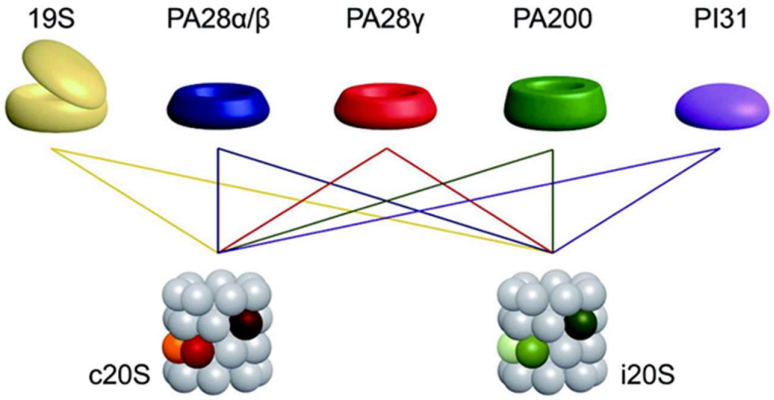


**Figure 4: Several cap complexes serve as proteasome activators, from (Meiners, Keller et al. 2014)**

Several proteasome activators are known already, namely 19S, the PA28 family, consisting of PA28α and PA28β, PA200 and PI31, the latter acting as an inhibitor *in vitro*. One big bundle of proteasomes with either constitutive 20S proteasome core particle (c20S) or immunoproteasome core particle (i20S) is imaginable as shown in (Meiners, Keller et al. 2014).

A recently published review by the Meiners lab aimed to highlight the importance of understanding how single proteasomal components as well as proteasomal super-complexes are regulated in disease and under physiological conditions. The authors offered a building block concept as a starting point for more systematic investigations on the diverse proteasome complexes. The authors highlight the identification of novel small molecule inhibitors to be a major step to generating a better understanding of proteasome function in disease and health and might additionally lead to future medical utilisation in humans (Wang, Meul et al. 2020). Interestingly, a PA200-

dependent impact on myofibroblast differentiation has been shown recently (Welk, Meul et al. 2019).

### 1.3.4 c20S constitutive proteasome core particle

The catalytic activity of the proteasome complexes resides in the CP, which is also known as the c20S particle. The barrel-like structured core particle consists of four stacked seven-membered rings with an inner diameter of 2 nm. The two outer rings are composed of seven α-subunits (α1-7, *PSMA1-PSMA7*) where the so-called proteasome activators can sit on, facilitating the entry of peptides into the CP (Stadtmueller and Hill 2011). The two inner rings consist of seven β-subunits (β1-7, *PSMB1-PSMB7*), which contain the proteolytically active sites (Kish-Trier and Hill 2013, Bard, Goodall et al. 2018). The enzymatic activity of the proteasome refers to three of the seven proteasomal β-subunits, namely β1, β2, and β5. Their active sites face the inner side of the barrel-shaped core particle. B1 cleaves after acid residues and has caspase-like (C-L) activity. B2 cleaves after basic residues and is characterised by trypsin-like (T-L) activity. B5 represents the chymotrypsin-like (CT-L) active site that cleaves after hydrophobic residues (Borissenko and Groll 2007, Finley 2009, Murata, Yashiroda et al. 2009). As an N-terminal-nucleophilic hydrolase-like enzyme, the proteasome's catalytic sites contain a threonine at position one (Thr1) which mediates peptide cleavage in an autocatalytic way. The proteasome does not release amino acids but peptides with a mean length of six to nine residues. This means the proteasome cleaves only 10 to 15 % of peptide bonds in proteins. The other 85 to 90 % of the peptide bonds are quickly hydrolysed by cellular endo- and exopeptidases (Kisselev, Akopian et al. 1999). Importantly, the access to the proteolytic chamber of the 20S CP is highly regulated by RPs that sit on one or both axial pores of the cylindrically shaped CP.

Considering the various combinations of subunits, it is theoretically possible to generate 36 different 20S core complexes that vary in their proteolytic capacity and specificity. This is a remarkable number of proteasome subtypes if one also includes

the different regulatory complexes (**Figure 4**) that can associate with each end to form either singly capped proteasomes (26S) or doubly capped proteasomes (30S) (Bhattacharyya, Yu et al. 2014). To add to this mosaic, one molecule each of 19S and PA28 form so-called hybrid proteasomes (Ferrington and Gregerson 2012).

### 1.3.5 i20S immunoproteasome core particle

Inflammatory stimuli lead to the assembly of the immunoproteasome with the insertion of three different catalytically active subunits instead of β1, β2, and β5 into the enzymatically active core, called i20S (Barton, Cruz et al. 2002). As the name suggests, immunoproteasomes are constitutively expressed in immune cells, but they are inducible in every parenchymal cell type as well as upon inflammatory stimuli such as interferon gamma (IFNγ) or tumour necrosis factor alpha (TNFα) (Kammerl and Meiners 2016, Liu, Wang et al. 2019). The catalytic β-subunits are called β1i, (or low molecular mass polypeptide-2 (LMP2, *PSMB9*), β2i (or multicatalytic endopeptidase complex-like 1 (MECL-1, *PSMB10*) and β5i (low molecular mass polypeptide-7 (LMP7, *PSMB8*) (Groettrup, Kirk et al. 2010). Both, the constitutive proteasome and the immunoproteasome generate peptides with the same length of around seven to nine amino acids and behave similarly in substrate turnover (Toes, Nussbaum et al. 2001). The three immunoproteasome subunits show a slightly different cleavage specificity which then leads to the generation of more hydrophobic and basic C-termini and fewer acidic C-termini (Groettrup, van den Broek et al. 2001, Kloetzel and Ossendorp 2004).
Besides the constitutive proteasome, intermediate proteasomes are abundant in normal human tissues as well. The intermediate proteasomes can contain only one or two of the three inducible catalytic subunits of the immunoproteasome, but the overall catalytic activity of these proteasomes is similar to those of the immunoproteasome (Guillaume, Chapiro et al. 2010, Ferrari, Stroobant et al. 2022).

**Table 1: Proteasomal and immunoproteasomal subunits**

| Category | Gene name | Protein name |
|---|---|---|
| 20S core α-subunits | *PSMA1* | proteasome subunit alpha type-1 |
| | *PSMA2* | proteasome subunit alpha type-2 |
| | *PSMA3* | proteasome subunit alpha type-3 |
| | *PSMA4* | proteasome subunit alpha type-4 |
| | *PSMA5* | proteasome subunit alpha type-5 |
| | *PSMA6* | proteasome subunit alpha type-6 |
| | *PSMA7* | proteasome subunit alpha type-7 |
| | *PSMA8* | proteasome subunit alpha type-8 |
| c20S core β-subunits | *PSMB1* | proteasome subunit beta type-1 |
| | *PSMB2* | proteasome subunit beta type-2 |
| | *PSMB3* | proteasome subunit beta type-3 |
| | *PSMB4* | proteasome subunit beta type-4 |
| | *PSMB5* | proteasome subunit beta type-5 |
| | *PSMB6* | proteasome subunit beta type-6 |
| | *PSMB7* | proteasome subunit beta type-7 |
| i20S core β-subunits | *PSMB8* | proteasome subunit beta type-8/ low molecular mass protein 7/ proteasome subunit beta 5i |
| | *PSMB9* | proteasome subunit beta type-9/ low molecular mass protein 2/ proteasome subunit beta 1i |
| | *PSMB10* | proteasome subunit beta type-10/ multicatalytic endopeptidase complex subunit 1/ proteasome catalytic subunit 2i |

### 1.3.6 Inhibitors of the proteasome

Proteasome inhibitors are mostly short peptides and can be grouped into chemical classes, referring to the peptide scaffold's electrophilic anchor. The latter might either be an aldehyde, a boronate, an epoxyketone, a vinyl sulfone or a β-lactone (Beck, Dubiella et al. 2012).

One major representative of the peptide aldehyde group is MG-132, the first synthetic proteasome inhibitor. The aldehyde group which binds reversibly to the proteasomes' CT-L active site has been replaced by proteasome investigators into a vinyl sulfone group which then binds irreversibly to the proteasome (Bogyo, McMaster et al. 1997).

Bortezomib is another reversible proteasome inhibitor, characterised by its peptide-like backbone being linked to a boronate group. Bortezomib thereby belongs to the peptide boronate proteasome inhibitors. The boronate group is known to bind more tightly to the proteasomes´ CT-L and C-L active sites when compared to an aldehyde group which leads to higher inhibitory potency (Beck, Dubiella et al. 2012, Huber and Groll 2012, Fricker 2020). Bortezomib belongs to the so-called first-generation proteasome inhibitors and is the first-line treatment for patients suffering from multiple myeloma (MM). Also, beneficial effects on pulmonary graft versus host disease were observed, a disease, in which fibrotic changes in the small airways are present (Jain, Budinger et al. 2018). Currently, a clinical trial of bortezomib in SSc-ILD is in progress (www.clinicaltrials.gov identifier NCT02370693).

One major representative of the epoxyketone proteasome inhibitors is carfilzomib, which irreversibly binds by double covalent bond formation to the CT-L active site of the proteasome and gets applied in MM treatment since 2012 (Herndon, Deisseroth et al. 2013, Thibaudeau and Smith 2019). Carfilzomib is injected intravenously (like bortezomib) and is used to overcome bortezomib resistance in MM patients (Allegra, Alonci et al. 2014). Oprozomib (former ONX012) is another well-known irreversibly binding but orally available epoxyketone proteasome inhibitor and provides CT-L site-specific inhibitory effects (Thibaudeau and Smith 2019). The last two mentioned drugs belong to the so-called second-generation proteasome inhibitors (Dick and Fleming 2010).

Finally, the peptide vinyl sulfone proteasome inhibitors represent irreversible proteasome inhibitors. As being cost-efficient and easily synthesised, peptide vinyl sulfone serves as a protease activity probe by being labelled with fluorophores or radioactive sites (Thibaudeau and Smith 2019).

In extracts of streptomyces, a non-peptide proteasome inhibitory molecule was found, called lactacystin. Lactacystines convert into β-lactones in neutral pH conditions which acylate and thereby irreversibly inhibit the proteasome. B-lactones are known to be the least stable proteasome inhibitors by fast hydrolysation in water (Kisselev and Goldberg 2001, Groll and Huber 2004, Thibaudeau and Smith 2019).

The above-mentioned groups mostly represent covalently binding and thereby irreversible proteasome inhibitors.

Irreversible proteasome inhibition is preferred to a reversible mechanism when targeting parasites, such as mycobacteria (Lin, Li et al. 2009). But when it comes to human proteasome targets, irreversible inhibitors are often limited by off-target effects and cytotoxicity which limit the dosage (Beck, Dubiella et al. 2012). Additionally, counteracting mechanisms such as proteasomal overexpression or mutation are known to dampen the effect of irreversible proteasomal inhibitors (Franke, Niewerth et al. 2012, Kumar, Lee et al. 2012). Restricted membrane permeability and simultaneously high plasma clearance limit peptide-based proteasome inhibitors as well, and so, reversible and non-peptide-based proteasome inhibitors are suggested to better withstand the mentioned counteracting biological and chemical drawbacks and might even exhibit higher target selectivity (Beck, Dubiella et al. 2012).

In general, non-covalently binding molecules act as reversible proteasome inhibitors. So far, no clinical trials were undertaken using non-covalently binding proteasome inhibitors (Huber and Groll 2021).

### 1.3.7 Proteasome dysfunction in fibrotic lung disease

It is well known that constitutive proteasome function is important in several lung diseases, such as COPD and asthma by impacting on cellular protein homeostasis network (Bouchecareilh and Balch 2011). Dysregulation of protein homeostasis was also shown for IPF (Korfei, Ruppert et al. 2008, Lawson, Crossno et al. 2008). Proteomic analysis revealed an overexpression of the proteasome activator PA28α to be associated with better clinical outcomes. These data suggest that proteasomal activity might be regulated in pulmonary fibrosis (Korfei, von der Beck et al. 2013). This hypothesis was confirmed by the Meiners lab showing activation of proteasome activity in fibrotic lungs using the bleomycin model (Semren, Welk et al. 2015). Proteasome expression was also shown to be upregulated in IPF lungs which might contribute to the pathophysiology of the disease (Baker, Bach et al. 2014). The 19S protein Rpn6 was

found to be upregulated in endstage IPF lung tissues compared to healthy lung donors. (Semren, Welk et al. 2015). Rpn6 is an essential subunit of the 19S RP and acts as a molecular clamp to facilitate binding to the 20S catalytic core (Pathare, Nagy et al. 2012). It thereby regulates the assembly of the 26S proteasome. The Meiners group found an increased assembly and activity of the 26S proteasome in the process of TGF-β1-induced myodifferentiation of pulmonary fibroblasts that depended on Rpn6 levels. Partial depletion of Rpn6 counteracted myofibroblast activation by attenuating TGF-β1-induced 26S proteasome formation in primary human lung fibroblasts (phLF) (Semren, Welk et al. 2015). Rpn6 expression was found to be high in AECII and Clara cells in the murine model of bleomycin-induced fibrosis and in a model of irreversible pulmonary lung fibrosis in gammaherpesvirus-68–infected mice. The authors concluded the 26S proteasome activation to potentially be an intrinsic feature of pulmonary fibrotic remodelling (Semren, Welk et al. 2015).

Targeting the proteasome in fibrosis and specifically in lung fibrosis with catalytic proteasome inhibitors was tested in several experimental models with divergent results. In 2012, the first-in-class pan-proteasome inhibiting agent bortezomib was found to prevent bleomycin-induced pulmonary fibrosis when administered on day seven of the bleomycin challenge by inhibiting TGF-β1-mediated target gene expression (Mutlu, Budinger et al. 2012). In contrast, another group of researchers showed that bortezomib reduced collagen mRNA expression in murine lung fibroblasts, as well as in human lung fibroblasts, but the authors also stated bortezomib failed in the prevention of bleomycin-induced pulmonary inflammation and fibrosis if administered daily, starting one day after bleomycin instillation (Fineschi, Reith et al. 2006, Fineschi, Bongiovanni et al. 2008). As in the latter study, the applied doses of bortezomib were sequential and quite high, the exact comparability of the studies is limited. Meiners et al. highlighted the crucial importance of the degree and the timepoint of proteasome inhibition on either cytotoxic or beneficial effects (Meiners, Ludwig et al. 2008, Meiners and Eickelberg 2012) and thereby contributed to resolving the apparent contradiction in pre-existing literature. Dose-dependent adverse effects of bortezomib were also described in models of dextran-sulfate-sodium (DSS)-induced

colitis in mice. Bortezomib treatment ameliorated DSS-induced inflammation in a dose-dependent manner by preventing tissue damage via diminishing infiltration of the colon by neutrophils and inflammatory T cells (Schmidt, Gonzalez et al. 2010).

Recently, a group of scientists stated that the anti-fibrotic effects of bortezomib might not be linked to proteasome inhibition (Penke, Speth et al. 2022).

The first study suggesting anti-fibrotic effects of a second-generation inhibitor targeting only one (CT-L) active site of the proteasome was presented by (Semren, Habel-Ungewitter et al. 2015). Oprozomib (former ONX0912) was shown to counteract TGF-β signalling and thereby provide anti-fibrotic effects in primary murine lung fibroblasts (pmLF). Reduction of Col1a1 and actin alpha 2 (Acta2) expression in pmLF could be demonstrated on the mRNA level. However, Oprozomib failed to prevent or reduce bleomycin-induced pulmonary fibrosis in mice when applied locally to the lung. Unfortunately, the site-specific inhibitor worsened fibrotic lung remodelling in bleomycin-treated mice. An increase of proteasomal activity was considered as a compensatory mechanism by the authors which then might have overcome the local proteasome inhibition (Semren, Habel-Ungewitter et al. 2015). One recently published paper highlighted the bottlenecks of therapeutic anti-fibrotic efficacy of proteasome inhibitors (Chen, Liu et al. 2022): (1) anti-fibrosis effects might be caused through mechanisms dissociated from proteasome inhibition (Penke, Speth et al. 2022); (2) proteasomal inhibition does not target a single specific protein (Wang, Shih et al. 2021); (3) drug resistance to proteasome inhibitors is achieved by compensatory activation of other catalytically active sites of the proteasome as many proteasome inhibitors act on one activity site (Raninga, Lee et al. 2020, Wang, Shih et al. 2021); and (4) difficult application of proteasome inhibitors due to their side effects (Ale, Bruna et al. 2014, Kaplan, Torcun et al. 2017).

Taken together, the anti-fibrotic effects of proteasomal inhibition are still not fully understood from a mechanistic view, and the discussion on their therapeutic application in the literature remains controversial.

### 1.3.8 Function and druggability of the immunoproteasome

The following chapter provides an overview of three main functions of the immunoproteasome, namely its role in MHC class I antigen presentation, its influence on preventing autoimmune reactions and its role in shaping innate immune responses. These activities make immunoproteasomes a novel emerging drug target for which specific inhibitors have been generated.

Immunoproteasomes have a dedicated role in MHC class I antigen presentation. Antigen processing is initiated by a specific generation of short peptides, consisting of eight or nine residues which are loaded onto the MHC I molecule's groove. Therefore, hydrophobic C-termini anchors of the peptides are required, of which the immunoproteasome is the major provider by its CT-L enzymatically active centre of LMP7, whereas in general other cytosolic proteases form peptides with a less hydrophobic C-terminus (Ferrington and Gregerson 2012). The immunoproteasome is thus an essential player in processing these antigenic epitopes. This function is particularly relevant upon viral infection of cells which results in the interferon-mediated induction of the immunoproteasome and subsequent processing of viral proteins into MHC I epitopes (Kloetzel and Ossendorp 2004). The subsequent detection of these "foreign" peptides by $CD8^+$ T cells results in the killing of the virus-infected cell. Timely induction of the immunoproteasome in parenchymal cells is thus a crucial part of the adaptive immune response (Kloetzel and Ossendorp 2004).

Besides its pivotal role in antigen presentation, the immunoproteasome is involved in the prevention of autoimmunity after infection (Basler, Mundt et al. 2015). Inappropriate immunoproteasomal expression was shown in experimental models of autoimmunity as well as in human autoimmune disorders. $LMP7^{-/-}$ mice were significantly less affected by experimentally DSS-induced colitis and thereby body weight loss due to a less extent of nuclear factor-κB (NF-κB) signalling (Schmidt, Gonzalez et al. 2010). Also, reduced disease severity in either $LMP2^{-/-}$ and $MECL\text{-}1^{-/-}$ mice was also observed in other studies using the DSS-induced colitis disease model.

LMP7-inhibited (PR-957, also known as ONX0914) mice developed less severe symptoms of DSS-induced colitis, probably due to suppressed cytokine production (Basler, Dajee et al. 2010). LMP7 inhibition was also shown to attenuate colitis-associated cancer in mice (Vachharajani, Joeris et al. 2017).

IL23, IFNγ, IL6, and IL8 release in lipopolysaccharide- (LPS-)stimulated peripheral blood mononuclear cells (PBMC) was potently decreased by the pan-proteasome inhibitor bortezomib and a selective LMP7 inhibitor ONX0914 (Pletinckx, Vassen et al. 2019). ONX0914 has been shown to impact positively on several murine inflammatory models, such as lupus nephritis, arthritis, autoimmune encephalomyelitis, and colitis (Muchamuel, Basler et al. 2009, Basler, Dajee et al. 2010, Ichikawa, Conley et al. 2012). T cell differentiation into T helper 17 cells (Th17) or T helper 1 cells (Th1) cells was altered by ONX0914 (Muchamuel, Basler et al. 2009, Kalim, Basler et al. 2012).

Psoriasis is a chronic autoimmune disease, which can be modelled in murine models, such as the Imiquimod (IMQ) mouse model, in which psoriasis-like skin lesions and inflammation are induced by Imiquimod, a TLR7/8 activator (van der Fits, Mourits et al. 2009). IMQ-treated mice that were subjected to immunoproteasome inhibition using ONX0914 were found to display interleukin 17A (*Il17a*) levels that were comparable to vaseline-treated mice, the control for IMQ. The weight of inguinal lymph nodes in IMQ mice was reduced by ONX0914 and fewer inflammatory infiltrates were found in ONX0914-treated mice's skin lesions (Del Rio Oliva, Mellett et al. 2022).

Mice, that are heterozygous for the caspase recruitment domain family member 14 (CARD14) gene, are characterised by spontaneous onset of chronic psoriasis-like skin lesions (Jordan, Cao et al. 2012, Mellett, Meier et al. 2018). Psoriasis-like skin lesions and histopathological signs of psoriasis in Card14DE138+/- mice were ameliorated by ONX0914. Comparable to the IMQ model, draining lymph nodes´ weight was reduced in ONX0914-treated mice.

In psoriasis-like altered tissue, interleukin 17 c (*Il17c*), Tnf, C-C Motif Chemokine Ligand 20 (*Ccl20*), interleukin 22 (*Il22*) and interleukin 23 (*Il23*) mRNA expression levels were decreased by ONX0914 treatment, while serum levels of Tnf and interleukin 6 (*Il6*) remained unaltered by immunoproteasome inhibition (Del Rio Oliva, Mellett et al.

2022). The binding of ONX0914 to the immunoproteasome was resolved in crystal structures showing only LMP7-site specific inhibition (Huber, Basler et al. 2012).
In 2014, another immunoproteasome inhibitor has been introduced, called LU-005i (de Bruin, Huber et al. 2014). LU-005i has been shown to act as an effective and selective inhibitor of MECL-1, LMP2 and LMP7. LU-005i lowered LPS-induced IFNγ-secretion of splenocytes, reduced Il6 production and fully blocked Il23 secretion in LPS-treated PBMCs, and inhibited IL17 production in $CD4^+$ T cells in a dose-dependent manner. In a DSS mouse model of colitis, the expression levels of tumour necrosis factor-α (TNFα), interleukin 1 beta (Il1β), and Il17 were significantly lower in LU-005i-treated mice compared to untreated ones. Inflammation and signs of crypt damage were described to be lower than in untreated mice (Basler, Maurits et al. 2018). In the following, LU-005i will be called a pan-reactive immunoproteasome inhibitor. Specific immunoproteasome inhibition attenuates cytokine release of mononuclear cells and reduces DC- and T-cell activity, and thereby lowering cardiac allograft rejection in mice (Sula Karreci, Fan et al. 2016).
These data indicate that both, subunit deficiency and specific site inhibition are promising instruments to ameliorate autoimmune diseases and diseases with autoimmune components.

### 1.3.9 Immunoproteasome regulation in the lung

Immunoproteasomes in the lung have been studied by the Meiners lab in detail. Keller, Vosyka et al. could show a potential induction of the immunoproteasomes in parenchymal cells in which a very low basal expression can be found. Besides primary alveolar type II cells (pmATII) and pmLF, the induction was observed in a human alveolar epithelial cell line A549 and even phLF. The induction of the immunoproteasome in parenchymal cells was initiated by IFNγ in a time-dependent manner, which is a major inflammatory cytokine, also found in viral infections (Keller, Vosyka et al. 2015).

Recently published data from the Meiners lab showed for the first time an inappropriate expression of the immunoproteasomal subunit LMP2 in lung tissue sections of IPF patients (Wang, Zhang et al. 2023). Remarkably, LMP2 overexpression was found in immune cells, such as invading alveolar macrophages and in parenchymal cells, such as epithelial cells (**Figure 5**).

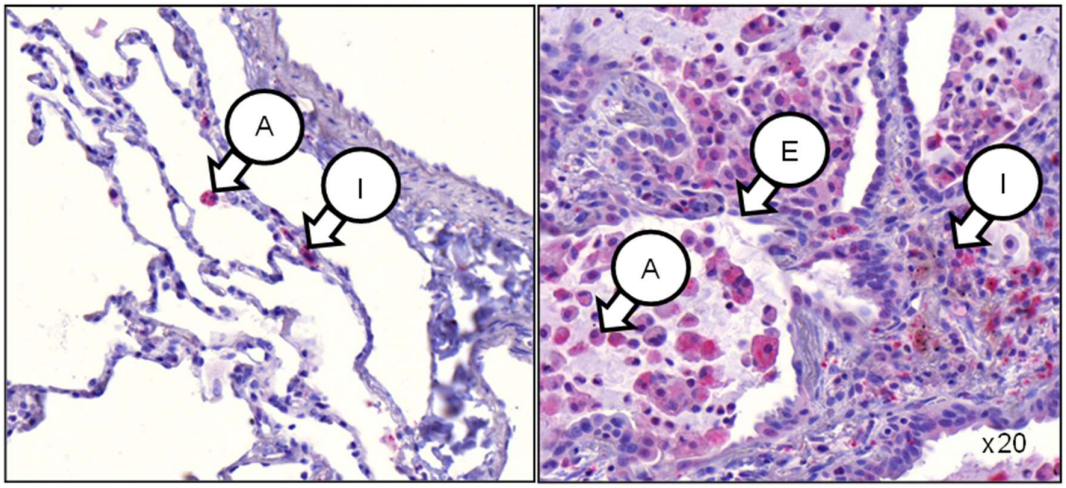


**Figure 5: Immunoproteasomal subunit LMP2 expression in healthy human lung tissue compared to IPF lung tissue**

Immunohistochemical LMP2-staining in human donor lung tissue (left) compared to IPF lung tissue (right) reveals immunoproteasomal expression not only in alveolar macrophages (A), but also in interstitial cells (I) and epithelial cells (E), derived from Dr. Ilona Kammerl, Shinji Takenaka, unpublished.

These data highly correlate with single-cell RNA sequencing data, provided by Lafyatis et al. on ipfcellatlas.com, demonstrating immunoproteasomal subunits PSMB8, PSMB9 and PSMB10 being overexpressed in parenchymal cells such as fibroblasts as well as myofibroblasts of IPF patients (ipfcellatlas.com).

Inappropriate induction of the immunoproteasome in lung parenchymal cells was also observed in a mouse model of experimental lung fibrosis. Mice, treated with 2 U/kg bleomycin, showed induction of immunoproteasomal subunits LMP2 and LMP7 in lung tissue homogenates as detected by Western blot analysis. Significant overexpression of LMP2 could also be detected on day 56 after bleomycin administration when

compared to the control. LMP7 has been shown to be increased significantly from day seven until the end of observation at day 56. Unpublished bleomycin data (**Figure 6**) were kindly provided by Dr. Ilona Kammerl and Dr. Isis Fernandez, both from the CPC, Helmholtz Munich.

Taken together, immunohistochemically stained IPF tissue sections, single-cell RNA sequencing data and analyses of experimentally induced pulmonary fibrosis highly suggest a potential role of immunoproteasomes in mammalian lung fibrosis. Its function and relevance for pulmonary fibrosis, however, are unknown.

Interestingly, immunoproteasomal subunits were also found to be overexpressed in parenchymal cells, such as fibroblasts in SSc-ILD patients when compared to healthy donors in a single-cell RNA sequencing study, provided by Misharin et al. on ipfcellatlas.com.

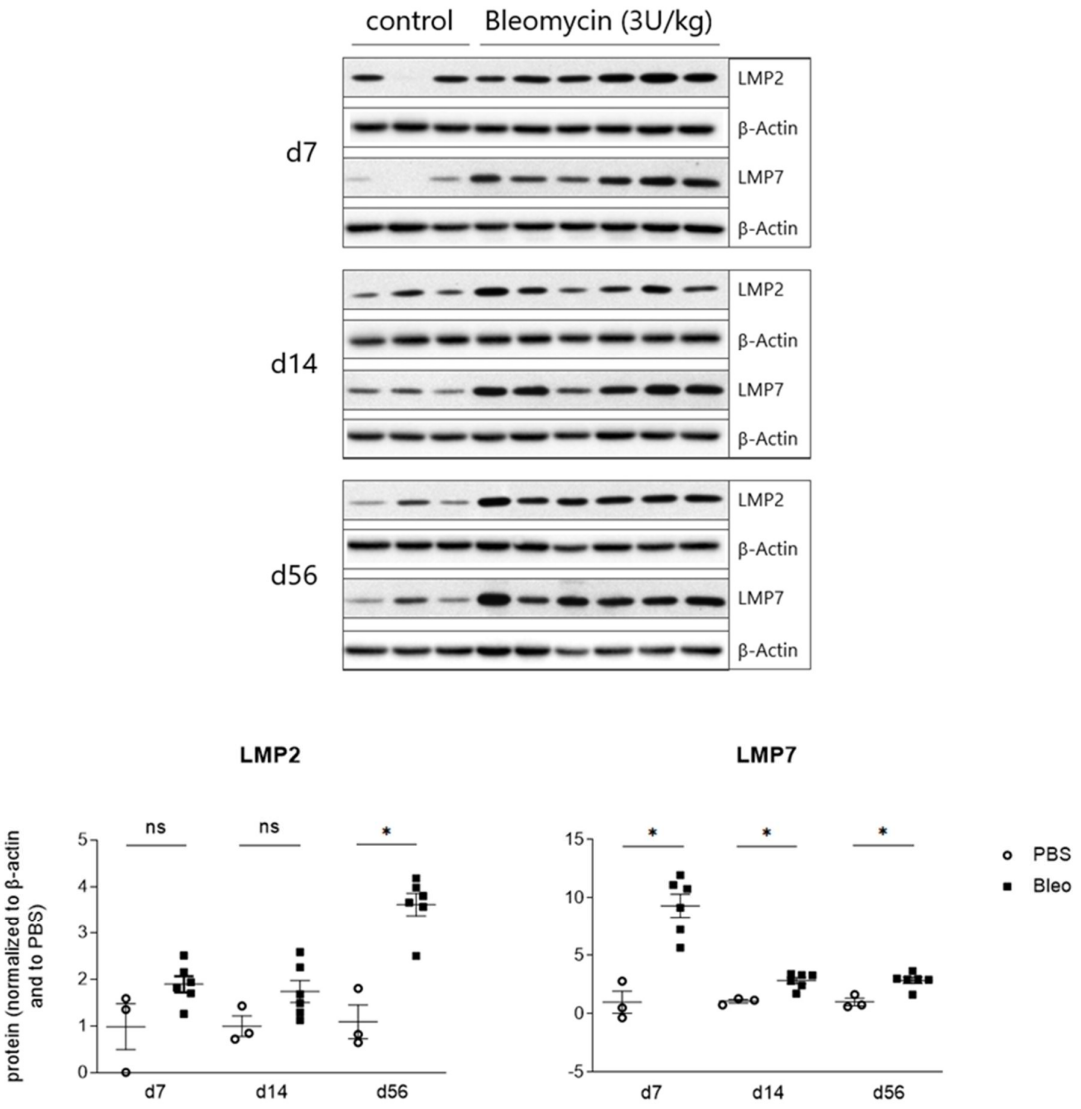


**Figure 6: Immunoproteasomal subunit expression is upregulated in bleomycin-treated mice**

Low molecular mass protein 2 (LMP2) and low molecular mass protein 7 (LMP7) protein staining in murine lung tissue homogenates reveals immunoproteasomal expression levels in mice, treated with 2 U/kg bleomycin (Bleo) intratracheally. Protein levels were analysed at day seven (d7), day 14 (d14), and day 56 (d56) after administration. PBS = phosphate buffered saline. (Mann-Whitney-test, ns = not significant, * $p < 0,05$, n = 3 per control group, 6 per bleo group). Derived from Dr. Ilona Kammerl and Dr. Isis Fernandez, unpublished.

# 2 Aims and hypotheses

IPF is a severe lung disease characterised by impaired gas exchange with a median survival of two to three years after diagnosis. For patients with advanced progression, lung transplantation remains the only treatment option as no pharmacological cure exists to date (Le Pavec, Dauriat et al. 2020). This outlines the need to gain new insights into the diseases' pathophysiology to identify new druggable targets. As described in **Chapter 1.3.9**, previous data of the Meiners lab suggested the immunoproteasome to be upregulated in a murine model of bleomycin-induced lung fibrosis. In accordance, immunohistochemically stained tissue sections of IPF patients revealed immunoproteasomal overexpression in parenchymal cells when compared to healthy lung donors. Based on these findings the present study aimed to shed more light on the potential role of the immunoproteasome in lung fibrogenesis and to evaluate whether the immunoproteasome might serve as a therapeutic target to ameliorate the course of the disease. In addition, this study also investigated lung tissue homogenates of SSc patients, as fibrotic alterations have also been shown to be present in these patients. Several sets of experiments were performed to address the following hypotheses.

**Hypothesis 1: Immunoproteasomal gene expression is upregulated in lung tissue homogenates of SSc patients when compared to healthy tissue donors.**

Relative gene expression of immunoproteasomal subunits was evaluated in lung tissue homogenates of SSc patients and compared to healthy donors.

**Hypothesis 2: The main pro-fibrotically acting mediator TGF-β1 affects immunoproteasomal expression in fibroblasts.**

Primary human lung fibroblasts (phLF) were subjected to TGF-β1-treatment *in vitro* and immunoproteasomal expression was quantified both on mRNA and protein levels.

**Hypothesis 3: Immunoproteasome function regulates myofibroblast differentiation.**

Immunoproteasome single-subunit-deficient lung fibroblasts (*in vitro*), murine lung sections (*ex vivo*) and mice (*in vivo*) were subjected to pro-fibrotic conditions and compared to their specific wildtype counterpart. Moreover, cells, tissue and mice were treated with an immunoproteasome inhibitor or solvent as a control. Marker gene expression of collagen (*Col1a1*), fibronectin (*Fn1*), tenascin (*Tnc*), and α-smooth muscle actin (*Acta2*) were investigated by RT-qPCR.

# 3 Materials

## 3.1 Drugs and treatments

| Drug | Solvent | Stock | Provider |
|---|---|---|---|
| IFNγ (human or mouse) | PBS | 20,000 U/ml | Roche, Basel, Switzerland |
| LPS | PBS | 1 mg/ml | Sigma-Aldrich, St. Louis, USA |
| LU-005i | DMSO | 10 µM | Prof. Overkleeft, Leiden University, Dep. of Organic Chemistry |
| KZR-504 | DMSO | 10 µM | Kezar Life Sciences, South San Francisco, USA |
| Amphotericin B | - | 250 µg/ml | Gibco, Thermo Fisher Scientific, Waltham, USA |
| Penicillin/Streptomycin | - | 10,000 U/ml, 10,000 µg/ml | Gibco, Thermo Fisher Scientific, Waltham, USA |
| TGF-β1 | 4 mM HCl + 1 mg/mL BSA | 1,000 ng/mL | R&D Systems, Minneapolis, USA |
| DMSO | - | 99,9 % | Carl Roth, Germany |

## 3.2 Enzymes

| Product | Provider |
|---|---|
| Collagenase Type CLS 240 U/mg | Biochrom GmbH, Berlin, Germany |
| DNase 2 U/µl | Peqlab, Erlangen, Germany |
| M-MLV Reverse Transcriptase 200 U/ml | Sigma-Aldrich, St. Louis, USA |
| Proteinase K min. 600 mAnson-U/ml | AppliChem, Darmstadt, Germany |
| Taq Polymerase 5 U/µl | Thermo Fisher Scientific, Waltham, USA |

## 3.3 Kits

| Product | Provider |
|---|---|
| LightCycler 480 SYBR Green I Master | Roche Diagnostics, Mannheim, Germany |
| PeqGOLD Total RNA-Kit | Peqlab, Erlangen, Germany |

| | |
|---|---|
| Pierce BCA Protein Assay Kit | Thermo Fisher Scientific, Waltham, USA |
| Roti-Quick RNA Extraction Kit | Carl Roth, Karlsruhe, Germany |

## 3.4 Markers

| **Product** | **Provider** |
|---|---|
| Protein Marker IV (10-245 kDa) | AppliChem, Darmstadt, Germany |
| DNA-ladder 100 bp Plus, peqGOLD | VWR Peqlab, Rednore, USA |
| DNA-ladder 1 kb Plus, peqGOLD | VWR Peqlab, Rednore, USA |

## 3.5 Buffers

All buffers were prepared with Milli-Q® water. Ingredients are listed in the relevant chapters.

## 3.6 Reagents

| **Product** | **Solvent** | **Stock** | **Provider** |
|---|---|---|---|
| 6 x DNA Loading Dye | - | 6 x | Thermo Fisher Scientific, Waltham, USA |
| Activity based probe LW124 | DMSO | 2.5 µM | Prof. Dr. H. Overkleeft, University of Leiden, Netherlands |
| Activity-based probe MV151 | DMSO | 50 µM | Prof. Dr. H. Overkleeft, University of Leiden, Netherlands |
| Activity-based probe MVB127 | DMSO | 25 µM | Prof. Dr. H. Overkleeft, University of Leiden, Netherlands |
| Antibody diluent | - | - | Dako, Hamburg, Germany |
| Bovine serum albumin (BSA) | - | - | AppliChem, Darmstadt, Germany |
| cOmplete™ protease inhibitor cocktail | $H_2O$ | 25 x | Roche, Basel, Switzerland |
| Dithiotreitol (DTT) | $H_2O$ | 1 M | Life Technologies, Carlsbad, USA |
| Entellan | - | - | Merck Millipore, Darmstadt, Germany |
| Eosin G 0.5 % | $H_2O$ | - | Carl Roth, Karlsruhe, Germany |
| First Strand Buffer | - | 5 x | Life Technologies, Carlsbad, USA |

| | | | |
|---|---|---|---|
| Fluorescent Mounting Medium | - | - | Dako, Hamburg, Germany |
| Hemalaun | - | - | Carl Roth, Karlsruhe, Germany |
| Luminata™ Classico Western HRP Substrate | - | - | Merck Millipore, Darmstadt, Germany |
| Luminata™ Forte Western HRP Substrate | - | - | Merck Millipore, Darmstadt, Germany |
| Nuclease-Free Water | - | - | Ambion, Thermo Fisher Scientific, Waltham, USA |
| Nucleotide Mix | - | 10 mM | Promega, Fitchburg, USA |
| Penicillin/Streptomycin | - | - | Gibco, Thermo Fisher Scientific, Waltham, USA |
| Random Hexamers | - | 250 µM | Promega, Fitchburg, USA |
| RNAsin RNAse Inhibitor | - | 40 U/µl | Promega, Fitchburg, USA |
| Roti-Block | - | 10x | Carl Roth, Karlsruhe, Germany |
| Roti-Immunoblock | - | 10x | Carl Roth, Karlsruhe, Germany |
| SYBR Safe | - | - | Thermo Fisher Scientific, Waltham, USA |
| Trypsin (0.25 % EDTA) | - | - | Thermo Fisher Scientific, Waltham, USA |

## 3.7 Chemicals

| **Product** | **Provider** |
|---|---|
| Citric acid monohydrate | AppliChem, Darmstadt, Germany |
| Dithiothreitol (DTT) | Life Technologies, Carlsbad, USA |
| DMSO | Carl Roth, Karlsruhe, Germany |
| EDTA | AppliChem, Darmstadt, Germany |
| Ethanol | AppliChem, Darmstadt, Germany |
| Glycerol | AppliChem, Darmstadt, Germany |
| Isopropanol (p. A.) | AppliChem, Darmstadt, Germany |
| Methanol (p. A.) | AppliChem, Darmstadt, Germany |
| Paraformaldehyde | AppliChem, Darmstadt, Germany |
| Sodiumdodecylsulfate (SDS) | AppliChem, Darmstadt, Germany |
| Tris | AppliChem, Darmstadt, Germany |
| Triton X-100 | Life Technologies, Carlsbad, USA |
| Tween-20 | AppliChem, Darmstadt, Germany |

| | |
|---|---|
| Xylene | AppliChem, Darmstadt, Germany |
| β-Mercaptoethanol | AppliChem, Darmstadt, Germany |

## 3.8 Consumables

| **Product** | **Provider** |
|---|---|
| 6/24/96 cell-culture-treated well plates | TPP, Trasadingen, Switzerland |
| 96 well plates, white, for luminescence detection | Berthold Technologies, Bad Wildbad, Germany |
| Cell culture dishes (6 cm, 10 cm, 15 cm) | Nunc, Wiesbaden, Germany |
| Cell culture flasks (75 $cm^2$, 175 $cm^2$) | Nunc, Wiesbaden, Germany |
| Cryovials 1.5 ml | Greiner Bio-One, Frickenhausen, Germany |
| Eppendorf Safe-Lock Tubes (1 ml, 1.5 ml) | Eppendorf, Wesseling-Berzdorf, Germany |
| Dismembrator Tubes (Nalgene Cryogenic Tubes) | Thermo Fisher Scientific, Waltham, USA |
| Falcon tubes (15 mL, 50 ml) | BD Bioscience, Heidelberg, Germany |
| Glass pasteur pipettes | VWR International, Darmstadt, Germany |
| Microplate 96-well, PS, flat bottom (for BCA assay) | Greiner Bio-One, Frickenhausen, Germany |
| PCR plates, white, 96 well | Biozym Scientific, Hessisch Oldendorf, Germany |
| Pipet tips | Biozym Scientific, Hessisch Oldendorf, Germany |
| Protein LoBind tube 1.5 ml | Eppendorf, Hamburg, Germany |
| PVDF membrane | Bio-Rad, Hercules, USA |
| Quali-PCR-Tube stripes | Kisker Biotech**,** Steinfurt, Germany |
| Sealing foil for qPCR plate | Kisker Biotech, Steinfurt, Germany |
| Serological pipettes Cellstar 2, 5, 10, 25, 50 ml | Greiner Bio-One, Frickenhausen, Germany |
| Sterican cannulas | BD Bioscience, Heidelberg, Germany |
| Super RX Fuji medical X-ray film | Fujifilm Corporation, Tokyo, Japan |
| Syringes (10 mL, 20 mL, 50 ml) | Neolab, Heidelberg, Germany |
| Whatman blotting paper 3 mm | GE Healthcare, Freiburg, Germany |

## 3.9 Technical devices and further equipment

| Technical device | Provider |
|---|---|
| -20 °C freezer MediLine LGex 410 | Liebherr, Biberach, Germany |
| -80 °C freezer | Eppendorf, Hamburg, Germany |
| -80 °C freezer U570 HEF | Eppendorf, Hamburg, Germany |
| Autoclave DX-45 | Systec, Wettenberg, Germany |
| Autoclave VX-120 | Systec, Wettenberg, Germany |
| Cell culture workbench Herasafe KS180 | Thermo Fisher Scientific, Waltham, USA |
| Centrifuge MiniSpin plus | Eppendorf, Hamburg, Germany |
| Centrifuge Rotina 420R | Hettich, Tuttlingen, Germany |
| Centrifuge with cooling, Micro220R | Hettich, Tuttlingen, Germany |
| Cytospin 2 centrifuge | Hettich, Tuttlingen, Germany |
| Dismembrator S | Satorius, Göttingen, Germany |
| Dry ice container Forma 8600 Series, 8701 | Thermo Fisher Scientific, Waltham, USA |
| Electrophoretic Transfer Cell, Mini Protean Tetra Cell | Bio-Rad, Hercules, USA |
| Film developer Curix 60 | AGFA, Morsel, Belgium |
| Fluorescent scanner Typhoon TRIO+ | Amersham Biosciences, Amersham, UK |
| Gel imaging system ChemiDoc XRS+ | Bio-Rad, Hercules, USA |
| Hyrax M55 microtome | Zeiss, Jena, Germany |
| Ice machine ZBE 110-35 | Ziegra, Hannover, Germany |
| Light Cycler LC480II | Roche Diagnostics, Mannheim, Germany |
| Liquid nitrogen cell tank BioSafe 420SC | Cryotherm, Kirchen/Sieg, Germany |
| Liquid nitrogen tank Apollo 200 | Cryotherm, Kirchen/Sieg, Germany |
| Mastercycler gradient | Eppendorf, Hamburg, Germany |
| Mastercycler Nexus | Eppendorf, Hamburg, Germany |
| Microm STP 420D Tissue Processor | Thermo Fisher Scientific, Waltham, USA |
| Milli-Q® Advantage A10 Ultrapure Water Purification System | Merck Millipore, Darmstadt, Germany |
| Milli-Q® Integral Water Purification System for Ultrapure Water | Merck Millipore, Darmstadt, Germany |
| Mini Centrifuge MCF-2360 | Schubert & Weiss Omnilab, Munich, Germany |
| Mirax scanner | Zeiss, Jena, Germany |
| Nalgene Freezing Container (Mister Frosty) | Omnilab, Munich, Germany |

| | |
|---|---|
| NanoDrop 1000 | PeqLab, Erlangen, Germany |
| pH meter InoLab pH 720 | WTW, Weilheim, Germany |
| Plate centrifuge 5430 | Eppendorf, Hamburg, Germany |
| Plate reader Sunrise | Tecan, Crailsheim, Germany |
| Plate reader TriStar LB941 | Berthold Technologies, Bad Wildbach, Germany |
| Research plus pipettes | Eppendorf, Hamburg, Germany |
| Vibratome Hyrax V50 | Zeiss, Jena, Germany |
| Shaker Duomax 1030 | Heidolph, Schwabach, Germany |
| Thermomixer compact | Eppendorf, Hamburg, Germany |
| Tissue Lyser II | Qiagen, Hilden, Germany |
| Vacuum pump NO22AN.18 with switch 2410 | KNF, Freiburg, Germany |
| Vortex mixer | IKA, Staufen, Germany |
| Water bath Aqua Line AL 12 | Lauda, Lauda-Königshofen, Germany |

## 3.10 Software

| **Software** | **Provider** |
|---|---|
| GraphPad Prism 5 and 7 | GraphPad Software, La Jolla, USA |
| Image Lab | Bio-Rad, Hercules, USA |
| ImageJ | National Institutes of Health, Bethesda, USA |
| LightCycler® 480 SW 1.5 | Roche Diagnostics, Mannheim, Germany |
| Magellan Software | Tecan, Crailsheim, Germany |
| Microsoft Office Professional Plus 2010 | Microsoft, Redmond, USA |
| Adobe Acrobat Reader DC 2019 | Adobe Inc., San José, USA |
| Endnote X9 | Alfasoft GmbH, Frankfurt, Germany |

# 4 Methods

## 4.1 Animal experiments

The applied animal models are based on homozygous mice that lack single immunoproteasomal subunits, namely LMP2 or LMP7. For the experiments, mice strains C57BL/6 LMP2$^{-/-}$ (Van Kaer, Ashton-Rickardt et al. 1994) and LMP7$^{-/-}$ were used that were initially described by (Fehling, Swat et al. 1994).

### 4.1.1 Genotyping

Lysis of murine ear clips was performed in 200 µl PBND buffer (**Table 2**) containing 1 µl proteinase K at 56 °C shaking at 1250 RPM overnight. PBND buffer contained the following ingredients:

**Table 2: PBND buffer components**

| Component | Concentration |
|---|---|
| KCl | 50 mM |
| Tris-HCl pH 8.3 | 10 mM |
| $MgCl_2$ | 2.5 mM |
| Gelatin | 0.01 % (w/v) |
| IGEPAL | 0.45 % (v/v) |
| Tween-20 | 0.45 % (v/v) |

Tail-cuts were lysed at the same conditions in 300 µl PBND buffer containing 3 µl proteinase K (AppliChem). After centrifugation at 13,000 RPM for one minute, 2 µl of the DNA containing supernatant was mixed with 23 µl of the following polymerase chain reaction (PCR) master mix (**Table 3**), depending on mouse line:

**Table 3: PCR master mix components**

| Component | Amount for LMP2 | Amount for LMP7 |
|---|---|---|
| 10x PCR Rxn buffer | 2.5 µl | 2.5 µl |

| | | |
|---|---|---|
| 10 mM dNTP Mix | 0.5 µl | 0.5 µl |
| 50 mM $MgCl_2$ | 1 µl | 0.6 µl |
| Primer 1 5 µM | 1.25 µl | 1.25 µ |
| Primer 2 5 µM | 1.25 µl | 1.25 µl |
| Primer 3 5 µM | 1.25 µl | 1.25 µl |
| 5 U/mL Taq | 0.125 µl | 0.125 µl |
| Template | 2 µl | 2 µl |
| $H_2O$ | 15,125 µl | 15,525 µl |

PCR was performed in the Mastercycler Nexus (Eppendorf) under the following conditions (**Table 4**) (italic steps were repeated for 30 cycles):

**Table 4: PCR conditions**

| **PCR step** | **Temperature [°C]** | **Time [min:sec]** |
|---|---|---|
| initial denaturation | 94 | 03:00 |
| *denaturation* | *95* | *00:45* |
| *annealing* | *56* | *00:30* |
| *elongation* | *72* | *01:30* |
| final elongation | 72 | 10:00 |
| hold | 4 | ever |

After PCR samples were mixed with 6x DNA loading dye and loaded on a 1 % agarose gel containing SYBR Safe (Thermo Fisher Scientific) which ran in TAE buffer (**Table 5**) for 30 min at 90 V. PCR product detection was performed using a ChemiDoc XRS+ system (Bio-Rad). A band of 396 base pair (bp) indicates the LMP2 wildtype allele, whereas $LMP2^{-/-}$ shows a band of 644 bp. Heterozygous mice were characterised by both bands. A band of 600 bp indicates the LMP7 wildtype allele, whereas $LMP7^{-/-}$ shows a band of 700 bp. Heterozygous mice were identified by both bands. Primers used for genotyping are listed in **Table 6**.

**Table 5: TAE buffer composition**

| Component | Concentration |
|---|---|
| Tris | 40 mM |
| Acetic acid | 20 mM |
| EDTA | 1 mM |

**Table 6: Primers for LMP2 and LMP7 genotyping**

| Primer | | Sequence 5'-3' |
|---|---|---|
| LMP2 | FW | GTAACACTAAGGCTCCCCTTCTG |
| | REV | TGACACTACTCACCCCGCTGAC |
| | PGK-Prom-Rev2 | TCCATCTGCACGAGACTAGTGAGAC |
| LMP7 | FW | GGACCAGGACTTTACTACGTAGATG |
| | REV | CTTGTACAGCAGGTCACTGACATCG |
| | neo | CCGACGGCGAGGATCTCGTCGTGA |

### 4.1.2 Experimental bleomycin-induced pulmonary fibrosis in mice

Animal experiments were conducted by Dr. Ilona E. Kammerl, a postdoctoral scientist at the CPC, and David Kutschke, a technician at the Institute for Lung Biology and Disease (ILBD), both at Helmholtz Munich – Deutsches Forschungszentrum für Gesundheit und Umwelt (HMGU) and the author of this thesis. Bleomycin experiments were performed using age- and sex-matched LMP7$^{-/-}$ and littermate wildtype mice at the age of eight to twelve weeks. Narcosis was performed by intraperitoneal injection of 500 µg Medetomidin, 5 mg Midazolam, and 50 µg Fentanyl per kg body weight. 50 µl installation, containing 2 U/kg bleomycin in phosphate-buffered saline (PBS) as control was administered intratracheally. For antagonising narcotics, 2.5 mg Atipamezole, 500 µg Flumazenil, and 1.2 mg Naloxone per kg body weight were injected subcutaneously. Until sacrifice at day 14, mice were examined every day after Bleomycin instillation. Body weight loss was tolerated up to a critical threshold of -15 %, and subjects were excluded from observation and sacrificed by cervical dislocation due to ethical reasons. At day seven (peak of pulmonary inflammation) or 14 (peak of pulmonary fibrosis), after weighing survivor mice, narcotics (100 mg Ketamine per kg

body weight, 5 mg Xylazine per kg body weight) were injected intraperitoneally and several minutes were given to achieve unconsciousness. Proper anesthetisation was validated by checking the toe pinch reflex before starting the surgery. Mice were introduced into the laminar flow hood and were moistened with 80 % ethanol, fixated lying on the back and a median incision from the umbilicus to the chin was performed. The peritoneum was opened, and the left renal artery was incised to allow bleeding out. Pneumothorax was carefully placed using forceps in order not to hurt visceral pleurae and the diaphragm was removed on both sides of the ribs. Thorax was opened by sternotomy and thorax walls were retracted to two sides in order to better expose the thoracic cavity. The heart was flushed with 20 ml pre-warmed PBS 1X (**Table 7**) via the right ventricle after the incision of the left auricle to flush the lung to remove blood. Washing was successful when lung tissue turned completely white. Mice were intubated intratracheally via tracheotomy and bronchoalveolar lavage (BAL) was performed by three times instillation of 500 µl PBS 1 X containing cOmplete® protease inhibitor cocktail (Roche). BAL fluid was kept on ice until further processing described below. Left lungs were filled with 4 % (w/v) paraformaldehyde (PFA) via infusion after ligation of the right main bronchus and explantation of the right lung. Right lungs were directly snap-frozen in liquid nitrogen for later RNA and protein analysis. Left lungs were kept in PFA for 24 hours at 4 °C before starting the histological procedure as described below.

**Table 7: PBS buffer composition**

| Component | Concentration |
|---|---|
| NaCl | 137 mM |
| KCl | 2.7 mM |
| $Na_2HPO_4$ | 10 mM |
| $KH_2PO_4$ | 2 mM |

### 4.1.3 Experimental LPS-induced lung injury in mice

Animal experiments were conducted by Dr. Ilona E. Kammerl, a postdoctoral scientist at the CPC, and David Kutschke, a technician at the Institute for Lung Biology and Disease (ILBD), both at Helmholtz Munich – Deutsches Forschungszentrum für Gesundheit und Umwelt (HMGU) and the author of this thesis. LPS experiments were performed using C57BL/6 wildtype mice at the age of eight to twelve weeks. Narcosis was performed as described above in **Chapter 4.1.2**. 50 µl instillation containing 10 mg/kg LPS dissolved in PBS was administered intratracheally. Control instillation consisted of 50 µl PBS. 5 mg/kg immunoproteasome inhibitor LU-005i or solvent solution was administered on either day one, day one and two or day one, two and three. For antagonising narcotics 2.5 mg Atipamezole, 500 µg Flumazenil, and 1.2 mg Naloxone per kg body weight were injected intraperitoneally. Mice were sacrificed on day three after LPS exposure and sample preparation was performed as described in **Chapter 4.1.2**.

### 4.1.4 Bronchoalveolar lavage

BAL acquisition was performed by Dr. Ilona E. Kammerl, postdoctoral scientist, and the author of this thesis. After centrifugation of the entire BAL fluid at 1,400 RPM for 10 min, the supernatant was snap-frozen and kept in liquid nitrogen for further analysis. After resuspension of the BAL cell pellet in 500 µl, PBS + cOmplete® protease inhibitor cells were counted in a Neubauer counting chamber. 30,000 BAL cells were transferred onto glass slides by centrifugation for six minutes at 400 RPM using a Cytospin 2 centrifuge. After the cells dried overnight at RT, May-Grünwald Giemsa staining was performed. After drying out, cells were covered using a mounting medium and a coverslip.

## 4.2 Cell culture

When cells reached 90 % confluency detaching was performed by incubation with Trypsin-EDTA (0.25 %) for two to four minutes after aspiration of old media and washing with pre-warmed PBS 1X. Trypsin-induced cell detachment was monitored under the light microscope. Added 10 % FBS-containing medium stopped the reaction and cells were collected and distributed on new culture dishes or flasks for subculturing. Cryopreservation was done after harvest and centrifugation at 500 x *g* for five minutes at 4 °C and one additional washing step with PBS 1X before resuspension in 1 ml of cell culture medium containing 10 % dimethylsulfoxide (DMSO) (Carl Roth). Cooling down was achieved gently by use of a Nalgene Freezing Container (Mister Frosty, Omnilab) and long-term storage was done in a liquid nitrogen tank.

PhLF and pmLF synchronisation was achieved by FBS starvation using 1 % as its concentration for 24 hours. Cells were treated with 5 or 2 ng/ml TGF-β1 (R&D Systems) and 75 U/ml IFNγ diluted in a fresh 20 % FBS-containing medium. Immunoproteasome was inhibited by 0.2 µM LU-005i or 0.2 µM KZR-504, beginning three hours before TGF-β1 treatment.

### 4.2.1 Cell lines

#### 4.2.1.1 Primary human lung fibroblast (phLF) cell lines

PhLFs (**Table 8**) were kindly provided by Prof. Dr. Andreas Günther from Universities of Giessen and Marburg Lung Center (UGMLC), Giessen, Germany. Experiments were performed until passage three and media (**Table 9**) were changed every three to four days.

**Table 8: PhLF lines**

| Lung | ID | Age | Sex | Tissue |
|---|---|---|---|---|
| Control | 406 | 50 | F | peripheral normal lung tissue, organ donor |
| Control | 409Sp | 51 | M | peripheral normal lung tissue, organ donor |
| Control | 411a | 44 | F | peripheral normal lung tissue, organ donor |

| | | | | |
|---|---|---|---|---|
| Control | 423g | 41 | F | peripheral normal lung tissue, organ donor |

**Table 9: PhLF culture medium components**

| Culture medium | Provider |
|---|---|
| MCDB 131 medium | PAN-Biotech, Aidenbach, Germany |
| FBS 10 % | PAA Laboratories, Cölbe, Germany |
| Penicillin/Streptomycin 100 U/ml | Gibco, Thermo Fisher Scientific, Waltham, USA |
| L-glutamine 2 mM | Life Technologies, Carlsbad, USA |
| basic-FGF 2 ng/ml | Life Technologies, Carlsbad, USA |
| EGF 0.5 ng/ml | Sigma-Aldrich, St. Louis, USA |
| Insulin 5 µg/ml | Life Technologies, Carlsbad, USA |

#### 4.2.1.2 Primary murine lung fibroblasts (pmLF) cell lines

PmLFs were obtained as described in **Chapter 4.1.8**. Cells were cultured. Experiments were done until passage two and media (**Table 10**) were changed every three to four days.

**Table 10: PmLF culture medium components**

| Culture medium | Provider |
|---|---|
| DMEM/F-12 | Life Technologies, Carlsbad, USA |
| Penicillin/Streptomycin 100 U/ml | Gibco, Thermo Fisher Scientific, Waltham, USA |
| Amphotericin B 2.5 µg/mL | Gibco, Thermo Fisher Scientific, Waltham, USA |
| FBS 20 % | PAA Laboratories, Cölbe, Germany |

#### 4.2.1.3 Immortalised murine lung fibroblast cell line CCL-206

The murine lung fibroblast cell line CCL-206 was obtained from American Type Culture Collection (ATCC) (Manassas, USA). Experiments were done until passage eight and media (**Table 11**) were changed every three to four days.

**Table 11: CCL-206 culture medium components**

| Culture medium | Provider |
|---|---|
| DMEM/F-12 | Life Technologies, Carlsbad, USA |
| Penicillin/Streptomycin 100 U/ml | Gibco, Thermo Fisher Scientific, Waltham, USA |
| FBS 20 % | PAA Laboratories, Cölbe, Germany |

### 4.2.2 Murine precision-cut lung slices

Murine precision-cut lung slices (mPCLS) experiments were conducted by Dr. Ilona E. Kammerl, postdoctoral scientist, Jie Chen, MD, and the author of this study. To generate tissue for mPCLS, mice were sacrificed, intubated intratracheally via tracheotomy, and the tube was fixated with two threads one above the tracheostomy, one below. The upper thread fixated the tube while the lower thread remained untied initially. 3 % low melting agarose tempered to about 42 °C solutions was slowly administered via the tube and a syringe pump allowed both lungs to slowly expand and get the airways filled and by that, the lung expanded. After injecting between 0.9 and 1.5 ml of agarose solution mice were extubated, and the lower thread was immediately closed to prevent agarose to exit the lungs. Lungs were explanted and put into an ice-cold mPCLS culture medium (**Table 12**) to achieve stiffening of the agarose. Lung lobes were separated and mounted onto the cutting surface of a Hyrax V55 vibratome (Zeiss) using instant adhesive. The tissue was cut into slices of 300 µm thickness using a speed of 1.2 mm/s with a frequency of 100 Hz and amplitude of 1 mm while being submerged completely in an mPCLS culture medium. Slices were carefully transferred into a 24-well plate (TPP) containing 0.5 µl pre-warmed mPCLS culture medium. After 30 minutes of incubation, the medium was changed. This washing step was repeated once after 30 more minutes. MPCLS were incubated at 37 °C, with 5 % $CO_2$, and 95 % humidity.

### 4.2.3 MPCLS culture conditions and treatment

MPCLS were cultured for five days maximum using the following medium, listed in **Table 12**:

**Table 12: MPCLS culture medium**

| Culture medium | Provider |
|---|---|
| DMEM/F-12 | Life Technologies, Carlsbad, USA |
| Penicillin/Streptomycin 100 U/ml | Gibco, Thermo Fisher Scientific, Waltham, USA |
| Amphotericin B 2.5 µg/mL | PAA Laboratories, Cölbe, Germany |
| FBS 0.1 % | PAA Laboratories, Cölbe, Germany |

MPCLS were treated with a pro-fibrotic cocktail, furthermore, called fibrosis cocktail (FC) (**Table 13**) for 48 hours containing recombinant transforming growth factor beta (TGF-β1), platelet-derived growth factor-AB (PDGF-AB), TNFα, and lysophosphatidic acid (LPA), while control cocktail contained solvents only.

**Table 13: Fibrosis cocktail (FC) composition, derived from (Alsafadi, Staab-Weijnitz et al. 2017)**

| Drug | Concentration | Provider | Product number |
|---|---|---|---|
| TGF-β1 | 5 ng/ml | R&D Systems, Minneapolis, USA | 240-B-002 |
| PDGF-AB | 5 µM | GIBCO, Karlsbad, California, USA | PHG0134 |
| TNFα | 10 ng/ml | R&D Systems, Minneapolis, USA | P06804 |
| LPA | 5 µM | Cayman Chemical, Ann Arbor, USA | 62215 |

LPS treatment was done for six hours using 500 ng/ml. Immunoproteasome pan-inhibition was achieved by three hours pre-treatment using 0.5 µM LU-005i, control samples were treated with the same amount of DMSO.

### 4.2.4 PmLF isolation

PmLF acquisition was performed by Dr. Ilona E. Kammerl, postdoctoral scientist, and the author of this thesis. After explantation, entire murine lungs were put into a 10 cm dish containing 5 ml pre-warmed DMEM/F-12 containing penicillin/streptomycin and amphotericin B and cut into 1-2 $mm^2$ pieces using two scalpels. The lung pieces were transferred into a 50 ml falcon tube and 50 µl collagenase I enzyme (5 mg/ 50 µl) was added to allow digestion at 37 °C for two hours at 400 RPM on the Thermomixer

compact (Eppendorf). Afterwards, digested tissue pieces were transferred onto a 70 µm nylon filter placed on a 50 ml falcon tube and pressed through it using the flat end of a 3 ml syringe piston. The filter was rinsed with 10 ml sterile PBS 1X and rinsing was repeated for at least one more time. Centrifugation at 300 x *g* was performed at 4 °C for 5 minutes and the supernatant was discarded. The cell pellet was resuspended in 10 ml pmLF medium (containing 20 % FBS) and seeded on a 10 cm dish and incubated at 37 °C in the incubator. Cell culture medium was changed if needed, at the latest every third day to get rid of non-adherent and dead cells. Experiments were performed using pmLFs in passage two only.

## 4.3 RNA analysis

### 4.3.1 RNA extraction of cells

Cells were scraped, or cell pellets were resuspended in 500 µl Roti®-Quick 1 solution (Carl Roth). 650 µl of well-mixed Roti®-Quick 2 solution was added. The mix was vortexed and incubated on ice for ten minutes. Now centrifugation was done at 10,000 RPM for 15 minutes at 4 °C to separate phases. The upper phase containing RNA was transferred into a fresh tube and 500 µl Roti®-Quick 3 solution was added, and the tube twisted. Incubation happened at -80 °C for at least 40 minutes, preferably overnight at -20 °C. Centrifugation at 13,000 RPM was done for 20 minutes at 4 °C and the supernatant was discarded. RNA attached to the tubes was washed two times with 600 µl of 70 % ethanol and ethanol was removed completely (i.e., vaporisation for ten to 15 minutes). Finally, 30 µl nuclease-free water (Ambion, Thermo Fisher Scientific) was added to resuspend the pellet. Measurement of RNA concentration was done with the NanoDrop 1000 (Thermo Fisher Scientific) at a wavelength of 260 nm. RNA purity was quantified by the ratio of A260/280 and values higher than 1.8 indicated purity over 90 %.

### 4.3.2 RNA isolation from murine lung tissues

Mikro-Dismembrator S (Sartorius) / TissueLyser II (Qiagen) was used to make powder of murine lung tissue that has been snap-frozen before the homogenisation. RNA was isolated using the peqGold Total Kit (VWR International). Homogenised and frozen samples were lysed with 600 µl RNA Lysis Buffer T containing 6 µl tris-2-carboxyethyl-phosphine (TCEP) (VWR International) for one hour on ice. The lysate was transferred into a new tube and 15 µl proteinase K (Thermo Scientific) was added before vortexing and incubating at 55 °C for ten minutes on a thermoblock while shaking at 700 RPM. The lysate was transferred into DNA-removing columns and centrifuged for one minute at 12,000 x *g*. Flowthrough was transferred into a new tube and one volume equivalent (at least 600 µl) of 70 % ethanol was added before transferring lysate on an RNA binding column (750 µl successively) and centrifugation at 10,000 x *g* for one minute. Flowthrough was discarded. 500 µl wash buffer 1 was added and centrifugation was done at 10,000 x *g* for 30 seconds. 600 µl wash buffer 2 was added and centrifugation was done at 10,000 x *g* for 15 seconds. The second washing step was repeated once, and the column was placed in a new collection tube and centrifugation was done at 1,000 x *g* for two minutes to completely dry the column matrix. After placing the column in a new tube, 40 µl RNase-free distilled water was added and incubated for five minutes before centrifugation at 5,000 x *g* for one minute to eluate RNA. Re-elution was done one more time using the flow-through. RNA concentration was determined using a NanoDrop1000 (Thermo Fisher Scientific) and RNA was kept on ice or stored at -80 °C.

### 4.3.3 Reverse transcription

In order to generate cDNA, 0.2 to 1 µg mRNA were diluted to 9.5 µl and incubated with 2 µl of 250 µM Random Hexamers (Thermo Fisher Scientific) for ten minutes at 70 °C. Ingredients for the following additional 8.5 µl of mastermix are listed in **Table 14**.

**Table 14: Reverse transcription mastermix components**

| component | final concentration | quantity per sample |
|---|---|---|
| 1x First Strand Buffer | | 4 µl |
| DTT | 0.1 M | 2 µl |
| dNTPs | 0.5 mM | 1 µl |
| RNAsin RNAse Inhibitor | 40 U/µL | 0.5 µl |
| M-MLV transcriptase | 200 U/µL | 1 µl |

8.5 µl of the mastermix was added to the incubated samples which had been put on ice immediately after the incubation. The mix was inverted and centrifuged two times. Next, the annealing step took place for five minutes at 25 °C, and afterwards, elongation was performed for 60 minutes at 37 °C to allow reverse transcription. Finally, 1 µl DNase (2 U/µl) was added, the mix was incubated at 37 °C for 15 minutes and heat inactivation was done at 75 °C for ten minutes. Before cDNA was used for qPCR, samples were diluted 1:5 with nuclease-free water (Ambion, Thermo Fisher Scientific).
To quantify distinct marker gene expression a SYBR Green LC480 system (Roche) was used. Each of the samples measured in duplicate in a 96-well plate format (TPP) contained 2.5 µl cDNA, 5 µl LC480 SYBR Green I Master mix (Roche), and 2.5 µl primer dilution containing both, forward and reverse primer at a final concentration of 0.5 µM. Plates were centrifuged for one minute at 1,000 RPM before starting a standard program of the Light Cycler 480II (Roche) with conditions listed in **Table 15** (italic steps were repeated for 45 cycles):

**Table 15: QPCR conditions**

| qPCR step | temperature | duration |
|---|---|---|
| initial denaturation | 95 °C | 5 minutes |
| *denaturation* | *95 °C* | *5 seconds* |
| *annealing* | *59 °C* | *5 seconds* |
| *elongation* | *72 °C* | *20 seconds* |
| melting curve | 60-95 °C (continuous acquisition) | 1 minute |

Target gene expression was normalised to housekeeping genes like hypoxanthine phosphoribosyl transferase gene (HPRT) or the 60S ribosomal protein L19 (RPL-19) using the $2^{-\Delta cT}$ (= $2^{-(cT(marker\ gene)\ -\ cT(housekeeper\ gene))}$ ) method. Primer specificity was validated by analysing the melting curves of PCR products. Used primers are listed in **Table 16**.

**Table 16: Primers for quantitative RT-PCR**

| Gene | Species | | Sequence 5'-3' |
|---|---|---|---|
| *ACTA2* | human | FW | CGAGATCTCACTGACTACCTCATGA |
| | | REV | AGAGCTACATAACACAGTTTCTCCTTGA |
| *CCND1* | human | FW | CGTGGCCTCTAAGATGAAGG |
| | | REV | CTGGCATTTTGGAGAGGAAG |
| *COL1A1* | human | FW | CAAGAGGAAGGCCAAGTCGAG |
| | | REV | TTGTCGCAGACGCAGATCC |
| *FN* | human | FW | CCGACCAGAAGTTTGGGTTCT |
| | | REV | CAATGCGGTACATGACCCCT |
| *HPRT* | human | FW | TGAAGGAGATGGGAGGCCA |
| | | REV | AATCCAGCAGGTCAGCAAAGAA |
| *PSMA1* | human | FW | CAGGGCAGGATTCATCAAAT |
| | | REV | CCAAACACTCCTGACGCATA |
| *PSMA3* | human | FW | AGATGGTGTTGTCTTTGGGG |
| | | REV | AACGAGCATCTGCCAACAA |
| *PSMB5* | human | FW | TCAGTGATGGTCTGAGCCTG |
| | | REV | CCATGGTGCCTAGCAGGTAT |
| *PSMC3* | human | FW | GTGAAGGCCATGGAGGTAGA |
| | | REV | GTTGGATCCCCAAGTTCTCA |
| *PSMD11* | human | FW | GCTCAACACCCCAGAAGATGT |
| | | REV | AGCCTGAGCCACGCATTTTA |
| *PSME1* | human | FW | CAAGGTGGATGTGTTTCGTG |
| | | REV | TGCTCAAGTTGGCTTCATTG |
| *PSME3* | human | FW | TAGCCATGATGGACTGGATGG |
| | | REV | CCTTGGTTCCTTGGAAGGCT |
| *PSME4* | human | FW | CCAACAGGAAAAGAATGCCGA |
| | | REV | CCAGGGCAGGTTTCTTTGCT |

| | | | |
|---|---|---|---|
| *PSMF1* | human | FW | AAAGCTCCTTGTGAAAGCCA |
| | | REV | CCCACTGCTCATGGATAGGT |
| *RPL19* | human | FW | TGTACCTGAAGGTGAAGGGG |
| | | REV | GCGTGCTTCCTTGGTCTTAG |
| *Acta2* | mouse | FW | GCTGGTGATGATGCTCCCA |
| | | REV | GCCCATTCCAACCATTACTCC |
| *Ccl17* | mouse | FW | AGTGGAGTGTTCCAGGGATG |
| | | REV | CTGGTCACAGGCCGTTTTAT |
| *Cxcl15* | mouse | FW | CGTCCCTGTGACACTCAAGA |
| | | REV | TAATTGGGCCAACAGTAGCC |
| *Fn1* | mouse | FW | GTGTAGCACAACTTCCAATTACGAA |
| | | REV | GGAATTTCCGCCTCGAGTCT |
| *Foxp3* | mouse | FW | TTCATGCATCAGCTCTCCAC |
| | | REV | CTGGACACCCATTCCAGACT |
| *Hprt* | mouse | FW | AATCCAGCAGGTCAGCAAAGAA |
| | | REV | TGAAGGAGATGGGAGGCCA |
| *Ifng* | mouse | FW | ACGGCACAGTCATTGAAAGCCTA |
| | | REV | GTCACCATCCTTTTGCCAGTTCC |
| *Il17a* | mouse | FW | TCCAGAAGGCCCTCAGACTA |
| | | REV | AGCATCTTCTCGACCCTGAA |
| *Il23a* | mouse | FW | GACTCAGCCAACTCCTCCAG |
| | | REV | GGCACTAAGGGCTCAGTCAG |
| *Il6* | mouse | FW | TTCCATCCAGTTGCCTTCTT |
| | | REV | CAGAATTGCCATTGCACAAC |
| *Psma3* | mouse | FW | TGAAGAAGGCTCCAATAAACGTCT |
| | | REV | AACGAGCATCTGCCAGCAA |
| *Psmb10* | mouse | FW | GAAGACCGGTTCCAGCCAA |
| | | REV | CACTCAGGATCCCTGCTGTGAT |
| *Psmb5* | mouse | FW | TGCTCGCTAACATGGTGTATCAGTA |
| | | REV | GGCCTCTCTTATCCCAGCCA |
| *Psmb6* | mouse | FW | AGACGCTGTCACTTACCAACTTGG |
| | | REV | AAGAGACTGGCGGCTGTGTG |
| *Psmb7* | mouse | FW | TGCCTTATGTCACCATGGGTTC |
| | | REV | TTCCTCCTCCATATCTGGCCTAA |

| | | | |
|---|---|---|---|
| *Psmb8* | mouse | FW | CGGGACAGATGTTTTCCACT |
| | | REV | CCAACCGTCTTCCTTCATGT |
| *Psmb9* | mouse | FW | GTACCGTGAGGACTTGTTAGCGC |
| | | REV | GGCTGTCGAATTAGCATCCCT |
| *Psmc3* | mouse | FW | AAGCTGAGCAAGATGGCATT |
| | | REV | TTCATGGGTGACTCGCAATA |
| *Psmd11* | mouse | FW | GAATGGGCCAAATCAGAGAA |
| | | REV | TGTACTTCCACCAAAAGGGC |
| *Psme4* | mouse | FW | CATCCTTCAAATAATGGGCG |
| | | REV | AAGCTTATGGCTTTCAGGCA |
| *Psmf1* | mouse | FW | ATGATCATCAACGTGCTGGA |
| | | REV | CCCACTGCTCATGGATAGGT |
| *Rpl19* | mouse | FW | CGGGAATCCAAGAAGATTGA |
| | | REV | TTCAGCTTGTGGATGTGCTC |
| *Tnc* | mouse | FW | GCTTCACTGGCAAAGACTGCAA |
| | | REV | CGTAAAGCCCTCATGGCAGATA |

### 4.4 Protein analysis

Cell and tissue lysis was carried out after resuspension of the cell pellets or tissue powder in OK lysis buffer (**Table 17**), containing 1X cOmplete™ protease inhibitor cocktail (Roche) on ice for 20 minutes. Centrifugation was performed at 15,000 RPM for 20 minutes at 4 °C and protein amount in the supernatant was quantified by use of the bicinchoninic acid (BCA) assay. A calibration curve was generated by the usage of bovine serum albumin (BSA) including a range from 0 to 2 µg/µl in PBS. 20 µl BSA standard, lysate containing 15 µg of protein diluted in 20 µl lysis buffer or pure lysis buffer, diluted 1:10 in PBS were mixed with 200 µl BCA reagent according to the manufacturer's protocol (Thermo Fisher Scientific). To determine protein abundance, a Sunrise™ plate reader (TECAN) was used, and absorbance was measured at 562 nm. One mm thick 15 % SDS polyacrylamide gels contained components, listed in **Table 18**.

**Table 17: OK lysis buffer components**

| component | Final concentration | Amount |
|---|---|---|
| Tris/HCl (pH 7.5, 100 mM | 50 mM | 5 ml |
| DTT (1 M) | 2 mM | 20 ml |
| MgCl2 (1 M) | 5 mM | 50 ml |
| Glycerol (87%) | 10% (v/v) | 1.15 ml |
| ATP | 2 mM | 12 mg |
| Digitonin (5%) | 0.05% (v/v) | 100 ml |
| ddH2O | n/a | Add up to 10 ml |

**Table 18: SDS Western Blot gel mix components**

| component | SDS resolving gel<br>15 % (ml/gel) | SDS stacking gel<br>3.6 % (ml/gel) |
|---|---|---|
| 4x Resolving buffer | 2.0 | --- |
| 4x Stacking buffer | --- | 1.0 |
| $H_2O$ | 2.0 | 2.52 |
| 30 % Acrylamide | 4.0 | 0.48 |
| TEMED | 0.012 | 0.012 |
| 10 % APS | 0.1 | 0.050 |

After adding TEMED to start the polymerisation of the SDS-resolving gel components, the mix was instantly filled into the glass chamber and an overlay of 5 ml of isopropanol was used to get a flat and smooth surface. After polymerisation, the overlay was aspirated, and the surface of the resolving gel was washed three times with water. After activating the stacking gel with TEMED, the mix was added on top of the already polymerised resolving gel and a Western Blot comb was carefully inserted to set up the pockets for the later analysed protein mixes.

Western blot gel pockets were equally loaded with 15 µg of protein diluted in equal volumes of MilliQ® water and 6x Laemmli sample buffer (**Table 19**) and samples were loaded onto 15 % SDS polyacrylamide gels made of 4x resolving buffer, 4x stacking buffer, $H_2O$, and 10 % APS. Gel electrophoresis was performed at 120 V for at least 120 minutes for proper band separation. For immunoblotting, proteins were

transferred on a methanol-activated polyvinylidene difluoride (PVDF) membrane (Bio-Rad) in an ice-cold transfer buffer (**Table 20**) at 250 mA for at least 90 minutes. After Western blot transfer, the membrane was initially blocked from unspecific antibody binding by the use of a Roti®-Block solution (Carl Roth) for at least one hour at room temperature while being pivoted by the shaker Duomax 1030 (Heidolph). After removing the blocking solution, PVDF membranes were incubated with primary antibodies (**Table 21**) diluted in RotiBlock overnight at 4 °C. Loading control by β-actin or GAPDH immunoblotting was performed by primary antibody incubation at room temperature for one hour. A secondary antibody (horseradish peroxidase-conjugated, diluted 1:20,000-40,000 in PBST), (**Table 22**) was added and incubated for one hour at room temperature after removal of the primary antibody after washing the PVDF membrane three times for ten minutes with PBS on the shaker Duomax 1030. After removal of the secondary antibody and washing of the membrane for 30 minutes, Luminata™ Classico reagent (Merck Millipore) – for less abundant proteins Luminata™ Forte – was administered to the membrane. Proteins were finally detected by exposure to X-ray films and developed with a film-developing machine (AGFA). Signal intensity was detected by use of the Chemidoc XRS+ system (Bio-Rad). Quantification of protein amounts was done by the Image Lab software (Bio-Rad).

**Table 19: Laemmli sample buffer composition**

| Component | Concentration |
|---|---|
| Tris | 300 mM |
| Glycerol | 50 % (v/v |
| SDS | 6 % (w/v) |
| Bromophenol blue | 0.01 % (w/v) |
| DTT | 600 mM |

**Table 20: Western Blot transfer buffer composition**

| Component | Concentration |
|---|---|
| Tris | 25 mM |

| | |
|---|---|
| Glycine | 192 mM |
| Methanol | 10 % (v/v) |

**Table 21: Primary antibodies for Western Blotting**

| Antigen | Provider | Dilution | Product number | Type |
|---|---|---|---|---|
| LMP2 | Abcam (Cambridge, UK) | 1:1,500 | ab3328 | polyclonal |
| β1 | Santa Cruz (Dallas, USA) | 1: 1,500 | sc-67345 | polyclonal |
| LMP7 | Abcam (Cambridge, UK) | 1:1,500 | ab3329 | polyclonal |
| β5 | Abcam Cambridge, UK) | 1:1,000 | ab90867 | polyclonal |
| β-actin (HRP-linked) | Sigma-Aldrich (St. Louis, USA) | 1:40,000 | b3854, clone ac-15 | monoclonal |

**Table 22: PBST buffer composition**

| Component | Concentration |
|---|---|
| NaCl | 137 mM |
| KCl | 2.7 mM |
| $Na_2HPO_4$ | 10 mM |
| $KH_2PO_4$ | 2 mM |
| Tween-20 | 1 % (v/v) |

## 4.5 Proteasome activity measurement

To quantify the number of proteasomes and immunoproteasomes in cells and tissue lysates and determine their activity, proteolytically active complexes were labelled with so-called activity-based probes (ABPs). The used ABPs are made of fluorescently labelled inhibitors for both, the immuno- and the constitutive subunits and allow specific discrimination of the enzymatic activities for both, the constitutive and the immune subunits of the proteasome counterpart-wise, namely β1/LMP2, β2/MECL-1, and β5/LMP7. This represents the pivotal feature of the activity-based probes, which is not provided in commercially available proteasome substrates first described by (Li, Kuo et al. 2013). MV151 binds all the active sites of both, the proteasome and the immunoproteasome, MVB127 binds to β5 of the constitutive proteasome and the LMP7 of the immunoproteasome, and LW124 binds to β1 and LMP2 (Li, Kuo et al. 2013).

The ABPs will from now on be termed MV, MWB, and LW in this study. 12 µg protein lysate was equally diluted with Milli-Q® water in a volume of 30 µl and further incubated with 0.5 µM MV151 or 1 µM MVB127 and 0.25 µM LW124 at 37 °C. After incubation at 37 °C at 600 RPM avoiding light exposure 6X Laemmli buffer was added for SDS-PAGE. Gels ran up to 120 minutes at 250 mA constantly. Active proteasomal and immunoproteasomal subunits were finally detected using a Typhoon TRIO+ fluorescence scanner (GE Healthcare) in the Cy3/TAMRA channel (MV151, MVB127) and Cy2 channel (LW124), respectively, at 450 PTM and a resolution of 50 microns. Staining for LW124 and MVB127 was performed on the same gel since the two probes were both administered together in one mastermix. The obtained signal was quantified using ImageLab software. After imaging, gels were stained with Page Blue staining solution (Thermo Fisher Scientific) to validate equal loading, as demonstrated in the following in one selected experiment, shown below in **Figure 7.**

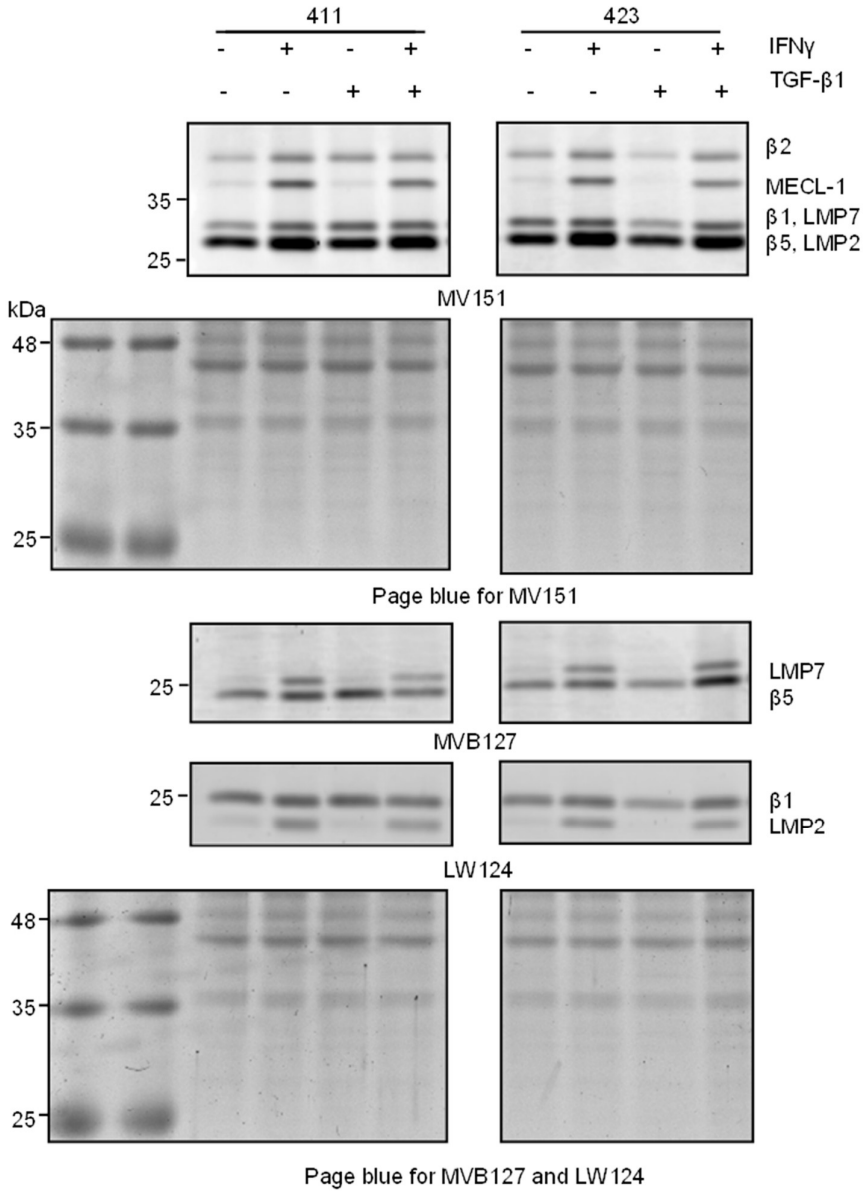


**Figure 7: Activity-based probes methodology**

Activity-based probes (ABP) assay of the same phLF. MV151 binds all the active sites of both, the proteasome and immunoproteasome, MVB127 binds to β5 of the constitutive proteasome and the LMP7 of the immunoproteasome, and LW124 binds to β1 and LMP2 (Verrecchia and Mauviel 2007, Li, Kuo et al. 2013). Primary human lung fibroblasts (phLF) of two donors (411 and 423, see **Table 8**). PhLF were either untreated, treated with either 75 U/ml IFNγ, 2 ng/ml TGF-β1 or both. ABP reveals lower immunoproteasomal activity in TGF-β1-treated phLF compared to control as well as in both, TGF-β1 and IFNγ-treated phLF compared to IFNγ-treated phLF. Constitutive subunits remain unaltered by treatment. Page blue staining confirms equal loading.

## 4.6 Histology

Left murine lungs were filled with 4 % PFA solution *via* an infusion system and PFA-submerged for 24 hours at 4 °C before preparing them for histological analysis using the tissue processor Microm STP 420D (Thermo Fisher Scientific). After paraffin embedding, tissue was cut into 3 µm thick sections using the Hyrax M55 microtome (Zeiss). Before starting the de-paraffinisation, tissue sections were initially incubated for one hour at 60 °C to melt excess paraffin. Next, two times incubation in xylene for five minutes each and rehydration was performed in an alcohol series, starting at 100 % in 10 % decreasing steps up to 70% (v/v) for one minute each. six minutes of incubation in Hemalaun (Carl Roth) was followed by 15 minutes rinse with tap water. Staining in 0.5 % Eosin G solution (Carl Roth) (with 1 % acetic acid) was done for ten minutes. Another time tissue sections were rinsed with tap water for five minutes and dehydration in 80 % (two times two minutes in 100 % ethanol) was performed. Before mounting slides with Entellan (Merck Millipore), tissue sections were incubated in xylene two times for five minutes. Tissues were finally imaged using the MIRAX scanning system (Zeiss).

## 4.7 Systemic sclerosis samples

The following table demonstrates the disease status, ID, age, sex, and ethnicity of all patient and control samples. Samples (**Table 23**) were kindly provided by Prof. Mauricio Rojas, UPMC, Pittsburgh, USA.

**Table 23: SSc and control samples**

| Lung | ID | Age | Sex | Ethnicity |
|---|---|---|---|---|
| Scleroderma | 2017-074-LT | 53 | M | Caucasian |
| Scleroderma | 2017-090-LT | 54 | M | Caucasian |
| Scleroderma | 2018-026-LT | 42 | M | African American |
| Scleroderma | 2017-012-LT | 67 | F | Caucasian |
| Scleroderma | 2018-012-LT | 64 | F | Caucasian |

| | | | | |
|---|---|---|---|---|
| Scleroderma | 2018-064-LT | 31 | F | Black American |
| Control | 2016-057-CORE | 50 | M | Caucasian |
| Control | 2016-174-CORE | 56 | M | Caucasian |
| Control | 2017-071-CORE | 41 | M | African American |
| Control | 2017-042-CORE | 69 | F | Caucasian |
| Control | 2017-005-CORE | 66 | F | Caucasian |
| Control | 2018-083-CORE | 32 | F | Caucasian |

No clinical patient data or treatment regimens were available.

# 5 Results

## 5.1 Proteasomal and immunoproteasomal subunit expression in lung homogenate of scleroderma patients and controls

Single-cell RNA sequencing data, provided by Misharin et al. on ipfcellatlas.com demonstrated immunoproteasomal subunits to be elevated in parenchymal cells of SSc-ILD patients when compared to healthy controls (Reyfman, Walter et al. 2019). The current study investigated mRNA expression levels of constitutive proteasomal and immunoproteasomal subunits in explanted lung homogenates derived from six SSc patients and six healthy donor lungs. Samples were kindly provided by Prof. Mauricio Rojas, UPMC, Pittsburgh, USA (**Table 23**).

With regard to the immunoproteasomal gene and regulatory particle expression, no significant differences between SSc tissue and healthy lung tissues were observed in our experiment. Likewise, no alterations in the gene expression levels of *IFNG* were detected (**Figure 8**).

Opposing hypothesis 1, these data suggest that there is no strong overall induction of the IP in systemic sclerotic lung tissue, but that upregulation of the IP might rather be cell-specific or a specific feature of IPF and experimental lung fibrosis. Immunohistological analysis would be required to investigate this further.

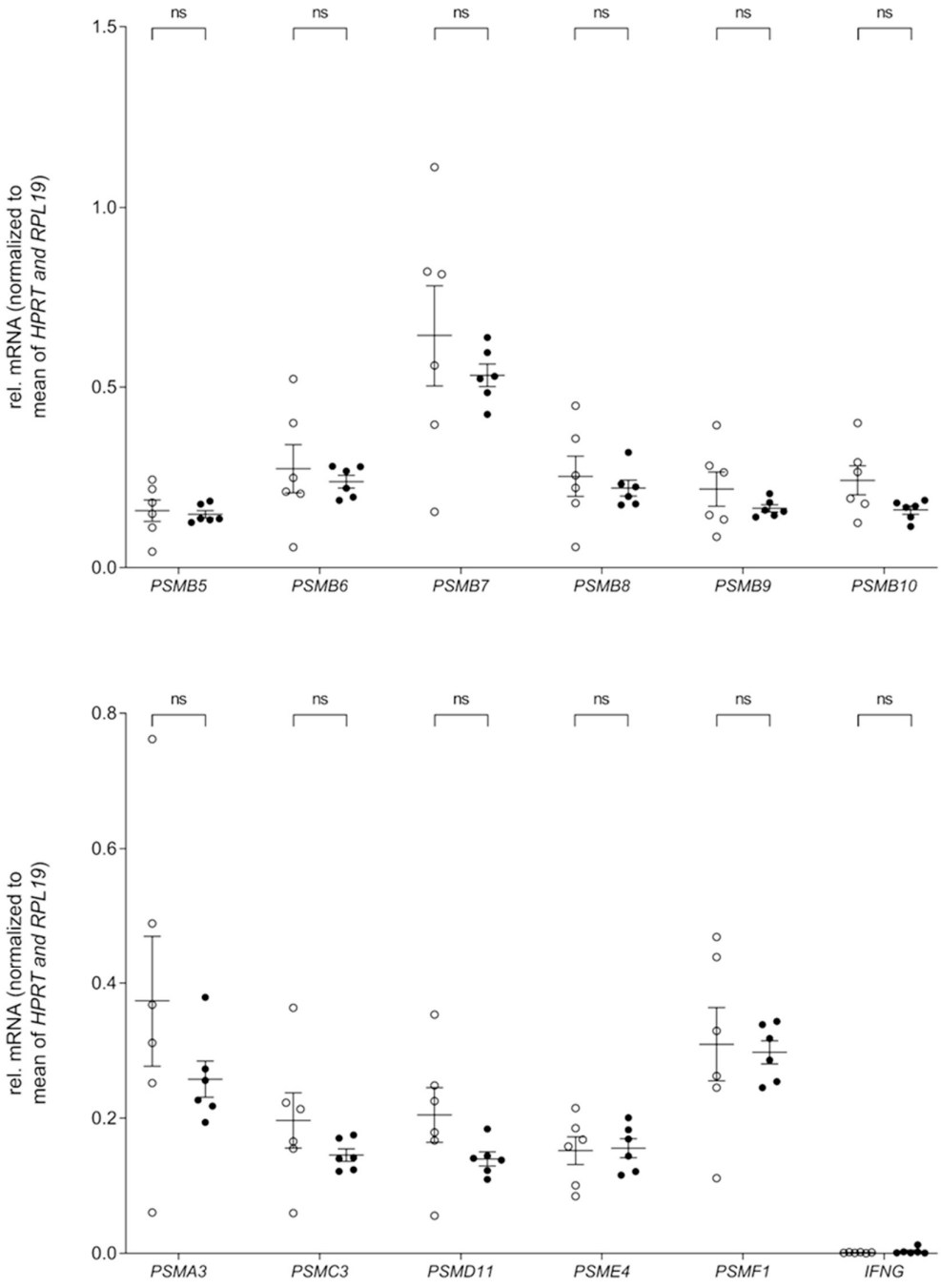


**Figure 8: RNA expression of proteasomal genes is similar in lung tissue of SSc patients and healthy donors**

Relative mRNA expression of proteasomal subunits in tissue homogenate of six healthy lung donors (○) and six Scleroderma (SSc) patients (●). Data points were normalised to the mean of hypoxanthine phosphoribosyltransferase (HPRT) and ribosomal protein L19 (RPL19). Proteasome 20S subunit beta 5-10 = PSMB5-10; proteasome 20S subunit alpha 3 = PSMA3; proteasome 26S subunit, ATPase 3 = PSMC3; proteasome 26S subunit, non-ATPase 11 = PSMD11; proteasome activator subunit 4 = PSME4; proteasome inhibitor subunit 1 = PSMF1; interferon gamma = IFNG. (Mann-Whitney test, n = 6 per group, ns = not significant).

## 5.2 Immunoproteasomal subunit expression in TGF β1-treated primary human lung fibroblasts

To investigate whether TGF-β1 as a main pro-fibrotic cytokine may be responsible for the alteration of immunoproteasomal subunits, healthy primary phLF from four different donors (**Table 8**: PhLF lines were treated with 2 ng/ml TGF-β1 or without (TGF-β1-buffer) in medium containing reduced FCS (1%) for 48 hours. The immunoproteasomal subunit expression was investigated on the mRNA level. The three immunoproteasomal active site-encoding genes *PSMB8*, *PSMB9*, and *PSMB10* were found to be significantly downregulated (**Figure 9A**) whereas *PSMA3,* a conserved alpha subunit of the 20S, was unaffected by the TGF-β1 treatment. Downregulation of LMP2 (significant) and LMP7 (non-significant) was also observed on the protein expression level. Immunoblotting for beta actin was performed to control for equal protein loading (**Figures 9B and C**). In conclusion, the immunoproteasome was downregulated by TGF-β1 treatment on both the mRNA and protein levels.

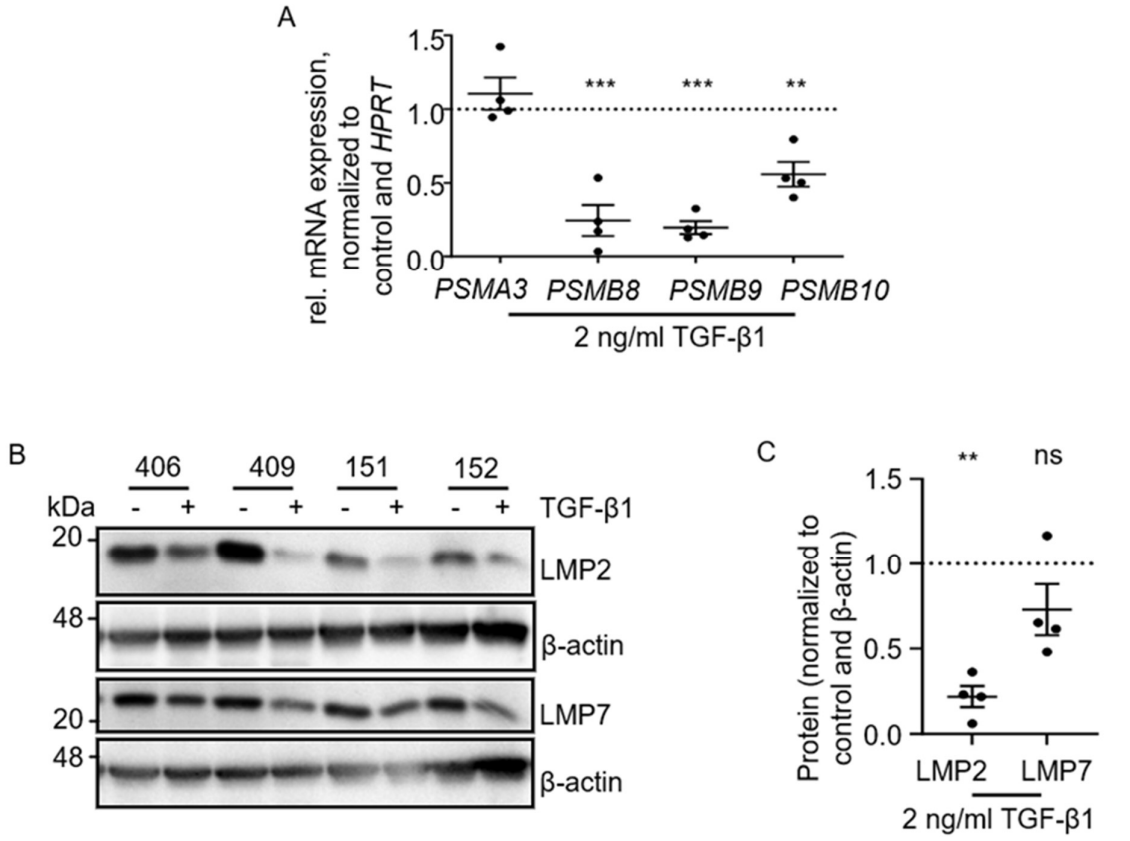


**Figure 9: TGF-β1 downregulates immunoproteasomal expression on mRNA and protein level in primary human lung fibroblasts**

A) mRNA expression of proteasomal (proteasome 20S subunit alpha 3 = *PSMA3*) and immunoproteasomal subunits (proteasome 20S subunit beta 8-10 = *PSMB8*, *PSMB9*, *PSMB10*) in primary human lung fibroblasts (phLFs) in four different donor samples (406, 409, 151, 152, **Table 8**) after transforming growth factor beta 1 (TGF-β1) treatment (2 ng/ml, 48 hours) and normalisation to untreated (TGF-β1-buffer) phLF and relative to hypoxanthine phosphoribosyl transferase (*HPRT*). B) Immunoblot of TGF-β1-treated phLF and staining for low molecular mass protein 2 and 7 (LMP2 and LMP7). β-actin served as a loading control. C) Immunoblot quantification. Data were normalised to untreated phLF and are relative to β-actin, as a loading control and. (One sample t test, ns = not significant, ** $p<0.01$, *** $p<0.001$, $n = 4$).

## 5.3 IFNγ-induced immunoproteasomal subunit expression in TGF-β1-treated primary human lung fibroblasts

To investigate whether TGF-β1 also downregulates IFNγ-inducible immunoproteasome expression, phLFs from two donors (411 and 423, see **Table 8**) were treated with 75 U/ml of IFNγ, 2 ng/ml of TGF-β1 for 48 hours, or both and compared to untreated controls.

Western blot analysis demonstrated that LMP2 and LMP7 expression was higher in IFNγ-treated donor cells. TGF-β1 treatment did not reduce IFNγ-induced LMP2 or LMP7 protein expression in a significant manner (**Figure 10**).

Analysis of immunoproteasome activities using the ABPs (**Chapter 4.5**), revealed a pronounced upregulation of all three activities, namely LMP2, MECL-1 and LMP7, by IFNγ. Likewise, TGF-β1 treatment did not reduce IFNγ-induced immunoproteasomal activity significantly (**Figure 11**, quantification **Figure 12**).

These data suggest that TGF-β1 downregulates basal immunoproteasome expression in lung fibroblasts (**Chapter 5.2**) but is unable to effectively counteract IFNγ-inducible protein induction and activation of the immunoproteasome.

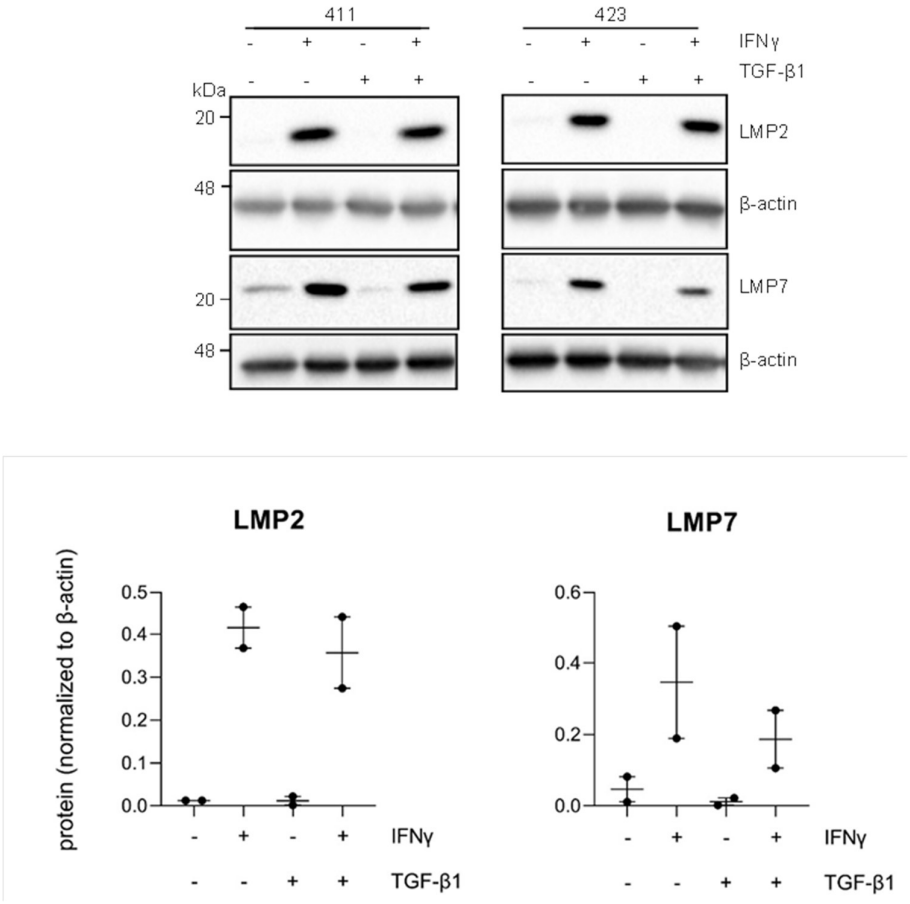


**Figure 10: Effect of TGF-β1 treatment on IFNγ-mediated immunoproteasome induction in primary human lung fibroblasts**

Primary human lung fibroblasts (phLF) of two donors (411 and 423, **Table 8**) were either untreated, treated with either 75 U/ml interferon gamma (IFNγ), 2 ng/ml transforming growth factor beta 1 (TGF-β1) or both. Immunoblotting and quantification of immunoproteasomal subunit LMP2 and LMP7 protein expression in two different primary human lung fibroblasts (phLF) donors (411 and 423, **Table 8**) on protein level. Low molecular mass protein 2 = LMP2; low molecular mass protein 7 = LMP7 (n = 2).

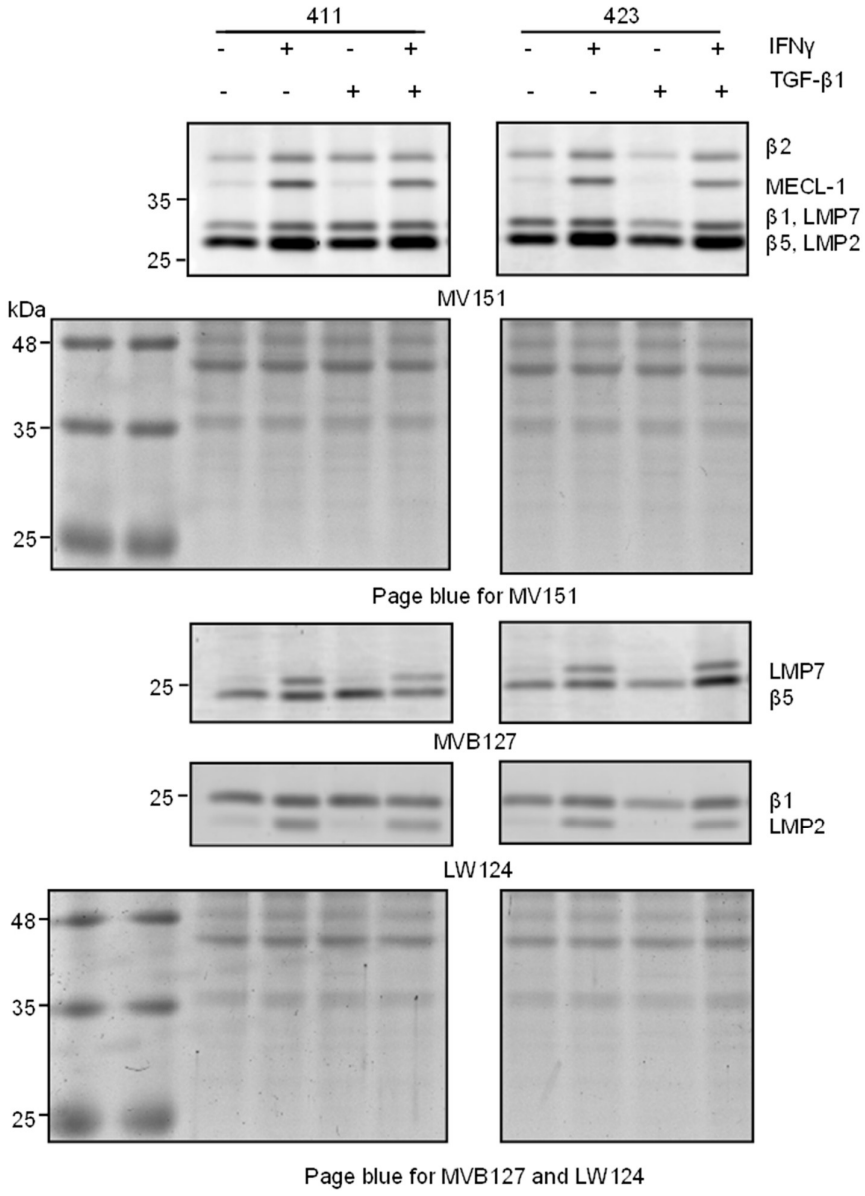


**Figure 11: Effect of TGF-β1 treatment on IFNγ-mediated immunoproteasome activity induction in primary human lung fibroblasts**

Primary human lung fibroblasts (phLF) of two donors (411 and 423, **Table 8**) were either untreated, treated with either 75 U/ml interferon gamma (IFNγ), 2 ng/ml transforming growth factor beta 1 (TGF-β1) or both. Activity-based probes (ABP) assay: Proteasome 20S subunit beta 1 = β1; proteasome 20S subunit beta 2 = β2; proteasome 20S subunit beta 5 = β5; low molecular mass protein 2 = LMP2; multicatalytic endopeptidase complex-like 1 = MECL-1; low molecular mass protein 7 = LMP7. MV151 binds all the active sites of both the proteasome and immunoproteasome, MVB127 binds to β5 of the constitutive proteasome and the LMP7 of the immunoproteasome, and LW124 binds to β1 and LMP2 (Verrecchia and Mauviel 2007, Li, Kuo et al. 2013). Page blue staining indicate equal loading conditions.

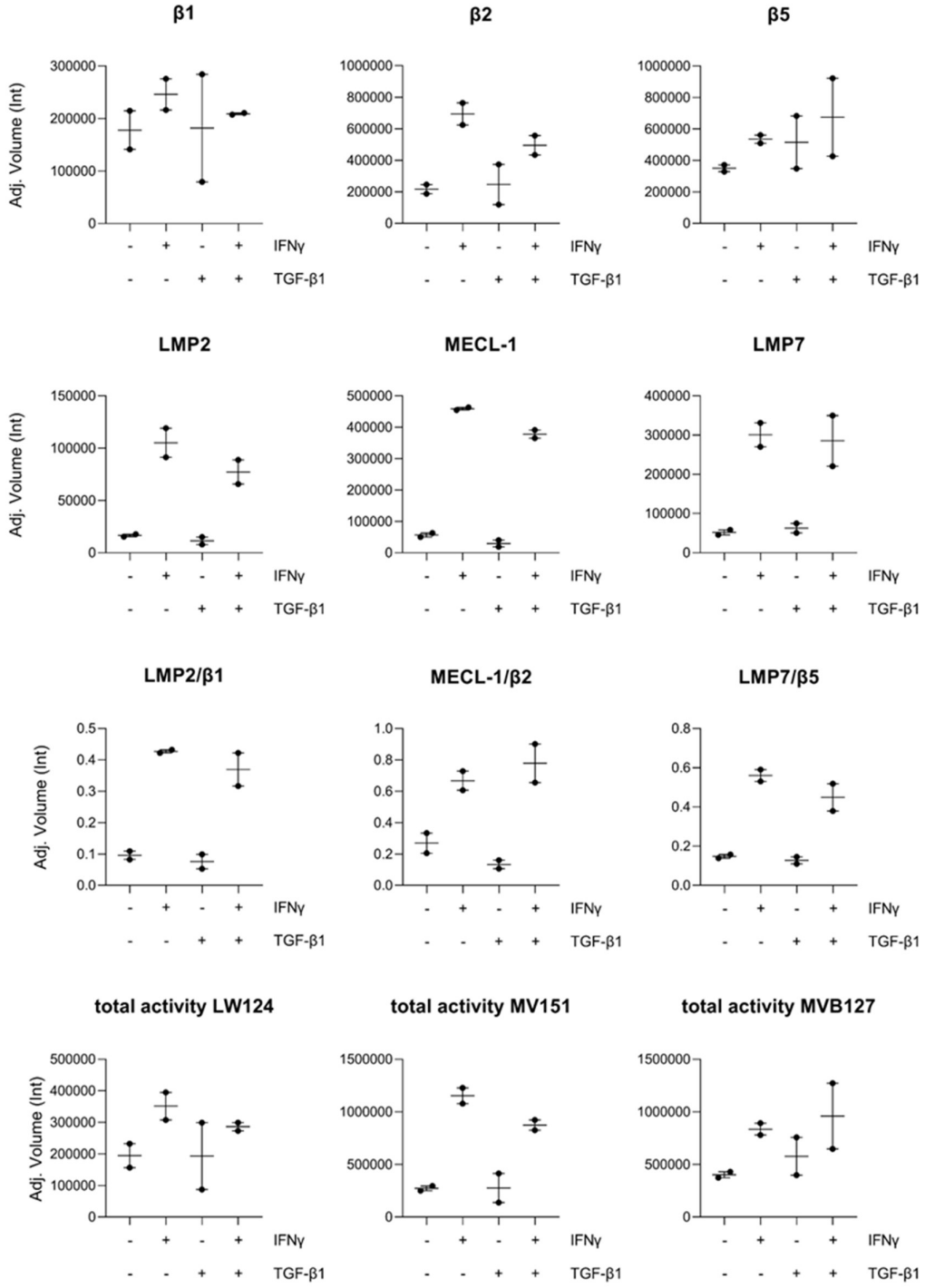


**Figure 12: Quantification of proteasomal and immunoproteasomal subunit activity in primary human lung fibroblasts of Figure 11**

Primary human lung fibroblasts (phLF) of two donors (411 and 423, **Table 8**) were either untreated, treated with either 75 U/ml interferon gamma (IFNγ), 2 ng/ml transforming growth factor beta 1 (TGF-β1) or both. Activity-based probes (ABP) assay quantification. Proteasome 20S subunit beta 1 = β1; proteasome 20S subunit beta 2 = β2; proteasome 20S subunit beta 5 = β5; low molecular mass protein 2 = LMP2; multicatalytic endopeptidase complex-like 1 = MECL-1; low molecular mass protein 7 = LMP7. LW124, MV152 and MVB127 refer to the activity-based probes, presented in **Chapter 4.5**. (n = 2).

## 5.4 TGF- β1-induced myodifferentiation in LMP2$^{-/-}$ primary murine lung fibroblasts

In the next step, it was investigated whether the presence of immunoproteasome subunit LMP2 affects TGF-β1-induced myodifferentiation of fibroblasts. For this, LMP2-deficient pmLFs isolated from nine LMP2$^{-/-}$ mice were treated with TGF-β1 (2 ng/ml, 48 hours) or left untreated and compared with the myodifferentiation potential of wildtype pmLFs isolated from nine wildtype mice. Myodifferentiation was determined by detecting mRNA levels of *Col1a1*, *Acta2*, *Fn1*, and *Tnc*. Significant TGF-β1-induced upregulation of *Col1a1* was observed in wildtype pmLF (**) but not in LMP2$^{-/-}$ pmLF. Downregulation of *Tnc* could be demonstrated in both, wildtype (**) and LMP2$^{-/-}$ (*) pmLF. *Acta2* and *Fn1* remained unaltered by the treatment. Baseline gene expression did not differ between wildtype and LMP2$^{-/-}$ pmLF (**Figure 13**).

This result indicates that wildtype mice and LMP2$^{-/-}$ mice do not significantly differ both, in either basal fibrosis-related marker gene expression or in their genotype-specific myodifferentiation response. As *Col1a1* and *Tnc* were upregulated in wildtype pmLF only but not in LMP2$^{-/-}$ pmLF, LMP2 deficiency might, however, interfere with pro-fibrotic TGF-β1signalling in phLF.

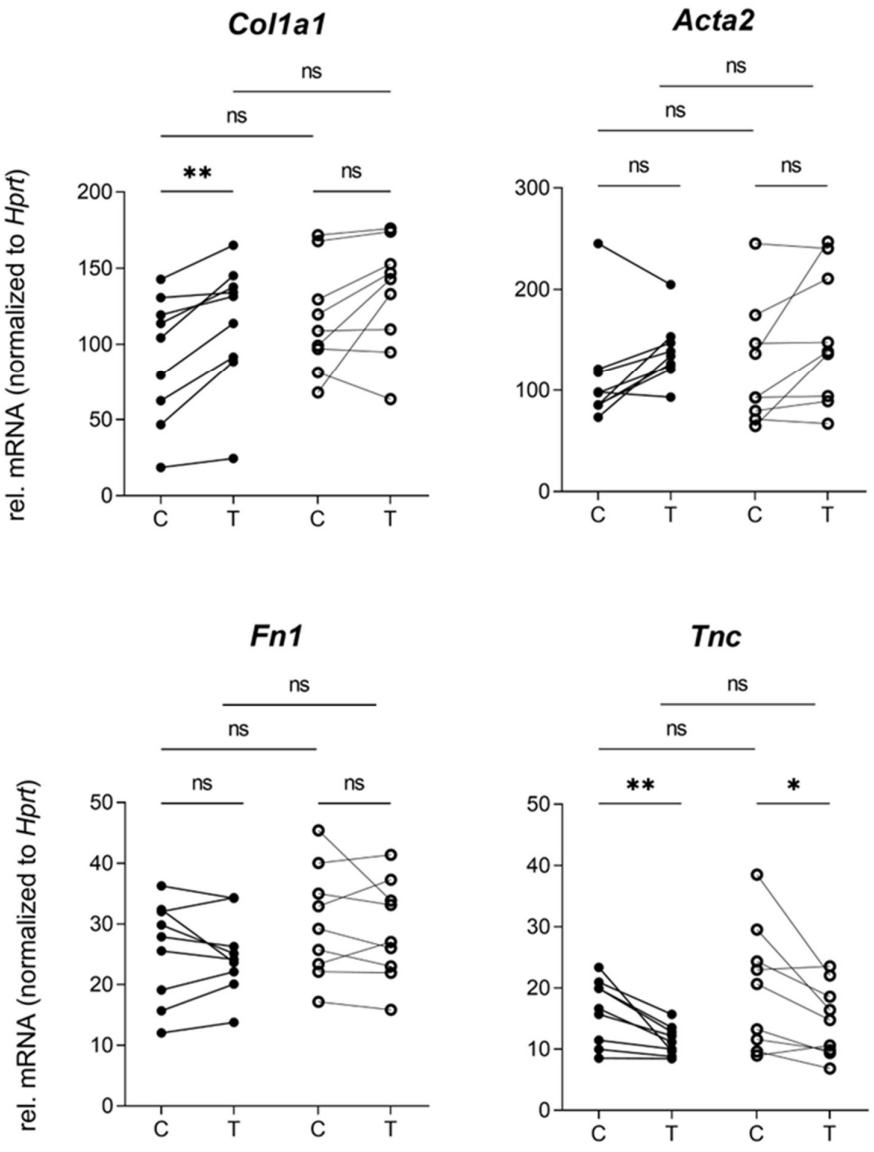


**Figure 13: Myodifferentiation marker gene expression in wildtype (●) and LMP2$^{-/-}$ (○) primary murine lung fibroblasts**

Wildtype and low molecular weight protein 2 (LMP2)$^{-/-}$ primary murine lung fibroblasts (pmLF) were treated with transforming growth factor beta 1 (TGF-β1) (2 ng/ml, 48 hours) (T) or without (TGF-β1 buffer) (C). Myodifferentiation marker gene expression of collagen (*Col1a1*), fibronectin (*Fn1)*, actin α2 (*Acta2*) and tenascin C (*Tnc*) was analysed. Genes of interest were normalised to *Hprt*. TGF-β1-treated vs. untreated mice (Wilcoxon test, ns = not significant, * $p<0.05$, ** $p<0.01$, n = 9 per group). Wildtype vs. knockout mice (Mann-Whitney-test, ns = not significant, n = 9 per group).

## 5.5 Fibrosis cocktail-induced myodifferentiation in LMP2$^{-/-}$ murine precision cut lung slices

Furthermore, the potential impact of immunoproteasome-single-subunit deficiency was investigated on mPCLS, a more representative model of the murine lung microenvironment when compared to 2D pmLF cultures on plastic. Therefore, mPCLS of ten wildtype and six LMP2$^{-/-}$ mice were subjected to pro-fibrotic conditions, using a fibrogenic cocktail: mPCLS were treated with fibrosis cocktail (FC), containing 5 ng/ml recombinant transforming growth factor beta (TGF-β), 5 µM platelet-derived growth factor-AB (PDGF-AB), 10 ng/ml tumour necrosis factor-α (TNFα) and 5 µM LPA, for 48 hours, while control cocktail (CC) contained solvents only (Alsafadi, Staab-Weijnitz et al. 2017). In most of the murine tissue sections, induction of *Col1a1* and *Fn1* was observed. FC-induced upregulation of *Col1a1* and *Fn1* was observed in wildtype mPCLS (**) but not in LMP2$^{-/-}$ mPCLS, which showed higher variability in their response. Baseline gene expression did not differ between wildtype and LMP2$^{-/-}$ mPCLS (**Figure 14**).

These data indicate that LMP2-deficient lung tissue shows a highly variable response to pro-fibrotic stimuli, which may indicate some protective effects compared to wildtype lung tissue.

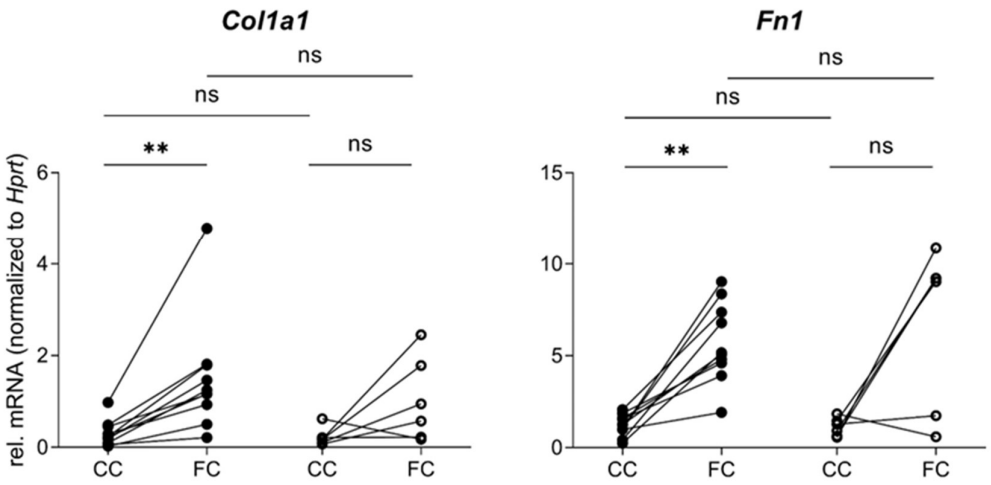


**Figure 14: Fibrosis-related marker gene expression in wildtype (●) and LMP2$^{-/-}$ (○) murine precision cut lung slices**

Wildtype- and low molecular weight protein 2 (LMP2)$^{-/-}$- murine precision cut lung slices (mPCLS) were treated with fibrosis cocktail (FC), containing 5 ng/ml transforming growth factor beta 1 (TGF-β1), 10 ng/ml platelet-derived growth factor-AB (PDGF-AB), 10 ng/ml tumour necrosis factor-α (TNFα) and 5 µM lysophosphatidic acid (LPA) for 48 hours) or not (solvents) and fibrosis-related marker gene expression of *collagen* (C*ol1a1*) and *fibronectin* (*Fn1*) was analysed. Genes of interest were normalised to *Hprt*. Treated vs. untreated mPCLS (Wilcoxon test, ns = not significant, ** $p<0.01$, n = 10 wildtype and 6 knockout). Wildtype vs. knockout mPCLS (Mann-Whitney-test, ns = not significant, n = 10 wildtype and 6 knockout).

## 5.6 Bleomycin-induced pulmonary fibrosis in LMP7$^{-/-}$ mice

We next aimed to gain insight into whether the ubiquitous deficiency of single immunoproteasome subunits in parenchymal as well as immune cells affects the development of bleomycin-induced lung fibrosis in vivo. Wildtype mice (n=10) and LMP7$^{-/-}$ mice (n=11) were intratracheally challenged with a single dose of bleomycin (2 U/kg, dissolved in 50 µl PBS). Weight and survival were monitored over 14 days until the mice were sacrificed, and lungs were harvested for pro-fibrotic marker gene analysis (time course in **Figure 15A**). A control group of four wildtype mice received PBS administration intratracheally. We abstained from treating LMP7-deficient mice with PBS as lab-own data from 2015 (Caniard, Ballweg et al. 2015) showed, that proteasomal and organismal function was comparable in LMP7$^{-/-}$ and wildtype mice. Wildtype mice were more severely affected by bleomycin-induced loss in body weight. Four out of ten wildtype mice (red squares) lost weight excessively and thereby fell below the critical threshold of -15 % change in body weight at day seven after bleomycin administration (**Figure 15B**). These four mice were excluded from observation and sacrificed by cervical dislocation. LMP7$^{-/-}$ mice were affected by body weight loss as well, but none critically. A significant survival benefit was shown for LMP7$^{-/-}$ mice at day 14 after bleomycin administration (**Figure 15B**) suggesting a potentially protective effect of LMP7 deficiency upon bleomycin challenge. On day 14, fibrosis-related marker gene expression of *Col1a1*, *Acta2*, *Fn1*, and *Tnc* was analysed in the lungs (**Figure 16**). *Col1a1* (*), *Acta2* (ns), *Fn1* (*), and *Tnc* (*) expression was altered by bleomycin when compared to control mice on day 14 after bleomycin administration. No significant alterations were observed in gene expression of bleomycin-treated LMP7$^{-/-}$ mice when compared to bleomycin-treated survivor wildtype mice, except a higher (**) expression of *Tnc*. In retrospect, one (green square) out of the ten wildtype mice was excluded from fibrosis-related marker gene evaluation and survival statistics, due to the presumption of insufficient intratracheal administration of bleomycin, which was suggested by both, the absence of body weight loss, and unaltered fibrosis-related marker gene expression. In total, five out of

ten wildtype mice were excluded from mRNA analysis and survival statistics due to either technical error or excessive body weight loss. Statistics were conducted using the five-day 14 survivor wildtype mice.

After the exclusion of the critically diseased wildtype mice on day seven after bleomycin administration, this experiment was not able to prove significant alterations in the fibrosis-related marker gene expression profiles in the lungs of survivor wildtype and LMP7$^{-/-}$ mice.

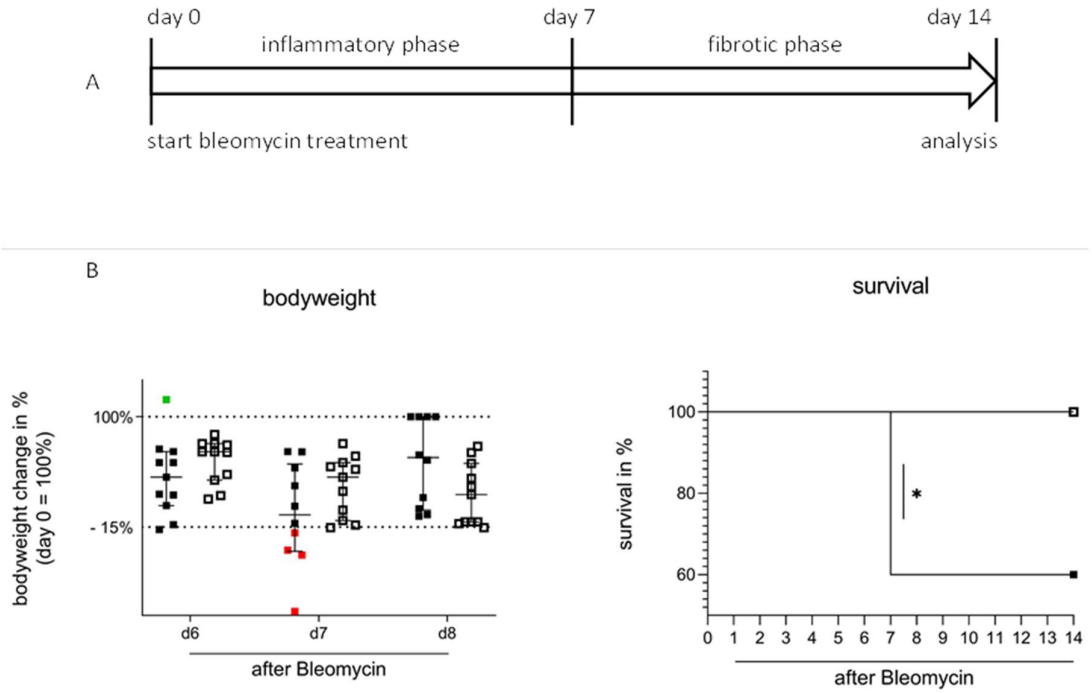


**Figure 15: Body weight course and survival of wildtype (■) and LMP7$^{-/-}$ (□) mice at day14 after intratracheal bleomycin challenge**

A) Timeline. Intratracheal administration of bleomycin (2 U/kg, dissolved in 50 µl PBS) or PBS in wildtype and LMP7$^{-/-}$ mice to induce experimental lung fibrosis. Day zero to seven: inflammatory phase, day seven to 14: fibrotic phase. B) Body weight change in %: four (red squares) out of ten wildtype mice fell below the lower threshold of -15 % change of body weight and were excluded at day seven, as 15 % body weight loss was one of the exclusion criteria. Green square = one wildtype mouse in which bleomycin administration presumably failed (excluded from fibrosis related marker gene evaluation and survival statistics). Kaplan-Mayer survival curve: Four out of ten wildtype mice were sacrificed on day seven due to excessive loss of body weight. At day 14 LMP7$^{-/-}$ showed a significant survival benefit compared to wildtype mice (red square), both after undergoing bleomycin-challenge (Log-Rank (Mantel-Cox) test and Gehan-Breslow-Wilcoxon test, * $p<0.05$).

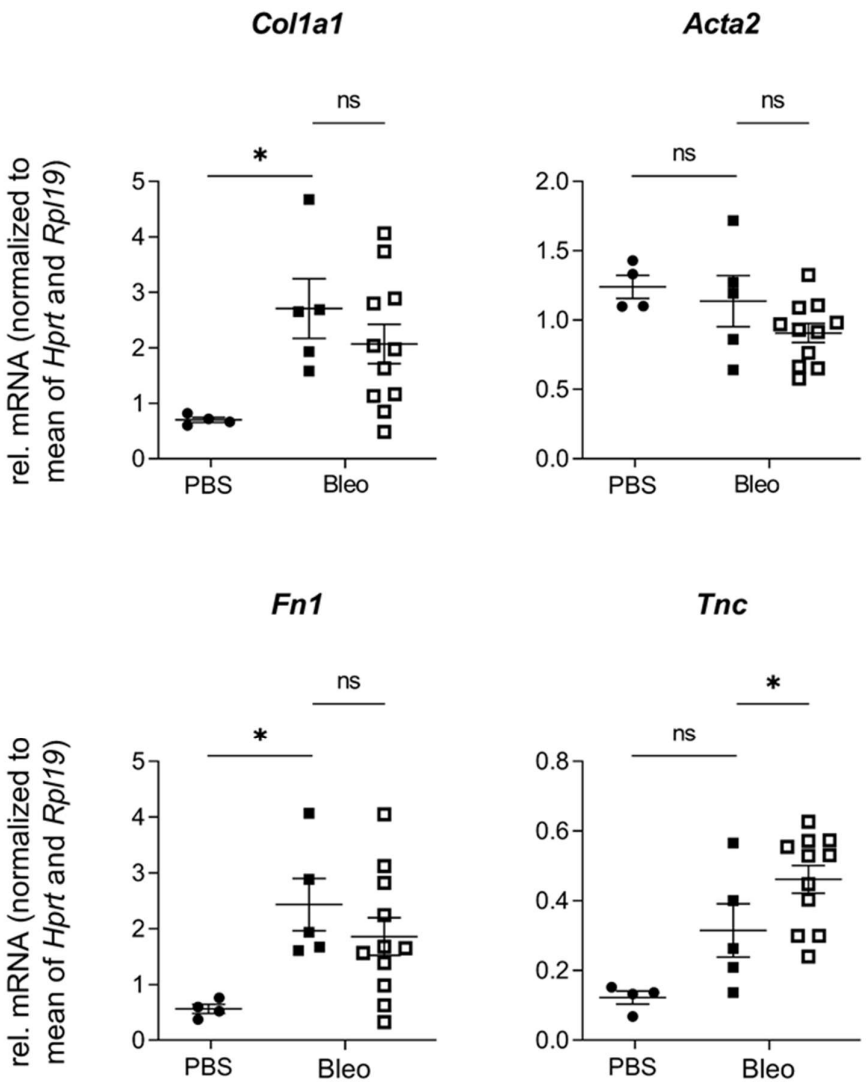


**Figure 16: Fibrosis-related marker gene expression of wildtype (■) and LMP7$^{-/-}$ (□) mice at day 14 after intratracheal bleomycin challenge, compared to PBS-treated (●)**

Fibrosis-related marker genes collagen (*Col1a1*), actin α2 (*Acta2*), fibronectin (*Fn1)*, and tenascin C (*Tnc*) were analysed. Genes of interest were normalised to mean of *Hprt* and *Rpl19*. (Kruskal Wallis test with Dunn´s Multiple Comparisons test, ns = not significant, * $p<0.05$, n = 4 per PBS group, initial n = 11 per bleomycin group).

## 5.7 Immunoproteasome inhibitor validation and dose-finding for *ex vivo* and *in vitro* experiments

Following the single-subunit-knockout experiments which suggested a potential protective effect of LMP2 and LMP7 deficiency upon *in vitro*, *ex vivo* and *in vivo* fibrotic stimulation, it was tested whether the inhibition of the entire immunoproteasome would impact response to pro-fibrotic challenges. For that, we used the pan-reactive immunoproteasome inhibitor LU-005i (de Bruin, Huber et al. 2014). First, the optimal dose for inhibition of the immunoproteasome *in vitro* was determined using the immortalised lung fibroblast cell line CCL-206 (American Type Culture Collection, Manassas, USA). Cells were treated with 75 U/ml IFNγ for 48 hours after seeding to induce immunoproteasomal subunits LMP2 and LMP7. Different doses of LU-005i were administered 24 hours after seeding to find a specific and efficient inhibitory concentration. Effective inhibition of the immunoproteasome was determined by molecular weight changes in Western blot analyses upon covalent binding of the low molecular weight inhibitor to the respective catalytic subunits. The specificity of inhibition was analysed by blotting for the corresponding constitutive proteasome subunits. 0.2 µM of LU-005i inhibited the immunoproteasome effectively and specifically, which is indicated by double-bands (LMP2+ LU-005i and LMP7+LU-005i), whereas β1 and β5 did not bind the inhibitor at that dose and thus remained unaffected by inhibitor treatment (**Figure 17**). For *ex vivo* immunoproteasome inhibition, 0.5 µM was taken as a sufficient and specific dose (data not shown).

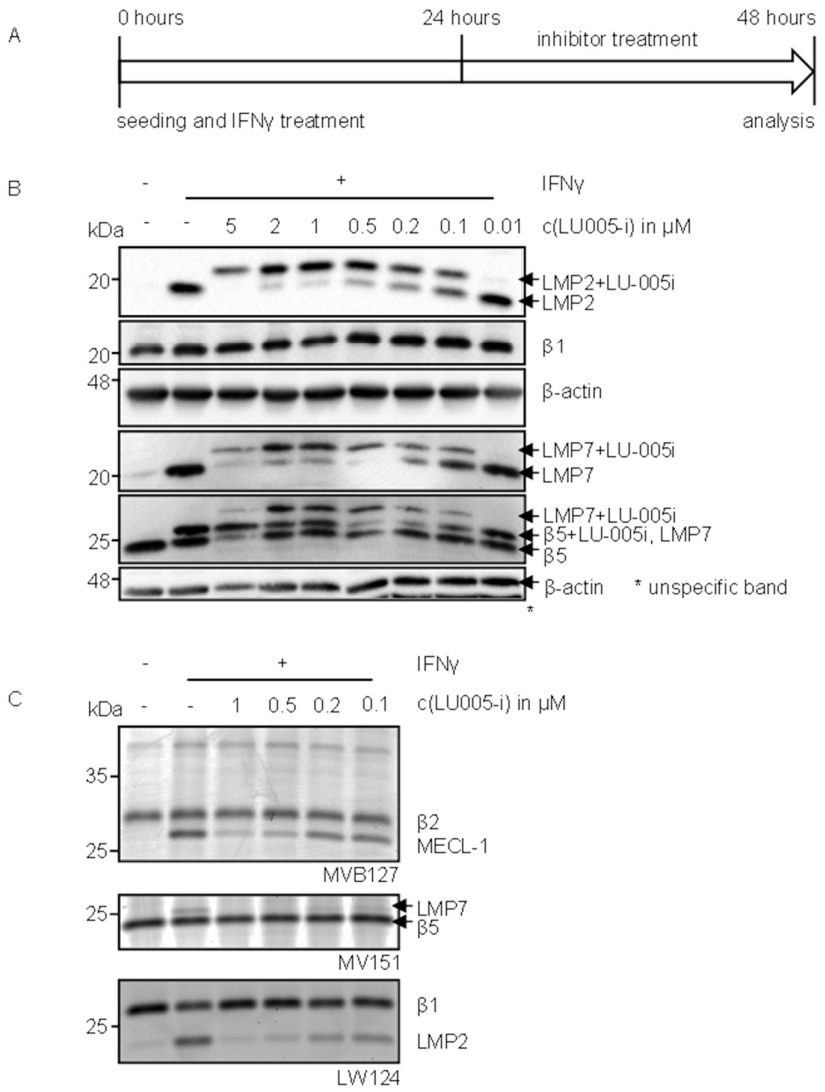


**Figure 17: Inhibitor dose finding in CCL-206 line**

A) Timeline. Fibroblasts were seeded and treated for 48 hours with IFNγ to induce immunoproteasome. Different concentrations of LU-005i (5 µM, 2 µM, 1 µM, 0.5 µM, 0.2 µM, 0.1 µM and 0.01 µM) were administered or not 24 hours after seeding and the start of IFNγ treatment. Harvesting after 24 more hours. B) Immunoblot. Double bands indicate covalent binding of inhibitor and thereby increase of detected protein weight (LMP2+ LU-005i and LMP7+LU-005i), whereas β1 and β5 remained unaffected. LU-005i at a concentration of 0.2 µM was taken to be specific and sufficient for immunoproteasome inhibition. C) Activity based probes (ABP) assay showed 0.2 µM LU-005i to sufficiently inhibit the immunoproteasome.

## 5.8 TGF- β1-induced myodifferentiation in primary human lung fibroblasts upon pan-reactive immunoproteasome inhibition

Subsequently, investigations on whether immunoproteasome inhibition leads to altered myofibroblast differentiation in primary human lung fibroblasts (phLFs) after TGF-β1-treatment were undertaken. Therefore, phLFs from four donors were treated with TGF-β1 (2 ng/ml, 48 hours) or without (TGF-β1 buffer) after pre-incubation with LU-005i (0.2 µM, three hours) or not (timeline **Figure 18A**). TGF-β1 induced myodifferentiation marker genes *COL1A1* (**), *ACTA2* (*), and *FN1* (***) in non-inhibited phLF and induced *COL1A1* (*), *ACTA2* (*) and *FN1* (*) in LU-005i-treated phLF. LU-005i pre-treatment did not alter phLF myodifferentiation marker gene expression. (**Figure 18B**).

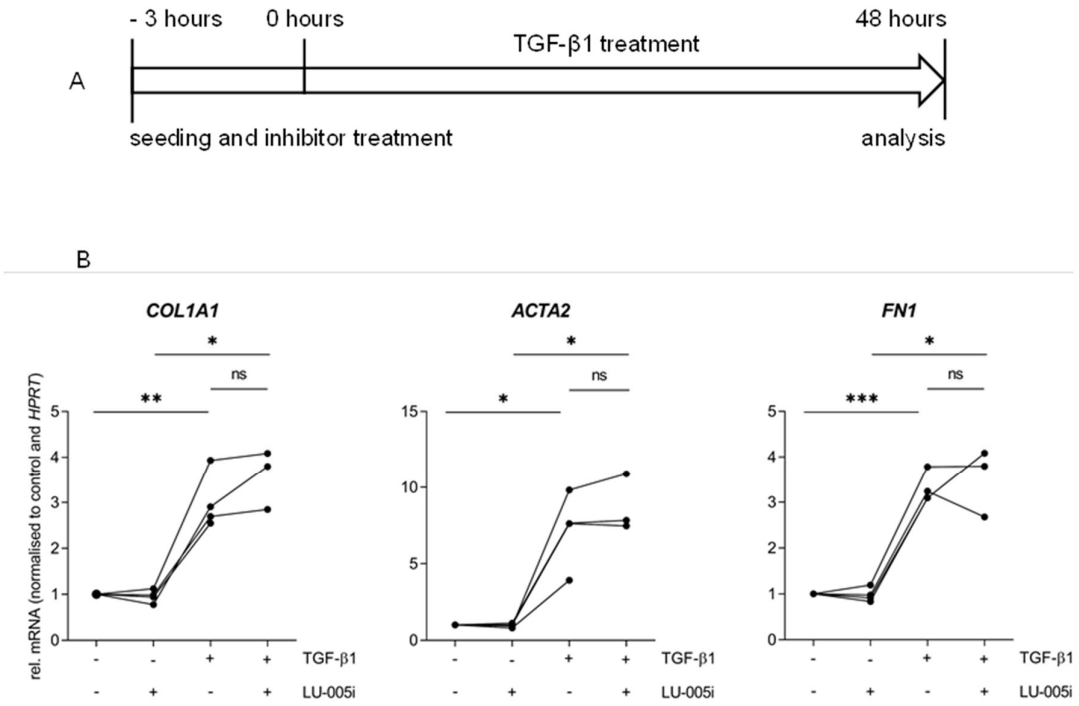


**Figure 18: Fibrosis-related marker gene expression in phLF upon immunoproteasome inhibition**

A) Timeline. Primary human lung fibroblasts (phLFs) of four donors were pre-incubated with LU-005i (0.2 µM) or not (DMSO) three hours prior to transforming growth factor beta 1 (TGF-β1) (2 ng/ml, 48 hours) or without (TGF-β1 buffer) to induce myodifferentiation. B) Gene expression of collagen (*COL1A1*), actin α2 (*ACTA2*) and fibronectin (*FN1*) was analysed. Genes of interest were normalised to *HPRT* (Paired t-test and Wilcoxon-test (due to lacking one data-point in LU-005i- and TGF-β1-treated group), ns = not significant, * $p<0.05$, ** $p<0.01$, *** $p<0.001$, n = 4).

## 5.9 Fibrosis cocktail-induced gene expression in murine precision-cut lung slices upon pan-reactive immunoproteasome inhibition

We also tested the pan-immunoproteasome inhibition in mPCLS of wildtype mice. FC was administered on immunoproteasome-inhibited (0.5 µM LU-005i, three hours prior) mPCLS (**Figure 19A**) for 48 hours as described by (Alsafadi, Staab-Weijnitz et al. 2017). In non-inhibited mPCLS, FC induced fibrosis-related marker gene expression of *Fn1* (**) and tenascin *C* (*Tnc*) (*), whereas in LU-treated mPCLS the FC induced protein expression of *Col1a1* (**), *Acta2* (***), (*Fn1*) (**) and tenascin *C* (*Tnc*) (***). We conclude that pan-reactive immunoproteasome inhibition was not able to alter fibrosis-related marker gene expression in FC-treated mPCLS (**Figure 19B**).

These data suggest that the activity of the immunoproteasome does not regulate myodifferentiation of lung cells in response to pro-fibrotic stimuli.

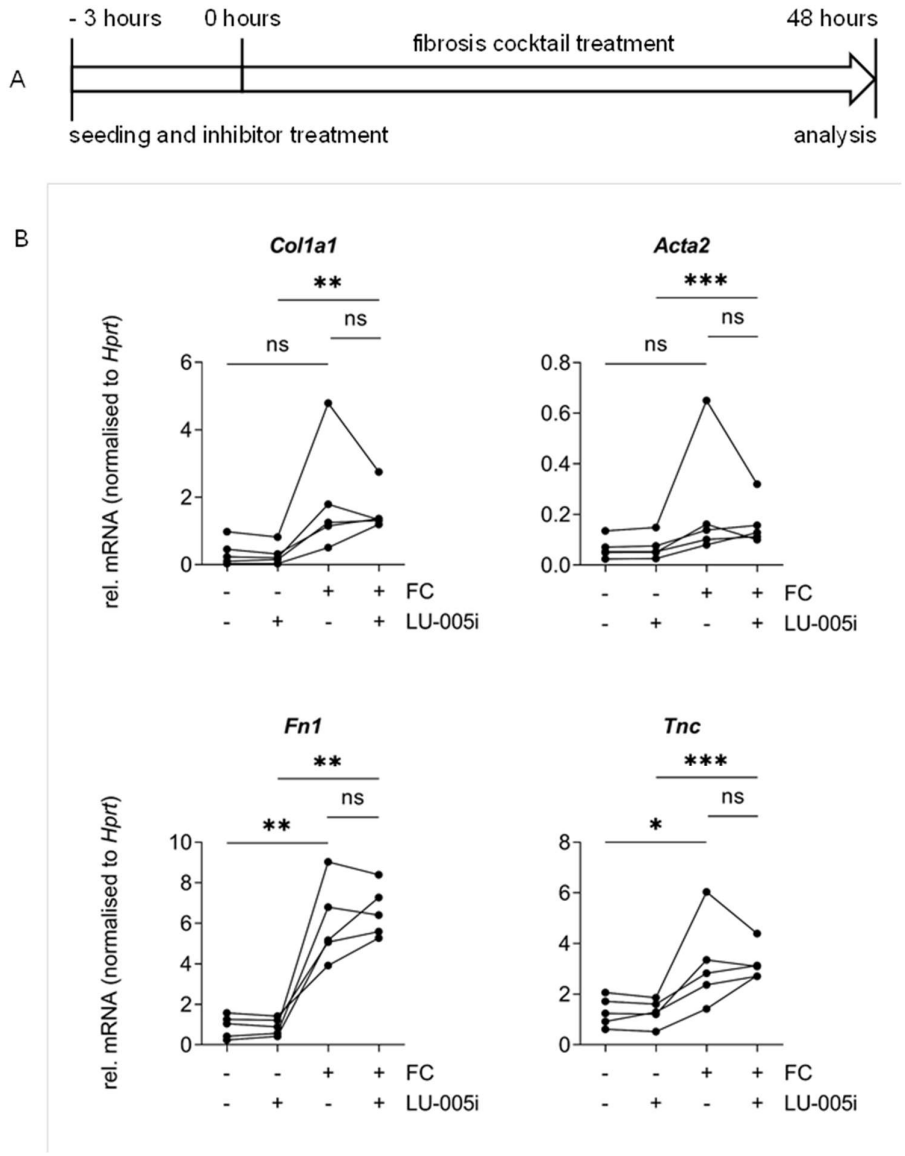


**Figure 19: Fibrosis-related marker gene expression in murine precision cut lung slices upon pan-reactive immunoproteasome inhibition**

A) Timeline. Wildtype murine precision cut lung slices (mPCLS) were pre-incubated with 0.5 µM LU-005i or solvent (DMSO) three hours before 48 hours treatment with fibrosis cocktail (FC), containing 5 ng/ml transforming growth factor beta 1 (TGF-β1), 10 ng/ml platelet-derived growth factor-AB (PDGF-AB), 10 ng/ml tumour necrosis factor-α (TNFα) and 5 µM lysophosphatidic acid (LPA) for 48 hours) or not (solvents). B) Fibrosis-related marker gene expression of collagen (*Col1a1*), fibronectin (*Fn1*), actin α2 (*Acta2*) and tenascin C (*Tnc*) was analysed. Genes of interest were normalised to *Hprt*. (Paired t-test, ns = not significant, * $p<0.05$, ** $p<0.01$, n = 5).

## 5.10 Immunoproteasome inhibitor dose finding for *in vivo* experiments

In preliminary experiments prior to this thesis, an immunoproteasome inhibitor dose-finding experiment was performed *in vivo* using LU-005i. Different concentrations of LU-005i (1, 5, and 10 mg/kg body weight) were dissolved in Captisol®, administered intratracheally and mice were sacrificed after two hours. The control group received only the solvent. BAL cells and PBMCs were collected, and lung and spleen tissues were prepared to determine the local and systemic effect of immunoproteasome application. Inhibition was analysed via Western blot analysis as outlined above (**Chapter 5.7**). Band shift indicated covalent binding of inhibitor and thereby an increase of detected protein weight (LMP7+LU-005i), whereas β5 remained unaltered. Western blots indicated sufficient immunoproteasome inhibition at 5 mg/kg, as most of LMP7 was shifted. At 10 mg/kg, LU-005i lost its specificity as it also bound to β5 (β5+LU-005i) (**Figure 20**).

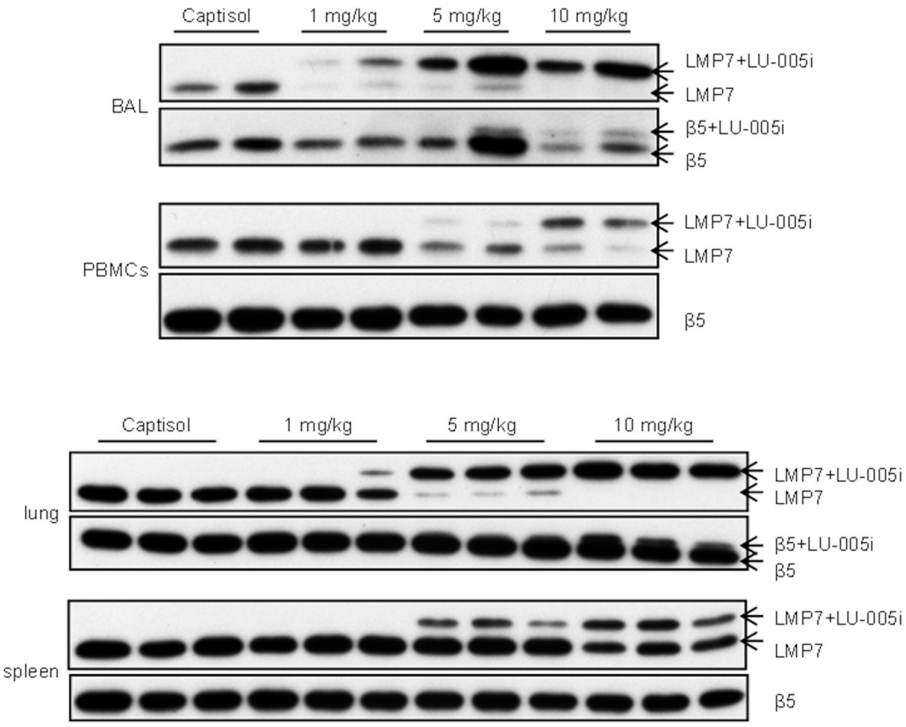


**Figure 20: Inhibitor dose finding *in vivo***

Three different concentrations (1 mg/kg, 5 mg/kg, or 10 mg/kg body weight) of the immunoproteasome inhibitor LU-005i were administered intratracheally into mice and BAL, PBMC, lung and spleen samples were collected after two hours. Double bands indicate covalent binding of inhibitor and thereby increase of detected protein weight (LMP7+LU-005i). LU-005i at a concentration of 5 mg/kg was taken to be sufficient for effective immunoproteasome inhibition. Western Blot staining shows specificity of LU-005i for immunoproteasome inhibition as β5 does not show any inhibitor binding at even high concentrations.

## 5.11 Bleomycin-induced acute lung injury in mice treated with pan-reactive immunoproteasome inhibitor

To investigate the potential impact of the immunoproteasome inhibitor at the inflammatory phase prior to the fibrotic phase in the bleomycin model, an *in vivo* experiment using 5 mg/kg of the pan-reactive immunoproteasome inhibitor LU-005i was performed in wildtype mice with or without bleomycin challenge for seven days. Body weight was determined at days three and seven (**Figure 21**), BAL cell composition was analysed (**Figure 22**) as well as expression of several inflammatory marker genes in whole lung tissues upon sacrificing the animals at day seven (**Figures 23, 24 and 25**).

In this experiment, one bleomycin- and captisol-treated mouse (red square, **Figure 21**) fell below the critical threshold and lost more than 15% of body weight on day three. This mouse was euthanised instantly and was thereby not included in statistics. One bleomycin- and captisol-treated mouse (blue square, **Figure 21**) fell below the critical body weight loss of over 15 % at day seven, was euthanised instantly and lung samples were prepared for day seven inflammatory marker gene evaluation. The application of LU-005i in PBS-treated mice slightly but not significantly reduced body weight on day three but not on day seven (**Figure 21**). A single intratracheal dose of bleomycin significantly reduced the body weight of treated mice at day seven. Mice co-treated with LU-005i varied in their response by either losing or gaining body weight, so there was no overall significant loss in body weight in co-treated animals. Although this was not significant in this experiment, this might suggest a protective effect of LU-005i.

BAL cell counting at day seven indicated that the numbers of lymphocytes and neutrophils were significantly induced in bleomycin- compared to PBS-treated mice, while macrophage numbers were significantly reduced. Pan-reactive immunoproteasome inhibition in bleomycin-treated mice did not significantly alter BAL cell composition at day seven compared to bleomycin-only mice but the influx of inflammatory cells tended to be lower as indicated by the loss of significance when comparing LU-005i-treated PBS with respective bleomycin-treated mice (**Figure 22**).

These data suggest that inhibition of the immunoproteasome slightly dampened the acute bleomycin-induced inflammatory response in some animals.

Several inflammatory genes were analysed in whole lung tissue by RT-qPCR on day seven (**Figures 23, 24 and 25**). The investigated genes can be grouped into three groups, namely a pro-fibrotic signalling cluster (**Figure 23**), represented by interleukin *Il17a*, *Il23a*, forkhead box P3 (*Foxp3*), chemokine (C-C motif) ligand 17 (*Ccl17*), *Il6*, chemokine (C-X-C motif) ligand 15 (*Cxcl15*) and interleukin 10 (*Il10*), a pro-inflammatory cluster (**Figure 24**), represented by *Ifng* and *Tnf* and a macrophage-related cluster (**Figure 25**), represented by arginase (*Arg1*) and mannose receptor, C type 1 (*Mrc1*), as described more in detail in the discussion. Some genes have mixed functions (**Chapter 6.5**).

At day seven, bleomycin neither altered the pro-fibrotic nor the pro-inflammatory cytokine expression profile in captisol-treated mice. Only expression of the macrophage M2 polarisation marker *Arg1* (*) was altered by bleomycin challenge in captisol-treated mice. LU-005i did not impact cytokine expression levels in PBS-treated mice. LU-005i was able to increase *Cxcl15* expression level (**) in bleomycin-treated mice. LU-005i and bleomycin co-treatment, however, increased lung-specific expression of *Il17a*, *Il23a* (**), *Arg1*, *Il6*, *Tnf* and *Foxp3* (*).

Summarised, this experiment is in line with the previously performed LMP7 knockout experiment (**Chapter 5.6**), which suggested a survival benefit of LMP7$^{-/-}$ mice compared to wildtype mice seven days after bleomycin administration. The LU-005i-treated mice tended towards a lower body weight loss seven days after bleomycin administration, which might correlate with less disease severity. So far, only *Cxcl15* gene expression was significantly higher in LU-005i-treated bleomycin mice, contradictory to the body weight data, as *Cxcl15* is supposed to correlate with a higher extent of pulmonary fibrosis.

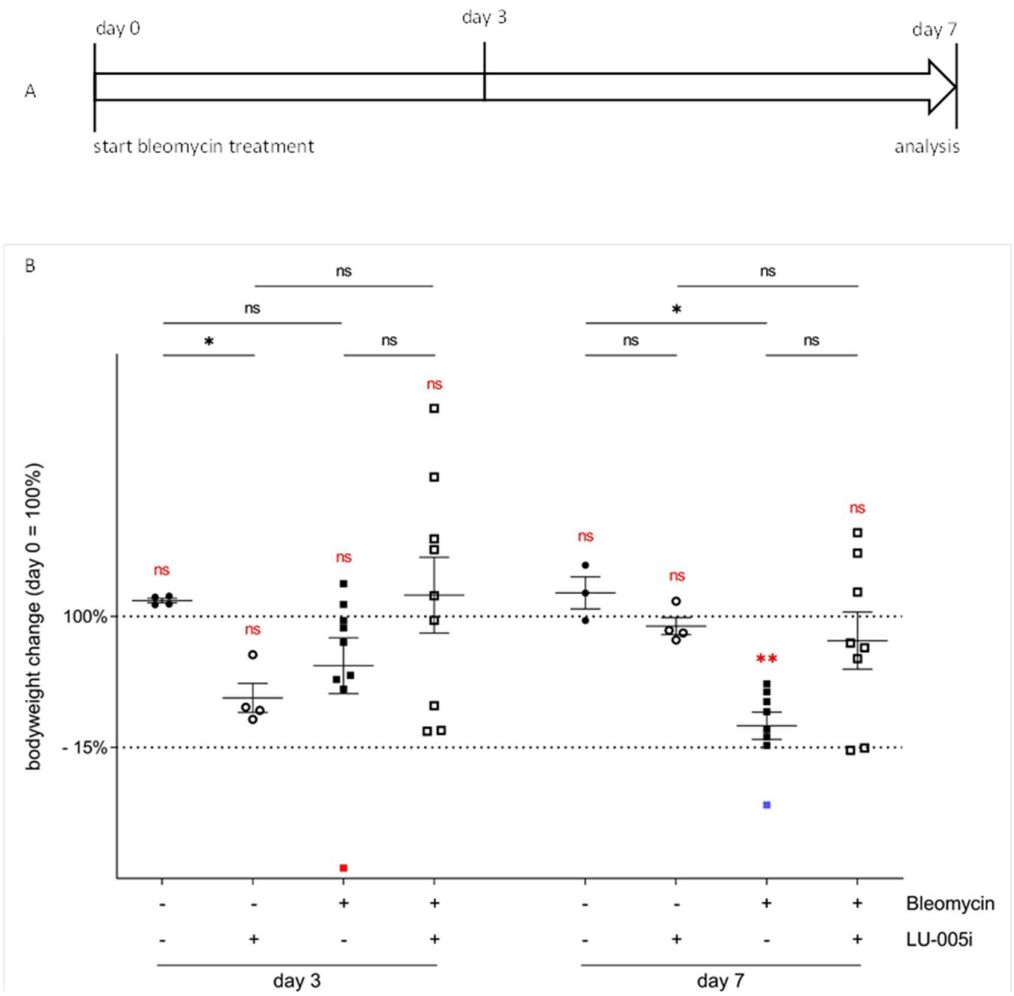


**Figure 21: Body weight of mice at day three and day seven after intratracheal bleomycin challenge and pan-reactive immunoproteasome inhibition**

A) Timeline. Intratracheal administration of (2 U/kg, dissolved in 50 µl PBS) or not (PBS) to wildtype mice to induce experimental lung injury. Administration of LU-005i (5mg/kg) or not (captisol). Mice were weighed at day three and day seven (sacrifice). B) Body weight change of mice at day three and day seven. Day zero was set as 100%. At day three, no significant alterations in body weight were induced by neither bleomycin, nor LU-005i, when compared to initial weight (Wilcoxon test, ns = not significant, n = 4 per PBS group, n = 8 per bleomycin group). Day three body weight loss of bleomycin-treated mice was not significantly higher when compared to PBS-treated mice (p = 0.0506) (Mann-Whitney test, ns = not significant, n = 4 per PBS group, n = 8 per bleomycin group). LU-005i-treated mice significantly (*) lost weight in comparison to captisol-treated mice (Mann-Whitney test, * = $p < 0.05$, n = 4 per PBS group). One bleomycin- and captisol-treated mouse (red square fell below the critical body weight loss over 15 % at day three and was euthanised instantly and thereby was not subjected to day seven inflammatory marker gene evaluation. At day seven, bleomycin-treated mice showed significant (red **) body weight loss, when compared to initial weight (Wilcoxon test, ** $p < 0.01$, n = 4 per PBS group, n = 8 per bleomycin group) and lost significantly more weight than PBS-treated mice (*) (Mann-Whitney test, ns = not significant, * $p < 0.05$, n = 4 per PBS group, n = 8 per bleomycin group). One bleomycin- and captisol-treated mouse (blue square) fell below the critical body weight loss over 15 % at day seven and was euthanised instantly but subjected to day seven inflammatory marker gene evaluation. One bleomycin- and LU-005i-treated mouse erroneously was not weighed at day seven and thereby not subjected to body weight statistics.

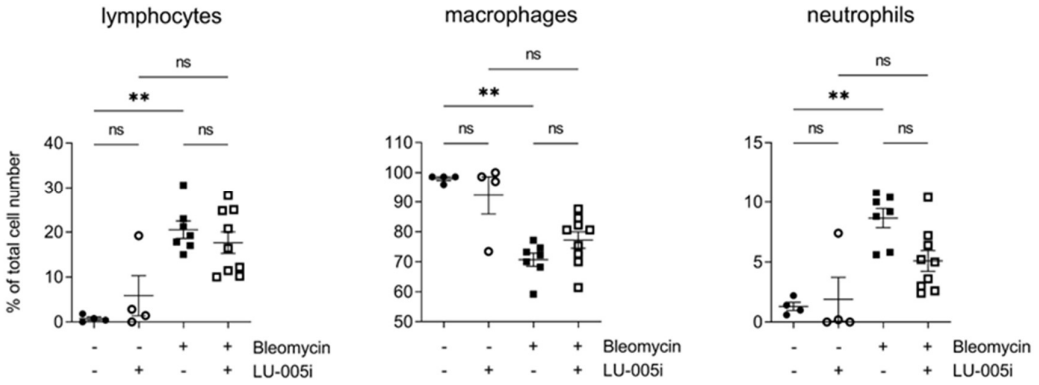


**Figure 22: BAL of mice at day seven after intratracheal bleomycin challenge and pan-reactive immunoproteasome inhibition**

Wildtype mice were treated with bleomycin (2 U/kg, dissolved in 50 µl PBS) or not (PBS) and LU-005i (5 mg/kg) or not (captisol) and BALs were acquired at day seven. (Kruskal Wallis test with Dunn´s Multiple Comparisons test, ns = not significant, * $p<0.05$, n = 4 per PBS group, n = 8 per bleomycin group).

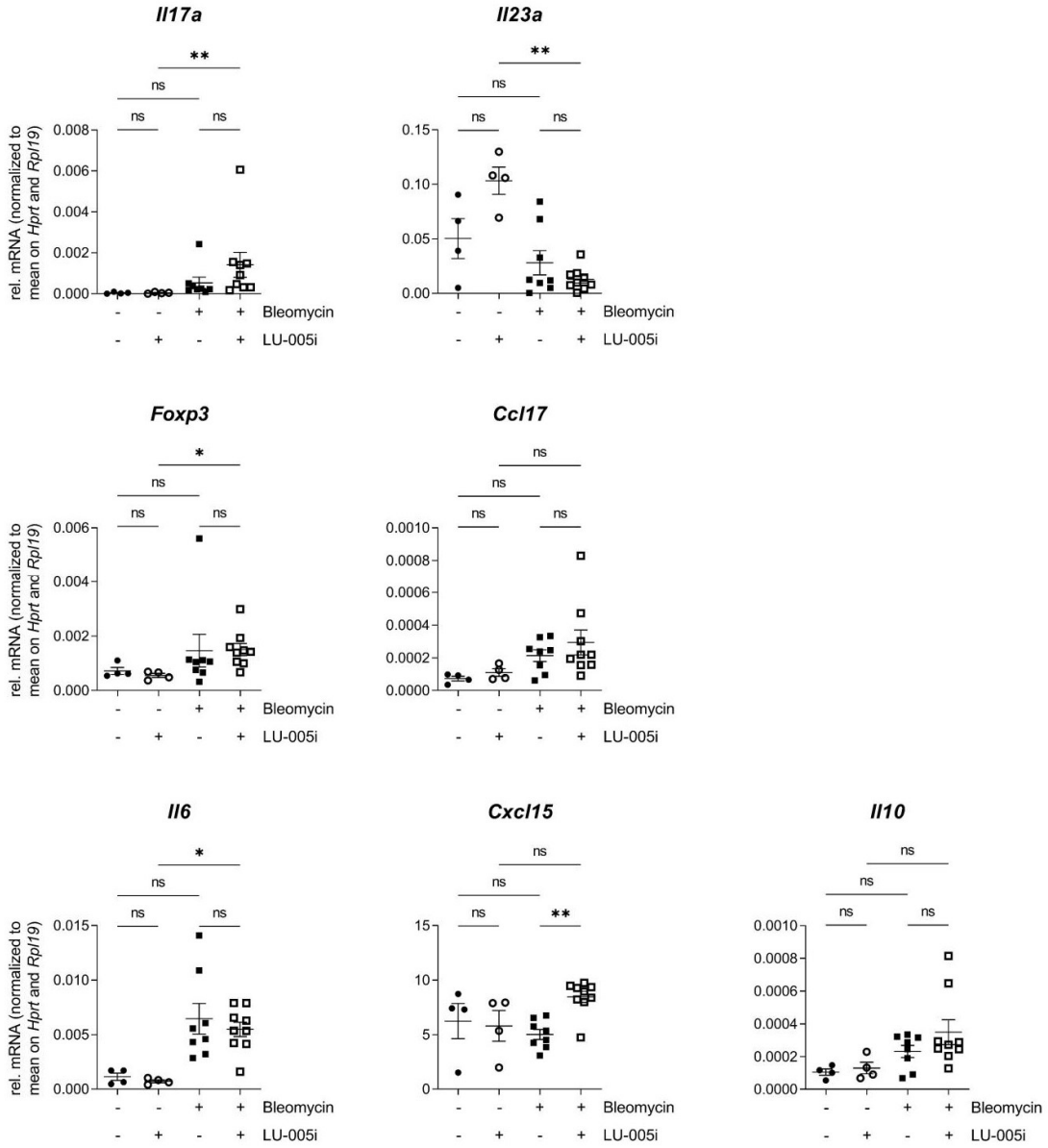


**Figure 23: Pro-fibrotic cytokine gene expression in mice at day seven after intratracheal bleomycin challenge and pan-reactive immunoproteasome inhibition**

Cytokine gene expression of interleukin 17A (*Il17a*), interleukin 23, alpha subunit p19 (*Il23a*), forkhead box P3 (*Foxp3*), chemokine (C-C motif) ligand 17 (*Ccl17*), interleukin 6 (*Il6*), chemokine (C-X-C motif) ligand 15 (*Cxcl15*) and interleukin 10 (*Il10*) was analysed at day seven after bleomycin administration. Genes of interest were normalised to the mean of *Hprt* and *Rpl19*. (Kruskal Wallis test with Dunn´s Multiple Comparisons test, ns = not significant, * $p<0.05$, n = 4-11 per group).

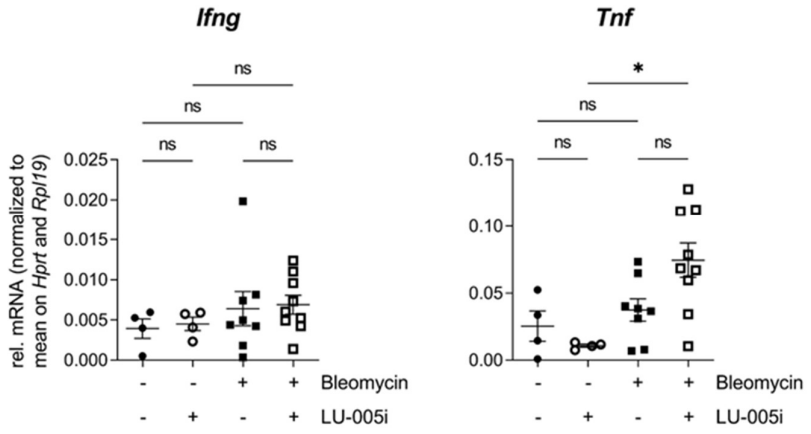


**Figure 24: Pro-inflammatory and anti-fibrotic cytokine gene expression in mice at day seven after intratracheal bleomycin challenge and pan-reactive immunoproteasome inhibition**

Cytokine gene expression of interferon gamma (*Ifng*) and tumour necrosis factor (*Tnf*) was analysed at day seven after bleomycin administration. Genes of interest were normalised to the mean of *Hprt* and *Rpl19*. (Kruskal Wallis test with Dunn´s Multiple Comparisons test, ns = not significant, * p<0.05, n = 4-8 per group).

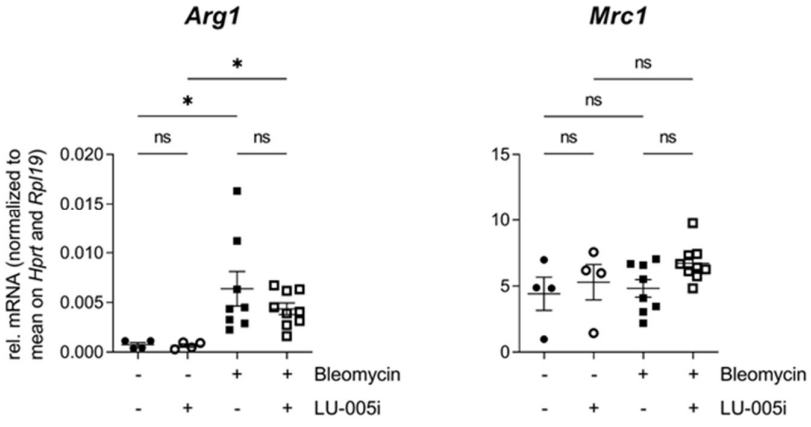


**Figure 25: Macrophage marker gene expression in mice at day seven after intratracheal bleomycin challenge and pan-reactive immunoproteasome inhibition**

Macrophage marker gene expression of arginase (*Arg1*) and mannose receptor C type 1 (*Mrc1*) was analysed at day seven after bleomycin administration. Genes of interest were normalised to the mean of *Hprt* and *Rpl19*. (Kruskal Wallis test with Dunn´s Multiple Comparisons test, ns = not significant, * p<0.05, n = 4-8 per group).

# 6 Discussion

One recently published study of the Meiners lab demonstrated an upregulation of immunoproteasomal subunits in lung tissue sections of IPF patients when compared to healthy lung tissue donors (Wang, Zhang et al. 2023). The same finding was made in experimentally induced pulmonary fibrosis.

This thesis intended to gain insights into a potential role of the immunoproteasome in lung fibrogenesis. Therefore, a set of *in vitro*, *ex vitro* and *in vivo* experiments was conducted. PmLF, as main drivers of lung fibrosis were treated with TGF-β1 to investigate a potential impact on immunoproteasomal expression. Surprisingly, immunoproteasomal expression was downregulated by pro-fibrotic treatment both on RNA and protein expression levels. Single-subunit-deficient pmLFs ($LMP2^{-/-}$) were analysed under pro-fibrotic conditions to investigate a potential impact on myodifferentiation *in vitro*. An analogous experiment was performed on mPCLS *ex vivo*, using a fibrosis cocktail. Furthermore, an *in vivo* bleomycin challenge was performed on wildtype and $LMP7^{-/-}$ mice in order to evaluate the impact of LMP7 deficiency in experimentally induced pulmonary fibrosis. While all these *in vitro*, *ex vivo* and *in vivo* experiments did not reveal any major impact of single immunoproteasome subunit deficiency on pro-fibrotic signalling and lung-fibrosis development, the data suggested some minor protective and attenuating effects upon single immunoproteasome subunit depletion.

Following this, investigations into the potential impact of pan-reactive immunoproteasome inhibition on fibrosis-related marker gene expression were undertaken. Primary human lung fibroblasts and mPCLS were treated with pro-fibrotic stimuli and the effect of the immunoproteasome pan inhibitor LU-005i was analysed upon co-treatment. No significant alterations in myofibroblast marker gene expression were observed by pan-reactive immunoproteasome inhibition. *In vivo* treatment of mice with LU-005i for seven days altered expression of some pro-fibrotic and inflammatory cytokines on the lung at baseline as well as under conditions of bleomycin challenge. The data suggest that the immunoproteasome has no or only a

minor effect on pro-fibrotic responses of the lung parenchyma but influences cytokine responses in the lung *in vivo* in a complex manner.

## 6.1 Immunoproteasomal expression did not differ in lung homogenate from SSc patients and healthy tissue donors

Systemic sclerosis, also called scleroderma is an autoimmune disease, causing fibrosis of multiple internal organs due to excessive collagen production (Chizzolini, Raschi et al. 2002, Solomon, Olson et al. 2013, Schoenfeld and Castelino 2017, Adigun and Bhimji 2018). The development of ILD and PAH represent the main cause of death in SSc patients (Tyndall, Bannert et al. 2010, Schoenfeld and Castelino 2017).

So far, immunoproteasomal and proteasomal subunit expression was only investigated in SSc-derived PBMCs. Subunit expression was measured in cells taken from four patients suffering from SSc and compared to healthy controls. Only one of the patients did not receive immunosuppressive drugs. *PSMB8* and *PSMB9* levels were similar to healthy controls, while *PSMB10* was significantly upregulated in SSc-PBMCs. Interestingly, LMP2 and LMP7 protein expression levels were significantly upregulated in SSc-PBMCs, while MECL-1 was not significantly altered when compared to healthy donors (Krause, Kuckelkorn et al. 2006). Single-cell RNA sequencing data suggest that immunoproteasomal subunits are elevated in parenchymal cells of SSc-ILD patients when compared to healthy donors (https://www.atsjournals.org/doi/full/10.1164/rccm.201712-2410OC). This thesis intended to investigate immunoproteasomal and proteasomal subunit expression levels in whole lung tissue homogenates from explanted lungs of SSc patients. No significant alterations were detected between SSc patients and healthy lung tissue donors.

Scleroderma patients usually undergo multiple drug therapies including immunosuppressive agents which may also impact the immunoproteasomal expression or function. This could explain why no significant alterations of proteasomal and immunoproteasomal expressions in SSc patients were found when compared to

healthy lung tissue donors. Additionally, the IFNγ mRNA expression levels were similar in both groups which may also indicate a comparable level of active inflammation in healthy lung donors and presumably immune-compromised SSc patients. As clinical data concerning lung function or patients' medical treatment were unavailable, the informative value of this experiment is limited. Also, no protein data were obtained from the samples, which limits the depth of analysis.

## 6.2 TGF-β1 downregulates baseline immunoproteasome expression in primary human lung fibroblasts

So far, no data about the impact of the pro-fibrotic mediator TGF-β1 on immunoproteasomal expression are available to our knowledge. In this study, TGF-β1 was observed to downregulate the immunoproteasome on both the mRNA and protein levels. This was an unexpected finding, as an upregulation seemed much more likely because overexpression of the immunoproteasome in parenchymal cells in the lungs of IPF patients compared to control lungs has been observed previously in our lab (Wang, Zhang et al. 2023). Of note, TGF-β1 only downregulated baseline levels of the immunoproteasome but was unable to significantly counteract its IFNγ-induced upregulation. However, this data set is limited as only two different phLF lines of lung-healthy donors were analysed and would require a more thorough analysis of other donors and even IPF-derived phLF lines.

TGF-β1 downregulated baseline levels of the immunoproteasome, which presumably explains why TGF-β1 was suggested to be a general repressor of MHC mRNA expression already 30 years ago (Geiser, Letterio et al. 1993). In our experiments, TGF-β1 was unable to significantly counteract IFNγ-induced upregulation of the immunoproteasome. This finding is also in line with observations which were obtained with murine and human fibroblast lines, in which downregulation of MHC induction was observed by IFNγ- and TGF-β1- co-treatment, compared to only IFNγ treatment (Darley, Morris et al. 1993).

It was previously demonstrated that TGF-β1 was able to suppress the antiviral and proinflammatory response to rhinosyncicial virus (RSV) in murine alveolar macrophages and human monocyte-derived macrophages. Also, the anti-inflammatory (M2) response was dampened by TGF-β1, while TGF-β1-induced macrophage apoptosis impacted negatively on efficient phagocytosis (Grunwell, Yeligar et al. 2018).

### 6.3 Single IP-subunit deficiency mildly dampens fibrogenic responses

In mice that are deficient in single immunoproteasomal subunits such as LMP2 or LMP7 KO mice, the missing immunosubunits are replaced by their constitutive counterpart subunits, i.e. β1 and β5, respectively, forming a hybrid proteasome (Basler, Lauer et al. 2012, Joeris, Schmidt et al. 2012). Any functional effects observed in single-immunoproteasome-subunit-deficient mice will thus relate to the absence of this single subunit and at the same time to the activity of these hybrid proteasomes. This is different from the effects of immunoproteasome inhibitors, which will inhibit fully assembled immunoproteasomes and where no hybrid proteasomes are formed. Before interpreting the LMP2-deficient data obtained with pmLF, the very low basal expression of immunoproteasome subunits in fibroblasts must be considered. Wildtype pmLF were treated with TGF-β1 and compared to LMP2$^{-/-}$ pmLF. Wildtype and LMP2$^{-/-}$ cells did not significantly differ in basal or in TGF-β1-induced pro-fibrotic marker gene expression. However, while *Col1a1* and *Tnc* levels were significantly upregulated in wildtype pmLF, they did not reach significance in LMP2$^{-/-}$ pmLF. Likewise, FC induced an upregulation of fibrosis-related marker gene expression in wildtype mPCLS but was not detectable in LMP2$^{-/-}$ mPCLS. This ineffective induction of profibrotic marker gene expression might indicate some mild protective effect of LMP2 deficiency on myofibroblast gene expression.

Our data obtained with pmLF are, however, limited as the profibrotic stimulation by TGF-β1 treatment was only minor: the profibrotic marker genes *Col1a1*, *Fn1*, *Acta2*, and *Tnc* were not significantly upregulated. This might be due to culture-related activation

of the pmLFs under baseline conditions. It is well known that cells activate a myogenic differentiation program after the very first physical contact with the plate due to its stiff surface (Arora, Narani et al. 1999, Landry, Rattan et al. 2019). Several types of primary fibroblasts have been shown to turn into pro-fibrotic states under common cell culture conditions without administration of pro-fibrotic agents (Santiago, Dangerfield et al. 2010) and the use of less stiff surfaces and matrices has been shown to dampen myodifferentiation of primary embryonic murine fibroblasts (Solon, Levental et al. 2007). This effect might thus have veiled genotype-specific alterations of the treated phLFs presented here.

To address the role of the immunoproteasome in lung fibrosis in vivo, we analysed fibrotic in LMP7$^{-/-}$ mice (Fehling, Swat et al. 1994) and compared it to wildtype mice. The bleomycin model belongs to the most commonly used pulmonary fibrosis models, although bleomycin-induced chronic lung damage does not resemble human idiopathic pulmonary fibrosis (Borzone, Moreno et al. 2001). Intratracheal administration of 1 to 5 U bleomycin per kg body weight induces pulmonary fibrosis in most mice strains while 80 to 150 U per kg are mostly used for systemic administration. After initially causing epithelial cell injury – verifiable by elevation of cytokines like *IL1β*, *IL6*, *TNFα* and *IFNγ* – fibrotic tissue remodelling follows between seven to nine days after intratracheal administration (Moeller, Ask et al. 2008), and peaks around day 14 as indicated by increased accumulation of ECM and expression of collagens and fibronectin (Lawson, Crossno et al. 2008).

Here we analysed fibrosis-related marker gene expression in ten wildtype and eleven LMP7$^{-/-}$ mice undergoing bleomycin challenge with four wildtype mice undergoing PBS treatment as a control group. LMP7 $^{-/-}$ mice were not subjected to PBS treatment, as they do not significantly differ from wildtype mice under physiological conditions (Caniard, Ballweg et al. 2015). LMP7-deficiency did not significantly prevent the development of bleomycin-induced lung fibrosis *in vivo*. Initially, in the presented experiment, however, LMP7$^{-/-}$ mice showed a significant survival benefit at day 14 and experienced less pronounced body weight reduction after bleomycin administration

when compared to wildtype mice. The latter is in line with the observation that DSS-fed LMP7$^{-/-}$ mice were protected from weight loss (Kalim, Basler et al. 2012).

The fibrosis-related mRNA expression data analysis revealed a significantly higher expression of *Tnc* in bleomycin-treated LMP7$^{-/-}$ compared to wildtype mice. The other fibrosis-related marker genes (*Col1a1*, *Acta2*, and *Fn1*) showed a tendency to be higher in bleomycin-treated survivor wildtype mice. These data suggest a potential protective effect of LMP7 deficiency upon bleomycin challenge. Considering the importance of LMP7 in protein homeostasis (Seifert, Bialy et al. 2010), a worse outcome in LMP7$^{-/-}$ bleomycin-treated mice could have been likely, due to the impaired formation of the immunoproteasome (Griffin, Nandi et al. 1998). Future studies should involve a repetition of the experiment with higher numbers of mice per group. This would allow for compensating the observed loss of primarily wildtype mice and would improve the statistical power. Additionally, histology and/or lung function data should be investigated. Likewise, only fibrosis-related but no inflammatory cytokine data were analysed, which might be of interest in future studies. As the presented data are promising, it would be interesting to investigate other single-subunit-deficient mice, such as LMP2$^{-/-}$ or MECL-1$^{-/-}$ mice, or potentially even double- or triple-subunit-deficient mice in future experiments.

Multiple studies using single immunoproteasome knockout mice have demonstrated the crucial role of the immunoproteasome subunits in controlling inflammatory processes. Here, the deficiency of single immunoproteasome subunits was mainly protective.

LMP7$^{-/-}$ mice were shown to be less affected by DSS-induced colitis and bodyweight loss when compared to wildtype mice (Schmidt, Gonzalez et al. 2010). Likewise, pro-inflammatory cytokines and chemokines were reduced in LMP7$^{-/-}$ mice, such as IL1α/β, IL6, and TNFα. Th1 cell cytokines IFNγ and IL17 were also found not to be induced in LMP7$^{-/-}$ mice, whereas the Th2 cytokines IL4, IL5, and IL13 were not altered by the single-subunit-knockout. DSS-treated LMP7$^{-/-}$ mice also lost less weight when compared to wildtype mice (Schmidt, Gonzalez et al. 2010). LMP7$^{-/-}$ mice were shown

to display less pronounced Th2 responses in ovalbumin-induced acute lung injury when compared to wildtype mice (Volkov, Hagner et al. 2013). In contrast, a study investigating lung inflammation on LMP7-deficient mice did also not detect significant alterations when compared to wildtype mice. The authors stated the increase of the constitutive subunit β5 in LMP7-deficient mice might substitute LMP7 (Oliveri, Basler et al. 2022). Likewise, LMP7-deficiency has also been shown to not aggravate the initiation and progression of atherosclerosis in Low density lipoprotein receptor (LDLR)-deficient mice (Hewing, Ludwig et al. 2017). Overexpression of LMP2 was observed in the colon of DSS-treated mice and disease symptoms were shown to be lower in LMP2$^{-/-}$ mice (Fitzpatrick, Khare et al. 2006). Reduced disease severity in either LMP2$^{-/-}$-, MECL-1$^{-/-}$-, and LMP7$^{-/-}$ mice was also observed in other studies using the DSS-induced colitis disease model. Also, LMP2$^{-/-}$-, LMP7$^{-/-}$-, and MECL-1$^{-/-}$- mice were characterised by a lower weight loss and less colon length reduction compared to wildtype mice (Basler, Dajee et al. 2010). Of note, deficiency of MECL-1 has been shown to impact positively in a model of cardiac fibrosis and inflammation in DOCA/salt hypertensive mice (Yan, Bi et al. 2017). In this model, MECL-1 was found to be markedly increased in the heart after DOCA/salt treatment. DOCA/salt-induced hypertension, accumulation of pro-inflammatory cells, cytokine expression, and myocardial fibrosis were significantly attenuated in MECL-1$^{-/-}$ mice and the authors claimed the results to be partially associated with the inhibition of IkBa/NF-κB and TGF-b1/Smad2/3 signalling pathways.

## 6.4 Immunoproteasome inhibition did not impact fibrosis-related marker gene expression in phLF or mPCLS

This study also tested the effects of immunoproteasome inhibitors on fibrotic responses. In contrast to the above-described experiments involving single-subunit-deficient cells or mice, immunoproteasome inhibitors block the activity of assembled immunoproteasomes but do not affect the composition of the immunoproteasomes. Both, TGF-β1 and FC significantly upregulated the myodifferentiation marker genes

*COL1A1*, *ACTA2* and *FN1* in phLF and mPCLS. Pan-reactive immunoproteasome inhibition was neither able to alter fibrosis-related marker gene expression profile in TGF-β1-treated phLF (**Figure 18B**), nor in FC-treated mPCLS (**Figure 19B**). Interestingly, LU-005i seemed to lower the TGF-β1-responsiveness of phLF, whereas the immunoproteasome pan-inhibitor increased the responsiveness to pro-fibrotic stimuli in the mPCLS model, both observations were not described in the existing literature.

In retrospect, the doses of the inhibitor (0.2 µM LU-005i for *in vitro* and 0.5 µM for *ex vivo* experiments, added both two hours prior to pro-fibrotic treatment) are specific but not very effective doses as they only partially inhibited IFNγ-induced induction of the immunoproteasome in CCL206 cells (**Figure 17**). With higher doses that immunoproteasome might have been inhibited more effectively. We did not control for the degree of immunoproteasome inhibition after 24 hours. Regarding cytotoxicity, we did not observe any effect on cell morphology and cell viability in pmLFs which is in line with the rather low baseline expression of the immunoproteasome in these non-immune cells. Moreover, as we observed that TGF-β1 downregulated immunoproteasomal subunits in phLFs, TGF-β1-treated pmLFs will have even lower baseline expression compared to untreated controls. Inhibitor data suggest that the activity of the immunoproteasome does not regulate the response of lung cells to pro-fibrotic stimuli, at least not *in vitro* or *ex vivo*. Summing up, the presented experiments were conducted using cells or tissues with a very low basal expression of the immunoproteasome, and additionally, without the influence of a (physiological) immune system, which limits the informative value of the presented inhibitor experiments.

## 6.5 Immunoproteasome inhibition partially altered inflammation-related marker gene expression profile *in vivo*

Besides a well-orchestrated fibroblast function, proper regulation of several immune cells and cytokines is crucial for tissue regeneration and fibrotic tissue remodelling, as

shown in **Figure 2**, derived by Wynn, 2011. The 14-day *in vivo* bleomycin challenge (**Chapter 5.6**) was based on a properly working immune system and focussed on the fibrogenic reactions of murine lung tissue two weeks after intratracheal bleomycin administration. Accordingly, we performed additional experiments to investigate the effects of immunoproteasome inhibition on bleomycin-induced lung inflammation, which precedes the development of lung fibrosis in mice (Schiller, Fernandez et al. 2015). Given the constitutive expression of the immunoproteasome in immune cells and its known central role in regulating innate and adaptive immune responses and cytokine expression (**Chapter 1.3.8**), we here aimed to interfere with overall immunoproteasome activity using a potent pan-immunoproteasome inhibitor. We reasoned that immunoproteasome inhibition might affect immune cell function in response to bleomycin challenge such as inflammatory and pro-fibrotic cytokine release. Evidence for this is based on multiple studies showing the anti-inflammatory effects of immunoproteasome inhibition as outlined in the introduction (**Chapter 1.3.8**) and described in the following.

The inflammatory phase of the bleomycin model of pulmonary fibrosis lasts approximately until day nine which can be determined by the mRNA expression level of several inflammation-related cytokines in total lung tissue, most of them decreasing significantly after day nine (Chaudhary, Schnapp et al. 2006). Subsequently, a fibrotic phase occurs which peaks at day 14 (Chaudhary, Schnapp et al. 2006), which was the read-out timepoint for the foregone experiment in **Chapter 5.6**.

As previous data from the Meiners lab had indicated that both, LMP7-deficiency, and LMP7-inhibition regulate alternative alveolar macrophage activation (Chen, Kammerl et al. 2016), we first focussed on the expression of macrophage-related genes. The proper balance of alveolar macrophages´ – so-called plasticity – is known to be crucial for maintaining a healthy lung environment (Hussell and Bell 2014). M1 macrophages act pro-inflammatory, while M2 macrophages induce cell proliferation and tissue reparation (Italiani and Boraschi 2014). M1 macrophages produce nitric oxide (NO), which effectively kills pathogens (Roszer 2015). M2 macrophages improve the resolution of airway inflammation (Alber, Howie et al. 2012), but excessive M2 activity

is known to drive chronic lung pathology, which has also been shown in pulmonary fibrosis (Wynn and Barron 2010). Macrophages isolated from IPF patients´ BAL were shown to display alternatively activated properties, leading to stimulation of collagen production by lung fibroblasts (Prasse, Pechkovsky et al. 2006). Pro-fibrotic properties of M2-polarised macrophages play a role in pulmonary fibrosis (Pechkovsky, Prasse et al. 2010). *Arg1* and *Mrc1* serve as M2 macrophage markers, and are essential for cell growth, differentiation, DNA replication and protein translation (Rath, Muller et al. 2014).

We observed that *Arg1* was upregulated in the lungs of bleomycin-treated animals independent of LU-005i-treatment, whereas *Mrc1* remained unaltered by either treatment.

Chemokines such as CCL17 drive fibrosis by increasing collagen production in lung fibroblasts and recruiting fibrocytes, respectively (Kolahian, Fernandez et al. 2016). *Ccl17* was shown to be increased in the lung tissue of bleomycin-treated mice and peaked between day five and day ten after bleomycin administration. Neutralisation of *Ccl17* led to attenuation of pulmonary fibrosis without altering collagen content or impacting fibroblast proliferation (Belperio, Dy et al. 2004). Chen et al. observed the induction of *Ccl17* by immunoproteasome inhibition (ONX0914) and LMP7 depletion in purified alveolar macrophages.

The M2-related *Ccl17* was not significantly upregulated by bleomycin and was not affected by LU-005i treatment in our experiment. Our *in vivo* experiments did not show any changes in *Ccl17* expression, which might be due to the analysis of total tissue and the resulting overall "dilution" of macrophage-derived signals in the RNA analysis of full lungs.

We next analysed the expression of the profibrotically acting Il17a and Foxp3, the latter a marker gene for regulatory T (Treg) cells. IL17A is known to contribute to the progression of pulmonary fibrosis (Piguet, Ribaux et al. 1993, Simonian, Roark et al. 2009), mainly produced by innate stimuli by Th17, $CD4^+$ IL17- and $CD8^+$ IL17 cells. IL17 promotes endothelial to mesenchymal transition (EndMT) and collagen production (Wilson, Madala et al. 2010, Mi, Li et al. 2011, Hasan, Eksteen et al. 2013). *IL17A* was

found to be upregulated in BAL of IPF patients, and bleomycin-induced pulmonary fibrosis is characterised by Il17a production (Wilson, Madala et al. 2010, Wynn 2011). In an IMQ model of murine psoriasis, ONX0914 decreased *Il17a* levels back to physiological amounts and could reduce the weight of lymph nodes as well as inflammatory infiltrates in IMQ-treated mice. ONX0914 was able to decrease *Il17c*, *Ccl20*, *Il22* and *Il23* expression levels, while serum levels of *Tnf* and *Il6* remained unaltered by LMP7 inhibition (Del Rio Oliva, Mellett et al. 2022). The pan-reactive immunoproteasome inhibitor LU-005i has been shown to act beneficial in a murine model of DSS-induced colitis: LU-005i-treated mice were significantly less affected by weight loss and showed only mild signs of inflammation and crypt damage compared to uninhibited mice. The expression levels of *Tnf*, interleukin 1 beta (*Il1b*), and *Il17a* were significantly lower in LU-005i-treated mice compared to uninhibited subjects (Basler, Maurits et al. 2018). Likewise, ONX0914-treated mice were characterised by less severe symptoms of DSS-induced colitis (Basler, Dajee et al. 2010), as described in the introduction (**Chapter 1.3.8**).

Like *Il17a*, *Foxp3* was also found to be increased by bleomycin in LU-005i-treated mice, but not in non-inhibited mice. Regulatory T (Treg) cells, characterised by the expression of *Foxp3*, are crucial players in modulating self-tolerance and maintaining immune homeostasis, and their impact on tissue fibrosis is controversial and potentially dependent on the particularly used disease model (Zhang and Zhang 2020). Depletion of Treg cells was shown to attenuate pulmonary fibrosis in a silica-fibrosis model in mice (Liu, Liu et al. 2010), whereas depletion of Treg cells lead to worsening of disease in an aspergillus fumigatus model of pulmonary fibrosis in mice (Ichikawa, Hirahara et al. 2019).

Il23a is another profibrotic cytokine that was previously found to be elevated in bleomycin-treated mice, and lung remodelling and fibrosis were shown to be Il23a-dependent (Gasse, Riteau et al. 2011). In our study, *Il23a* was downregulated by LU-005i in the bleomycin-treated group of mice compared to bleomycin-treated and PBS plus captisol controls. Specific LMP7 inhibition was able to lower *Il23a*, *Tnf*, *Ifng* and *Il6* production in endotoxin-stimulated PBMCs *in vitro* and reduced cytokine gene

expression and autoantibody levels in murine sera in a mouse model of collagen antibody-induced arthritis. T cell differentiation into T helper 17 cells (Th17) or T helper 1 cells (Th1) cells was prevented by ONX0914 (Muchamuel, Basler et al. 2009). Less Th1 and Th17 cells were found in lamina propria lymphocytes in ONX0914-treated mice having undergone DSS treatment, whereas more FoxP3$^{+}$ cells were found to be present in mesenteric lymph nodes 6 days after DSS treatment. Like LMP7$^{-/-}$ mice, ONX0914-treated subjects also were protected from body weight loss (Kalim, Basler et al. 2012). IL23, IFNy, IL6, and IL8 release in LPS-stimulated PBMCs was potently decreased by bortezomib ONX0914 (Pletinckx, Vassen et al. 2019). LU-005i has been shown to lower LPS-induced IFNγ-secretion of splenocytes, reduce Il6 production, fully block Il23 secretion in LPS-treated PBMCs, and inhibit Il17 production in CD4$^{+}$ T cells in a dose-dependent manner (Basler, Maurits et al. 2018). IL23 is required for the maintenance of IL6- and IL1β-induced Th17 cells and thereby for IL17 production (Aggarwal, Ghilardi et al. 2003, Bettelli, Carrier et al. 2006). ONX0914 blocked IL23 secretion in LPS-stimulated human PBMCs and has been stated to be a suppressor for Th17 cell development, which might make the immunoproteasome become a valuable target for autoimmunity diseases by impacting the IL-23/IL-17 immune axis (Basler, Claus et al. 2019). All this suggests the beneficial effects of immunoproteasome inhibition on autoimmune diseases or diseases characterised by autoimmunity.

In our experiment, LU-005i was able to induce *Tnf* expression in bleomycin-treated mice. Pro-inflammatory *Tnf* was shown to be markedly increased in both, bleomycin-treated mice (Piguet 1990, Piguet and Vesin 1994) and IPF patients derived macrophages (Zhang, Lee et al. 1993). TNFα was demonstrated to inhibit collagen synthesis in cardiac fibroblasts and thereby also acts anti-fibrotic (Siwik, Chang et al. 2000). TNFα$^{-/-}$ mice suffer from prolonged fibrotic response when compared to wildtype mice (Redente, Keith et al. 2014).

IFNγ has been shown to act suppressively on ECM production, by lowering collagen and fibronectin in human skin fibroblasts (Duncan and Berman 1989). Additionally, IFNγ has been demonstrated to reduce TGF-β1-induced proliferation and migration of

healthy and IPF lung fibroblasts by inhibiting matrix metalloprotease 2 (MMP-2) activation, whereas tissue inhibitor of metalloproteinases (TIMP-1 and -2) were not affected (Vu, Chen et al. 2019). ECM degrading MMP (MMP2, MMP7, MMP9, MMP13) expression was shown to be upregulated by IFNγ which might attenuate tissue fibrosis (Zhang and Zhang 2020).

Il6 has also pro-fibrotic properties by blocking fibroblast apoptosis and thereby contributing to the development of lung fibrosis (Liu, Das et al. 2007). We did not observe alterations in *Il6* or *Ifng* levels in all groups. In the bleomycin model of pulmonary fibrosis, using 2.2 mg/kg ($\sim 3.\overline{6}\ \mathrm{U/kG}$), pro-inflammatory cytokines, such as Il6 and IFNγ were found to be expressed and regulated similarly in lung homogenates. After a rapid upregulation until day 3, *Il6* and *Ifng* have been demonstrated to be highly elevated up until day 9, before rapidly decreasing to baseline levels at day 14 (Chaudhary, Schnapp et al. 2006).

We also investigated whether LU-005i treatment of bleomycin-challenged mice altered the expression of *Cxcl15*, also known as interleukin 8 (*Il8*). Il8 has been identified as a driver of fibrotic progression by promoting mesenchymal progenitor cells' self-renewal and stimulating macrophage migration and thereby developing fibrotic lesions (Yang, Herrera et al. 2018). LU-005i increased *Cxcl15* expression in bleomycin-treated mice, but bleomycin alone was not able to induce *Cxcl15* upregulation.

The absence of a bleomycin-induced increase of pro-inflammatory and pro-fibrotic cytokine expression levels might indicate only mild inflammatory or fibrotic signalling in our conducted experiment. This issue suggests considering the applied dose of bleomycin in our experiment and in the literature.

One study investigated the dose-dependent effect of intratracheal administration of 1 mg/kg ($\sim 1.\overline{6}\ \mathrm{U/kG}$), 2 mg/kg ($\sim 3.\overline{3}\ \mathrm{U/kG}$) and 4 mg/kg ($\sim 6.\overline{6}\ \mathrm{U/kG}$) and observed ECM deposition, interstitial alterations and total BAL cell count in bleomycin-treated mice were dose-dependent (Kim, Lee et al. 2010). Another group instilled 2.2 mg/kg ($\sim 3.\overline{6}\ \mathrm{U/kG}$) bleomycin to Wistar rats, as the dose was proven to not reduce body weight and survival of the rats (Chaudhary, Schnapp et al. 2006). Both mentioned studies did not observe significant changes in body weights between bleomycin-

treated and control rodents, which is inconsistent with our data using a relatively low dose, 1.2mg/kg (~2 U/kG), as severe bodyweight losses were observed in our bleomycin-treated mice at day 7, which lead to sacrification of the most affected subjects due to ethical reasons. This sensible disparity cannot fully be explained.

Concludingly, in our experiment, LU-005i and bleomycin co-treatment, however, increased lung-specific expression of *Il17a*, *Arg1*, *Il6*, *Tnf* and *Foxp3* and decreased *Il23a* levels.

It must be noted that in this study no inhibitor confirmation tests, such as Western Blots of immunoproteasome subunits of murine lung tissue homogenates were performed. This way, the extent and specificity of immunoproteasome inhibition could have been analysed. Consequently, as the degree of IP inhibition in the lung at the day of harvesting was not quantified, the presented results need to be interpreted with caution.

# 7 Concluding remarks and outlook

The present study aimed to shed light onto a potential role of the immunoproteasome in lung fibrosis.

In a first step, it was analysed whether the main pro-fibrotic acting mediator TGF-β1 might be responsible for overexpression of IP subunits in myodifferentiated lung fibroblasts. Surprisingly, the immunoproteasome was downregulated in phLF by TGF-β1 treatment on both the mRNA and protein levels, which might have effects on virus infections of parenchymal cells. This finding was unexpected and indicated that other factors may lead to IP overexpression in lung fibrosis which might counteract and exceed the inhibitory effects of TGF-β1.

Followingly, it was investigated whether IP subunit gene deficiency might impact fibrogenesis by subjecting LMP2$^{-/-}$-deficient pmLFs and mPCLS to pro-fibrotic conditions. No alterations were observed between LMP2$^{-/-}$ and wildtype groups.

For future cell experiments we recommend using other cell types than parenchymal cells, as fibroblasts are known for very low expression levels of the immunoproteasome.

LMP7$^{-/-}$ mice and wildtype littermates were treated with bleomycin to induce experimental lung fibrosis. No significant alterations in fibrotic gene expression levels were detected between the investigated groups. LMP7$^{-/-}$ mice undergoing a 14-day bleomycin challenge were characterised by significant survival benefit and less bodyweight alterations, when compared to wildtype littermates. Future studies should consider higher numbers of animals to compensate the detrimental effects of bleomycin.

Finally, immunoproteasome-inhibited wildtype fibroblasts, murine tissue sections (data not shown) and mice were subjected to pro-fibrotic and pro-inflammatory conditions. LU-005i and bleomycin co-treatment, however, increased lung-specific expression of *Il17a*, *Arg1*, *Il6*, *Tnf* and *Foxp3* and decreased *Il23a* levels.

The generated inhibitor data are partially contradictory to published literature and are not fully homogeneous within the presented manuscript. Future studies should use

higher inhibitor concentrations for the *ex vivo* and *in vitro* settings and include quantification of the inhibition levels of the treated subjects.

We recommend using higher number of mice for comparable *in vivo* experiments for compensating a potential loss due to excessive disease, induced by bleomycin. More endpoints of the bleomycin challenge should be investigated to generate a more detailed understanding of the effects of immunoproteasome inhibition or its deficiency. A physiological readout such as lung function will help to uncover the impact of the cell organelle on lung fibrotisation in mice.

# 8 List of abbreviations

| | |
|---|---|
| °C | Degree Celsius |
| µl | Microliter |
| µM | Micromolar |
| αSMA | Alpha smooth muscle actin |
| ABP | Activity-based probe |
| ACE | Angiotensin-converting enzyme |
| ALS | Autophagy-lysosome-system |
| Arg1 | Arginase 1 |
| ATCC | American Type Culture Collection |
| BAL | Bronchoalveolar lavage |
| BCA | Bicinchoninic acid assay |
| Bleo | Bleomycin |
| bp | Base pairs |
| BSA | Bovine serum albumin |
| c20S | Constitutive 20S proteasome |
| C-L | Caspase-like activity |
| CARD14 | Caspase recruitment domain family member 14 |
| CC | Control cocktail |
| CCL12 | C-C motif chemokine 12 |
| CCL17 | C-C motif chemokine ligand 17 |
| CCL20 | C-C Motif Chemokine Ligand 20 |
| CCND1 | Cyclin D1 |
| COL1A1 | Collagen alpha 1 chain type I |
| CP | Core particle |
| CT-L | Chymotrypsin-like activity |
| CXCL15 | C-X-C motif chemokine 15 |
| DMSO | Dimethylsulfoxide |
| DNA | Deoxyribonucleic acid |

List of abbreviations

| | |
|---|---|
| DSS | Dextran-sulfate-sodium |
| ECM | Extracellular matrix |
| ECMO | Extracorporeal membrane oxygenation |
| EMT | Epithelial to mesenchymal transition |
| EndMT | Endothelial to mesenchymal transition |
| FC | Fibrosis cocktail |
| FGF | Fibroblast growth factor |
| FN | Fibronectin |
| FoxP3 | Forkhead box P3 |
| FVC | Forced vital capacity |
| FW | Forward |
| GERD | Gastroesophageal reflux |
| HPRT | Hypoxanthin-Guanin-Phosphoribosyl-Transferase |
| HRCT | High resolution computed tomography |
| i20S | Immuno 20S proteasome |
| IFNγ | Interferon gamma |
| IL1β | Interleukin 1 beta |
| IL6 | Interleukin 6 |
| IL8 | Interleukin 8 |
| IL10 | Interleukin 10 |
| IL17a | Interleukin 17a |
| IL22 | Interleukin 22 |
| IL23a | Interleukin 23a |
| ILBD | Institute for Lung Biology and Disease |
| ILD | Interstitial lung disease |
| IMQ | Imiquimod |
| IPF | Idiopathic pulmonary fibrosis |
| kDa | Kilodalton |
| LDLR | Low density lipoprotein receptor |
| LMP2 | Low-molecular-weight protein 2 |

| | |
|---|---|
| LMP7 | Low-molecular-weight protein 7 |
| LPA | Lysophosphatidic acid |
| LPS | Lipopolysaccharide |
| MDa | Megadalton |
| MECL-1 | Multicatalytic endopeptidase complex subunit 1 |
| MHC | Major histocompatibility complex |
| ml | Millilitre |
| mM | Millimolar |
| MMP | Matrix metalloproteinase |
| mPCLS | Murine precision cut lung slices |
| Mrc1 | Mannose receptor C-type 1 |
| mRNA | Messenger ribonucleic acid |
| MUC5B | Mucin 5B |
| NF-κB | Nuclear factor-κB |
| NO | Nitric oxide |
| ns | not significant |
| OSA | Obstructive sleep apnoea |
| PAH | Pulmonary arterial hypertension |
| PBMC | Peripheral blood mononuclear cell |
| PBS | Phosphate-buffered saline |
| PCR | Polymerase chain reaction |
| PDGF | Platelet-derived growth factor |
| PFA | Paraformaldehyde |
| phLF | Primary human lung fibroblasts |
| pmATII | Primary alveolar type II cells |
| pmLF | Primary murine lung fibroblasts |
| PSMA1 | Proteasome 20S subunit alpha 1 |
| PSMA3 | Proteasome 20S subunit alpha 3 |
| PSMB10 | Proteasome 20S subunit beta 10 |
| PSMB5 | Proteasome 20S subunit beta 5 |

| | |
|---|---|
| PSMB6 | Proteasome 20S subunit beta 6 |
| PSMB7 | Proteasome 20S subunit beta 7 |
| PSMB8 | Proteasome 20S subunit beta 8 |
| PSMB9 | Proteasome 20S subunit beta 9 |
| PSMC3 | Proteasome 26S subunit, ATPase 3 |
| PSMD11 | Proteasome 26S subunit, non-ATPase 11 |
| PSME4 | Proteasome activator subunit 4 |
| PSMF1 | Proteasome inhibitor subunit 1 |
| PVDF | Polyvinylidene difluoride |
| qPCR | Quantitative polymerase chain reaction |
| REV | Reverse |
| ROS | Reactive oxygen species |
| RPL-19 | Ribosomal protein L19 |
| RPM | Rotations per minute |
| Rpn | Regulatory particle non-ATPase |
| Rpt | Regulatory particle triple A ATPase |
| RT-PCR | Real time polymerase chain reaction |
| SDS | Sodium dodecyl sulfate |
| SFTPA2 | Pulmonary surfactant-associated protein A2 |
| SFTPC | Pulmonary surfactant-associated protein C |
| SSc | Systemic sclerosis |
| SSc-ILD | Systemic sclerosis with Idiopathic lung disease |
| T-L | Trypsin-like activity |
| TERC | Telomerase RNA component |
| TERT | Telomerase reverse transcriptase |
| TGF-β1 | Transforming growth factor beta |
| Th1 | T helper 1 cells |
| Th17 | T helper 17 cells |
| TIMP-1 | Tissue inhibitor of metalloproteinase-1 |
| TNC | Tenascin |

List of abbreviations

| | |
|---|---|
| TNFα | Tumour necrosis factor-alpha |
| TNFβ | Tumour necrosis factor-beta |
| Treg | Regulatory T cells |
| UGMLC | Universities of Giessen and Marburg Lung Center |
| UIP | Usual interstitial pneumonia |
| UPS | Ubiquitin proteasome system |
| VEGF | Vascular endothelial growth factor |
| vWF | Von-Willebrand-Faktor |
| x *g* | Times gravity |

# 9 Register of figures

Register of figures

# 10 Register of tables

# 11 List of references

Adigun, R. and S. S. Bhimji (2018). Systemic Sclerosis (CREST syndrome). StatPearls. Treasure Island (FL).

Aggarwal, S., N. Ghilardi, M. H. Xie, F. J. de Sauvage and A. L. Gurney (2003). "Interleukin-23 promotes a distinct CD4 T cell activation state characterized by the production of interleukin-17." J Biol Chem **278**(3): 1910-1914.

Ahmad, K. and S. D. Nathan (2018). "Novel management strategies for idiopathic pulmonary fibrosis." Expert Rev Respir Med **12**(10): 831-842.

Alber, A., S. E. Howie, W. A. Wallace and N. Hirani (2012). "The role of macrophages in healing the wounded lung." Int J Exp Pathol **93**(4): 243-251.

Ale, A., J. Bruna, X. Navarro and E. Udina (2014). "Neurotoxicity induced by antineoplastic proteasome inhibitors." Neurotoxicology **43**: 28-35.

Allegra, A., A. Alonci, D. Gerace, S. Russo, V. Innao, L. Calabro and C. Musolino (2014). "New orally active proteasome inhibitors in multiple myeloma." Leuk Res **38**(1): 1-9.

Alsafadi, H. N., C. A. Staab-Weijnitz, M. Lehmann, M. Lindner, B. Peschel, M. Konigshoff and D. E. Wagner (2017). "An ex vivo model to induce early fibrosis-like changes in human precision-cut lung slices." Am J Physiol Lung Cell Mol Physiol **312**(6): L896-L902.

Aravena, C., G. Labarca, C. Venegas, A. Arenas and G. Rada (2015). "Pirfenidone for Idiopathic Pulmonary Fibrosis: A Systematic Review and Meta-Analysis." PLoS One **10**(8): e0136160.

Armanios, M. Y., J. J. Chen, J. D. Cogan, J. K. Alder, R. G. Ingersoll, C. Markin, W. E. Lawson, M. Xie, I. Vulto, J. A. Phillips, 3rd, P. M. Lansdorp, C. W. Greider and J. E. Loyd (2007). "Telomerase mutations in families with idiopathic pulmonary fibrosis." N Engl J Med **356**(13): 1317-1326.

Arora, P. D., N. Narani and C. A. McCulloch (1999). "The compliance of collagen gels regulates transforming growth factor-beta induction of alpha-smooth muscle actin in fibroblasts." Am J Pathol **154**(3): 871-882.

Ask, K., P. Bonniaud, K. Maass, O. Eickelberg, P. J. Margetts, D. Warburton, J. Groffen, J. Gauldie and M. Kolb (2008). "Progressive pulmonary fibrosis is mediated by TGF-beta isoform 1 but not TGF-beta3." Int J Biochem Cell Biol **40**(3): 484-495.

Baker, T. A., H. H. t. Bach, R. L. Gamelli, R. B. Love and M. Majetschak (2014). "Proteasomes in lungs from organ donors and patients with end-stage pulmonary diseases." Physiol Res **63**(3): 311-319.

Bard, J. A. M., E. A. Goodall, E. R. Greene, E. Jonsson, K. C. Dong and A. Martin (2018). "Structure and Function of the 26S Proteasome." Annu Rev Biochem.

Barnes, J. and M. D. Mayes (2012). "Epidemiology of systemic sclerosis: incidence, prevalence, survival, risk factors, malignancy, and environmental triggers." Curr Opin Rheumatol **24**(2): 165-170.

Barratt, S. L., A. Creamer, C. Hayton and N. Chaudhuri (2018). "Idiopathic Pulmonary Fibrosis (IPF): An Overview." J Clin Med **7**(8).

Barton, L. F., M. Cruz, R. Rangwala, G. S. Deepe, Jr. and J. J. Monaco (2002). "Regulation of immunoproteasome subunit expression in vivo following pathogenic fungal infection." J Immunol **169**(6): 3046-3052.

Basler, M., M. Claus, M. Klawitter, H. Goebel and M. Groettrup (2019). "Immunoproteasome Inhibition Selectively Kills Human CD14(+) Monocytes and as a Result Dampens IL-23 Secretion." J Immunol **203**(7): 1776-1785.

Basler, M., M. Dajee, C. Moll, M. Groettrup and C. J. Kirk (2010). "Prevention of experimental colitis by a selective inhibitor of the immunoproteasome." J Immunol **185**(1): 634-641.

Basler, M., C. Lauer, J. Moebius, R. Weber, M. Przybylski, A. F. Kisselev, C. Tsu and M. Groettrup (2012). "Why the structure but not the activity of the immunoproteasome subunit low molecular mass polypeptide 2 rescues antigen presentation." J Immunol **189**(4): 1868-1877.

Basler, M., E. Maurits, G. de Bruin, J. Koerner, H. S. Overkleeft and M. Groettrup (2018). "Amelioration of autoimmunity with an inhibitor selectively targeting all active centres of the immunoproteasome." Br J Pharmacol **175**(1): 38-52.

Basler, M., S. Mundt, A. Bitzer, C. Schmidt and M. Groettrup (2015). "The immunoproteasome: a novel drug target for autoimmune diseases." Clin Exp Rheumatol **33**(4 Suppl 92): S74-79.

Baumgartner, K. B., J. M. Samet, C. A. Stidley, T. V. Colby and J. A. Waldron (1997). "Cigarette smoking: a risk factor for idiopathic pulmonary fibrosis." Am J Respir Crit Care Med **155**(1): 242-248.

Beck, P., C. Dubiella and M. Groll (2012). "Covalent and non-covalent reversible proteasome inhibition." Biol Chem **393**(10): 1101-1120.

Behr, J., A. Gunther, F. Bonella, J. Dinkel, L. Fink, T. Geiser, K. Geissler, S. Glaser, S. Handzhhiev, D. Jonigk, D. Koschel, M. Kreuter, G. Leuschner, P. Markart, A. Prasse, N. Schonfeld, J. C. Schupp, H. Sitter, J. Muller-Quernheim and U. Costabel (2020). "[German Guideline for Idiopathic Pulmonary Fibrosis]." Pneumologie **74**(5): e1-e2.

Behr, J., A. Gunther, F. Bonella, J. Dinkel, L. Fink, T. Geiser, K. Geissler, S. Glaser, S. Handzhiev, D. Jonigk, D. Koschel, M. Kreuter, G. Leuschner, P. Markart, A. Prasse, N. Schonfeld, J. C. Schupp, H. Sitter, J. Muller-Quernheim and U. Costabel (2021). "S2K Guideline for Diagnosis of Idiopathic Pulmonary Fibrosis." Respiration **100**(3): 238-271.

Behr, J., M. Kreuter, M. M. Hoeper, H. Wirtz, J. Klotsche, D. Koschel, S. Andreas, M. Claussen, C. Grohe, H. Wilkens, W. Randerath, D. Skowasch, F. J. Meyer, J. Kirschner, S. Glaser, F. J. Herth, T. Welte, R. M. Huber, C. Neurohr, M. Schwaiblmair, M. Kohlhaufl, G. Hoffken, M. Held, A. Koch, T. Bahmer and D. Pittrow (2015). "Management of patients with idiopathic pulmonary fibrosis in clinical practice: the INSIGHTS-IPF registry." Eur Respir J **46**(1): 186-196.

Behr, J., S. D. Nathan, W. A. Wuyts, N. Mogulkoc Bishop, D. E. Bouros, K. Antoniou, J. Guiot, M. R. Kramer, K. U. Kirchgaessler, M. Bengus, F. Gilberg, A. Perjesi, S. Harari and A. U. Wells (2021). "Efficacy and safety

of sildenafil added to pirfenidone in patients with advanced idiopathic pulmonary fibrosis and risk of pulmonary hypertension: a double-blind, randomised, placebo-controlled, phase 2b trial." Lancet Respir Med **9**(1): 85-95.

Belperio, J. A., M. Dy, L. Murray, M. D. Burdick, Y. Y. Xue, R. M. Strieter and M. P. Keane (2004). "The role of the Th2 CC chemokine ligand CCL17 in pulmonary fibrosis." J Immunol **173**(7): 4692-4698.

Benanti, J. A. (2012). "Coordination of cell growth and division by the ubiquitin-proteasome system." Semin Cell Dev Biol **23**(5): 492-498.

Betensley, A., R. Sharif and D. Karamichos (2016). "A Systematic Review of the Role of Dysfunctional Wound Healing in the Pathogenesis and Treatment of Idiopathic Pulmonary Fibrosis." J Clin Med **6**(1).

Bettelli, E., Y. Carrier, W. Gao, T. Korn, T. B. Strom, M. Oukka, H. L. Weiner and V. K. Kuchroo (2006). "Reciprocal developmental pathways for the generation of pathogenic effector TH17 and regulatory T cells." Nature **441**(7090): 235-238.

Bhattacharyya, S., H. Yu, C. Mim and A. Matouschek (2014). "Regulated protein turnover: snapshots of the proteasome in action." Nat Rev Mol Cell Biol **15**(2): 122-133.

Bleisch, B., M. M. Schuurmans, R. Klaghofer, C. Benden, A. Seiler and J. Jenewein (2019). "Health-related quality of life and stress-related post-transplant trajectories of lung transplant recipients: a three-year follow-up of the Swiss Transplant Cohort Study." Swiss Med Wkly **149**(07-08).

Bogyo, M., J. S. McMaster, M. Gaczynska, D. Tortorella, A. L. Goldberg and H. Ploegh (1997). "Covalent modification of the active site threonine of proteasomal beta subunits and the Escherichia coli homolog HslV by a new class of inhibitors." Proc Natl Acad Sci U S A **94**(13): 6629-6634.

Bonnans, C., J. Chou and Z. Werb (2014). "Remodelling the extracellular matrix in development and disease." Nat Rev Mol Cell Biol **15**(12): 786-801.

Borissenko, L. and M. Groll (2007). "20S proteasome and its inhibitors: crystallographic knowledge for drug development." Chem Rev **107**(3): 687-717.

Borzone, G., R. Moreno, R. Urrea, M. Meneses, M. Oyarzun and C. Lisboa (2001). "Bleomycin-induced chronic lung damage does not resemble human idiopathic pulmonary fibrosis." Am J Respir Crit Care Med **163**(7): 1648-1653.

Bouchecareilh, M. and W. E. Balch (2011). "Proteostasis: a new therapeutic paradigm for pulmonary disease." Proc Am Thorac Soc **8**(2): 189-195.

Brown, A. W., H. Kaya and S. D. Nathan (2016). "Lung transplantation in IIP: A review." Respirology **21**(7): 1173-1184.

Burgess, J. K., T. Mauad, G. Tjin, J. C. Karlsson and G. Westergren-Thorsson (2016). "The extracellular matrix - the under-recognized element in lung disease?" J Pathol **240**(4): 397-409.

Caniard, A., K. Ballweg, C. Lukas, A. O. Yildirim, O. Eickelberg and S. Meiners (2015). "Proteasome function is not impaired in healthy aging of the lung." Aging (Albany NY) **7**(10): 776-792.

Chaudhary, N. I., A. Schnapp and J. E. Park (2006). "Pharmacologic differentiation of inflammation and fibrosis in the rat bleomycin model." Am J Respir Crit Care Med **173**(7): 769-776.

Chen, I. C., Y. C. Liu, Y. H. Wu, S. H. Lo, Z. K. Dai, J. H. Hsu and Y. H. Tseng (2022). "Evaluation of Proteasome Inhibitors in the Treatment of Idiopathic Pulmonary Fibrosis." Cells **11**(9).

Chen, S., I. E. Kammerl, O. Vosyka, T. Baumann, Y. Yu, Y. Wu, M. Irmler, H. S. Overkleeft, J. Beckers, O. Eickelberg, S. Meiners and T. Stoeger (2016). "Immunoproteasome dysfunction augments alternative polarization of alveolar macrophages." Cell Death Differ **23**(6): 1026-1037.

Chioma, O. S. and W. P. Drake (2017). "Role of Microbial Agents in Pulmonary Fibrosis." Yale J Biol Med **90**(2): 219-227.

Chizzolini, C., E. Raschi, R. Rezzonico, C. Testoni, R. Mallone, A. Gabrielli, A. Facchini, N. Del Papa, M. O. Borghi, J. M. Dayer and P. L. Meroni (2002). "Autoantibodies to fibroblasts induce a proadhesive and proinflammatory fibroblast phenotype in patients with systemic sclerosis." Arthritis Rheum **46**(6): 1602-1613.

Chu-Ping, M., C. A. Slaughter and G. N. DeMartino (1992). "Purification and characterization of a protein inhibitor of the 20S proteasome (macropain)." Biochim Biophys Acta **1119**(3): 303-311.

Collins, G. A. and A. L. Goldberg (2017). "The Logic of the 26S Proteasome." Cell **169**(5): 792-806.

Coux, O., K. Tanaka and A. L. Goldberg (1996). "Structure and functions of the 20S and 26S proteasomes." Annu Rev Biochem **65**: 801-847.

Darley, R., A. Morris, J. Passas and W. Bateman (1993). "Interactions between interferon gamma and retinoic acid with transforming growth factor beta in the induction of immune recognition molecules." Cancer Immunol Immunother **37**(2): 112-118.

de Bruin, G., E. M. Huber, B. T. Xin, E. J. van Rooden, K. Al-Ayed, K. B. Kim, A. F. Kisselev, C. Driessen, M. van der Stelt, G. A. van der Marel, M. Groll and H. S. Overkleeft (2014). "Structure-based design of beta1i or beta5i specific inhibitors of human immunoproteasomes." J Med Chem **57**(14): 6197-6209.

Del Rio Oliva, M., M. Mellett and M. Basler (2022). "Immunoproteasome inhibition attenuates experimental psoriasis." Front Immunol **13**: 1075615.

Dick, L. R. and P. E. Fleming (2010). "Building on bortezomib: second-generation proteasome inhibitors as anti-cancer therapy." Drug Discov Today **15**(5-6): 243-249.

Duncan, M. R. and B. Berman (1989). "Differential regulation of collagen, glycosaminoglycan, fibronectin, and collagenase activity production in cultured human adult dermal fibroblasts by interleukin 1-alpha and beta and tumor necrosis factor-alpha and beta." J Invest Dermatol **92**(5): 699-706.

Esmon, C. T. (2005). "The interactions between inflammation and coagulation." Br J Haematol **131**(4): 417-430.

Estany, S., V. Vicens-Zygmunt, R. Llatjos, A. Montes, R. Penin, I. Escobar, A. Xaubet, S. Santos, F. Manresa, J. Dorca and M. Molina-Molina (2014). "Lung fibrotic tenascin-C upregulation is associated with other extracellular matrix proteins and induced by TGFbeta1." BMC Pulm Med **14**: 120.

Fehling, H. J., W. Swat, C. Laplace, R. Kuhn, K. Rajewsky, U. Muller and H. von Boehmer (1994). "MHC class I expression in mice lacking the proteasome subunit LMP-7." Science **265**(5176): 1234-1237.

Ferrari, V., V. Stroobant, J. Abi Habib, S. Naulaerts, B. J. Van den Eynde and N. Vigneron (2022). "New Insights into the Mechanisms of Proteasome-Mediated Peptide Splicing Learned from Comparing Splicing Efficiency by Different Proteasome Subtypes." J Immunol.

Ferrington, D. A. and D. S. Gregerson (2012). "Immunoproteasomes: structure, function, and antigen presentation." Prog Mol Biol Transl Sci **109**: 75-112.

Finley, D. (2009). "Recognition and processing of ubiquitin-protein conjugates by the proteasome." Annu Rev Biochem **78**: 477-513.

Finley, D. and M. A. Prado (2020). "The Proteasome and Its Network: Engineering for Adaptability." Cold Spring Harb Perspect Biol **12**(1).

Fitzpatrick, L. R., V. Khare, J. S. Small and W. A. Koltun (2006). "Dextran sulfate sodium-induced colitis is associated with enhanced low molecular mass polypeptide 2 (LMP2) expression and is attenuated in LMP2 knockout mice." Dig Dis Sci **51**(7): 1269-1276.

Franke, N. E., D. Niewerth, Y. G. Assaraf, J. van Meerloo, K. Vojtekova, C. H. van Zantwijk, S. Zweegman, E. T. Chan, C. J. Kirk, D. P. Geerke, A. D. Schimmer, G. J. Kaspers, G. Jansen and J. Cloos (2012). "Impaired bortezomib binding to mutant beta5 subunit of the proteasome is the underlying basis for bortezomib resistance in leukemia cells." Leukemia **26**(4): 757-768.

Fricker, L. D. (2020). "Proteasome Inhibitor Drugs." Annu Rev Pharmacol Toxicol **60**: 457-476.

Gabbiani, G. (2003). "The myofibroblast in wound healing and fibrocontractive diseases." J Pathol **200**(4): 500-503.

Gasse, P., N. Riteau, R. Vacher, M. L. Michel, A. Fautrel, F. di Padova, L. Fick, S. Charron, V. Lagente, G. Eberl, M. Le Bert, V. F. Quesniaux, F. Huaux, M. Leite-de-Moraes, B. Ryffel and I. Couillin (2011). "IL-1 and IL-23 mediate early IL-17A production in pulmonary inflammation leading to late fibrosis." PLoS One **6**(8): e23185.

Geiser, A. G., J. J. Letterio, A. B. Kulkarni, S. Karlsson, A. B. Roberts and M. B. Sporn (1993). "Transforming growth factor beta 1 (TGF-beta 1) controls expression of major histocompatibility genes in the postnatal mouse: aberrant histocompatibility antigen expression in the pathogenesis of the TGF-beta 1 null mouse phenotype." Proc Natl Acad Sci U S A **90**(21): 9944-9948.

Geng, F., S. Wenzel and W. P. Tansey (2012). "Ubiquitin and proteasomes in transcription." Annu Rev Biochem **81**: 177-201.

Gordon, M. K. and R. A. Hahn (2010). "Collagens." Cell Tissue Res **339**(1): 247-257.

Gosain, A. and L. A. DiPietro (2004). "Aging and wound healing." World J Surg **28**(3): 321-326.

Griffin, T. A., D. Nandi, M. Cruz, H. J. Fehling, L. V. Kaer, J. J. Monaco and R. A. Colbert (1998). "Immunoproteasome assembly: cooperative incorporation of interferon gamma (IFN-gamma)-inducible subunits." J Exp Med **187**(1): 97-104.

Groettrup, M., C. J. Kirk and M. Basler (2010). "Proteasomes in immune cells: more than peptide producers?" Nat Rev Immunol **10**(1): 73-78.

Groettrup, M., M. van den Broek, K. Schwarz, A. Macagno, S. Khan, R. de Giuli and G. Schmidtke (2001). "Structural plasticity of the proteasome and its function in antigen processing." Crit Rev Immunol **21**(4): 339-358.

Groll, M. and R. Huber (2004). "Inhibitors of the eukaryotic 20S proteasome core particle: a structural approach." Biochim Biophys Acta **1695**(1-3): 33-44.

Gross, T. J. and G. W. Hunninghake (2001). "Idiopathic pulmonary fibrosis." N Engl J Med **345**(7): 517-525.

Grunwell, J. R., S. M. Yeligar, S. Stephenson, X. D. Ping, T. W. Gauthier, A. M. Fitzpatrick and L. A. S. Brown (2018). "TGF-beta1 Suppresses the Type I IFN Response and Induces Mitochondrial Dysfunction in Alveolar Macrophages." J Immunol **200**(6): 2115-2128.

Guillaume, B., J. Chapiro, V. Stroobant, D. Colau, B. Van Holle, G. Parvizi, M. P. Bousquet-Dubouch, I. Theate, N. Parmentier and B. J. Van den Eynde (2010). "Two abundant proteasome subtypes that uniquely process some antigens presented by HLA class I molecules." Proc Natl Acad Sci U S A **107**(43): 18599-18604.

Guo, S. and L. A. Dipietro (2010). "Factors affecting wound healing." J Dent Res **89**(3): 219-229.

Hasan, S. A., B. Eksteen, D. Reid, H. V. Paine, A. Alansary, K. Johannson, C. Gwozd, K. A. Goring, T. Vo, D. Proud and M. M. Kelly (2013). "Role of IL-17A and neutrophils in fibrosis in experimental hypersensitivity pneumonitis." J Allergy Clin Immunol **131**(6): 1663-1673.

Herndon, T. M., A. Deisseroth, E. Kaminskas, R. C. Kane, K. M. Koti, M. D. Rothmann, B. Habtemariam, J. Bullock, J. D. Bray, J. Hawes, T. R. Palmby, J. Jee, W. Adams, H. Mahayni, J. Brown, A. Dorantes, R. Sridhara, A. T. Farrell and R. Pazdur (2013). "U.s. Food and Drug Administration approval: carfilzomib for the treatment of multiple myeloma." Clin Cancer Res **19**(17): 4559-4563.

Hershko, A. and A. Ciechanover (1998). "The ubiquitin system." Annu Rev Biochem **67**: 425-479.

Hewing, B., A. Ludwig, C. Dan, M. Potzsch, C. Hannemann, A. Petry, D. Lauer, A. Gorlach, E. Kaschina, D. N. Muller, G. Baumann, V. Stangl, K. Stangl and N. Wilck (2017). "Immunoproteasome subunit ss5i/LMP7-deficiency in atherosclerosis." Sci Rep **7**(1): 13342.

Hubbard, R., A. Venn, C. Smith, M. Cooper, I. Johnston and J. Britton (1998). "Exposure to commonly prescribed drugs and the etiology of cryptogenic fibrosing alveolitis: a case-control study." Am J Respir Crit Care Med **157**(3 Pt 1): 743-747.

Huber, E. M., M. Basler, R. Schwab, W. Heinemeyer, C. J. Kirk, M. Groettrup and M. Groll (2012). "Immuno- and constitutive proteasome crystal structures reveal differences in substrate and inhibitor specificity." Cell **148**(4): 727-738.

Huber, E. M. and M. Groll (2012). "Inhibitors for the immuno- and constitutive proteasome: current and future trends in drug development." Angew Chem Int Ed Engl **51**(35): 8708-8720.

Huber, E. M. and M. Groll (2021). "A Nut for Every Bolt: Subunit-Selective Inhibitors of the Immunoproteasome and Their Therapeutic Potential." Cells **10**(8).

Hussell, T. and T. J. Bell (2014). "Alveolar macrophages: plasticity in a tissue-specific context." Nat Rev Immunol **14**(2): 81-93.

Hutchinson, J., A. Fogarty, R. Hubbard and T. McKeever (2015). "Global incidence and mortality of idiopathic pulmonary fibrosis: a systematic review." Eur Respir J **46**(3): 795-806.

Ichikawa, H. T., T. Conley, T. Muchamuel, J. Jiang, S. Lee, T. Owen, J. Barnard, S. Nevarez, B. I. Goldman, C. J. Kirk, R. J. Looney and J. H. Anolik (2012). "Beneficial effect of novel proteasome inhibitors in murine lupus via dual inhibition of type I interferon and autoantibody-secreting cells." Arthritis Rheum **64**(2): 493-503.

Ichikawa, T., K. Hirahara, K. Kokubo, M. Kiuchi, A. Aoki, Y. Morimoto, J. Kumagai, A. Onodera, N. Mato, D. J. Tumes, Y. Goto, K. Hagiwara, Y. Inagaki, T. Sparwasser, K. Tobe and T. Nakayama (2019). "CD103(hi) Treg cells constrain lung fibrosis induced by CD103(lo) tissue-resident pathogenic CD4 T cells." Nat Immunol **20**(11): 1469-1480.

Italiani, P. and D. Boraschi (2014). "From Monocytes to M1/M2 Macrophages: Phenotypical vs. Functional Differentiation." Front Immunol **5**: 514.

Izbicki, G., M. J. Segel, T. G. Christensen, M. W. Conner and R. Breuer (2002). "Time course of bleomycin-induced lung fibrosis." Int J Exp Pathol **83**(3): 111-119.

Jain, M., G. Budinger, B. Jovanovic, J. Dematte, S. Duffey and J. Mehta (2018). "Bortezomib is safe in and stabilizes pulmonary function in patients with allo-HSCT-associated pulmonary CGVHD." Bone Marrow Transplant **53**(9): 1124-1130.

Joeris, T., N. Schmidt, D. Ermert, P. Krienke, A. Visekruna, U. Kuckelkorn, S. H. Kaufmann and U. Steinhoff (2012). "The proteasome system in infection: impact of beta5 and LMP7 on composition, maturation and quantity of active proteasome complexes." PLoS One **7**(6): e39827.

Jordan, C. T., L. Cao, E. D. Roberson, S. Duan, C. A. Helms, R. P. Nair, K. C. Duffin, P. E. Stuart, D. Goldgar, G. Hayashi, E. H. Olfson, B. J. Feng, C. R. Pullinger, J. P. Kane, C. A. Wise, R. Goldbach-Mansky, M. A. Lowes, L. Peddle, V. Chandran, W. Liao, P. Rahman, G. G. Krueger, D. Gladman, J. T. Elder, A. Menter and A. M. Bowcock (2012). "Rare and common variants in CARD14, encoding an epidermal regulator of NF-kappaB, in psoriasis." Am J Hum Genet **90**(5): 796-808.

Juarez, M. M., A. L. Chan, A. G. Norris, B. M. Morrissey and T. E. Albertson (2015). "Acute exacerbation of idiopathic pulmonary fibrosis-a review of current and novel pharmacotherapies." J Thorac Dis **7**(3): 499-519.

Kalim, K. W., M. Basler, C. J. Kirk and M. Groettrup (2012). "Immunoproteasome subunit LMP7 deficiency and inhibition suppresses Th1 and Th17 but enhances regulatory T cell differentiation." J Immunol **189**(8): 4182-4193.

Kammerl, I. E. and S. Meiners (2016). "Proteasome function shapes innate and adaptive immune responses." Am J Physiol Lung Cell Mol Physiol **311**(2): L328-336.

Kaplan, G. S., C. C. Torcun, T. Grune, N. K. Ozer and B. Karademir (2017). "Proteasome inhibitors in cancer therapy: Treatment regimen and peripheral neuropathy as a side effect." Free Radic Biol Med **103**: 1-13.

Keller, I. E., O. Vosyka, S. Takenaka, A. Kloss, B. Dahlmann, L. I. Willems, M. Verdoes, H. S. Overkleeft, E. Marcos, S. Adnot, S. M. Hauck, C. Ruppert, A. Gunther, S. Herold, S. Ohno, H. Adler, O. Eickelberg and S. Meiners (2015). "Regulation of immunoproteasome function in the lung." Sci Rep **5**: 10230.

Kendall, R. T. and C. A. Feghali-Bostwick (2014). "Fibroblasts in fibrosis: novel roles and mediators." Front Pharmacol **5**: 123.

Kim, S. N., J. Lee, H. S. Yang, J. W. Cho, S. Kwon, Y. B. Kim, J. D. Her, K. H. Cho, C. W. Song and K. Lee (2010). "Dose-response Effects of Bleomycin on Inflammation and Pulmonary Fibrosis in Mice." Toxicol Res **26**(3): 217-222.

Kim, Y. E., M. S. Hipp, A. Bracher, M. Hayer-Hartl and F. U. Hartl (2013). "Molecular chaperone functions in protein folding and proteostasis." Annu Rev Biochem **82**: 323-355.

King, C. S. and S. D. Nathan (2017). "Idiopathic pulmonary fibrosis: effects and optimal management of comorbidities." Lancet Respir Med **5**(1): 72-84.

King, T. E., Jr., A. Pardo and M. Selman (2011). "Idiopathic pulmonary fibrosis." Lancet **378**(9807): 1949-1961.

Kish-Trier, E. and C. P. Hill (2013). "Structural biology of the proteasome." Annu Rev Biophys **42**: 29-49.

Kisselev, A. F., T. N. Akopian, K. M. Woo and A. L. Goldberg (1999). "The sizes of peptides generated from protein by mammalian 26 and 20 S proteasomes. Implications for understanding the degradative mechanism and antigen presentation." J Biol Chem **274**(6): 3363-3371.

Kisselev, A. F. and A. L. Goldberg (2001). "Proteasome inhibitors: from research tools to drug candidates." Chem Biol **8**(8): 739-758.

Kloetzel, P. M. and F. Ossendorp (2004). "Proteasome and peptidase function in MHC-class-I-mediated antigen presentation." Curr Opin Immunol **16**(1): 76-81.

Kolahian, S., I. E. Fernandez, O. Eickelberg and D. Hartl (2016). "Immune Mechanisms in Pulmonary Fibrosis." Am J Respir Cell Mol Biol **55**(3): 309-322.

Korfei, M., C. Ruppert, P. Mahavadi, I. Henneke, P. Markart, M. Koch, G. Lang, L. Fink, R. M. Bohle, W. Seeger, T. E. Weaver and A. Guenther (2008). "Epithelial endoplasmic reticulum stress and apoptosis in sporadic idiopathic pulmonary fibrosis." Am J Respir Crit Care Med **178**(8): 838-846.

Korfei, M., D. von der Beck, I. Henneke, P. Markart, C. Ruppert, P. Mahavadi, B. Ghanim, W. Klepetko, L. Fink, S. Meiners, O. H. Kramer, W. Seeger, C. Vancheri and A. Guenther (2013). "Comparative proteome analysis of lung tissue from patients with idiopathic pulmonary fibrosis (IPF), non-specific interstitial pneumonia (NSIP) and organ donors." J Proteomics **85**: 109-128.

Krause, S., U. Kuckelkorn, T. Dorner, G. R. Burmester, E. Feist and P. M. Kloetzel (2006). "Immunoproteasome subunit LMP2 expression is deregulated in Sjogren's syndrome but not in other autoimmune disorders." Ann Rheum Dis **65**(8): 1021-1027.

Kreuter, M., S. Ehlers-Tenenbaum, M. Schaaf, U. Oltmanns, K. Palmowski, H. Hoffmann, P. A. Schnabel, C. P. Heussel, M. Puderbach, F. J. Herth and A. Warth (2015). "Treatment and outcome of lung cancer in idiopathic interstitial pneumonias." Sarcoidosis Vasc Diffuse Lung Dis **31**(4): 266-274.

Kumar, S. K., J. H. Lee, J. J. Lahuerta, G. Morgan, P. G. Richardson, J. Crowley, J. Haessler, J. Feather, A. Hoering, P. Moreau, X. LeLeu, C. Hulin, S. K. Klein, P. Sonneveld, D. Siegel, J. Blade, H. Goldschmidt, S. Jagannath, J. S. Miguel, R. Orlowski, A. Palumbo, O. Sezer, S. V. Rajkumar, B. G. Durie and G. International Myeloma Working (2012). "Risk of progression and survival in multiple myeloma relapsing after therapy with IMiDs and bortezomib: a multicenter international myeloma working group study." Leukemia **26**(1): 149-157.

Lander, G. C., E. Estrin, M. E. Matyskiela, C. Bashore, E. Nogales and A. Martin (2012). "Complete subunit architecture of the proteasome regulatory particle." Nature **482**(7384): 186-191.

Landry, N. M., S. G. Rattan and I. M. C. Dixon (2019). "An Improved Method of Maintaining Primary Murine Cardiac Fibroblasts in Two-Dimensional Cell Culture." Sci Rep **9**(1): 12889.

Lawson, W. E., P. F. Crossno, V. V. Polosukhin, J. Roldan, D. S. Cheng, K. B. Lane, T. R. Blackwell, C. Xu, C. Markin, L. B. Ware, G. G. Miller, J. E. Loyd and T. S. Blackwell (2008). "Endoplasmic reticulum stress in alveolar epithelial cells is prominent in IPF: association with altered surfactant protein processing and herpesvirus infection." Am J Physiol Lung Cell Mol Physiol **294**(6): L1119-1126.

Le Pavec, J., G. Dauriat, P. Gazengel, S. Dolidon, A. Hanna, S. Feuillet, P. Pradere, A. Crutu, V. Florea, D. Boulate, D. Mitilian, D. Fabre, S. Mussot, O. Mercier and E. Fadel (2020). "Lung transplantation for idiopathic pulmonary fibrosis." Presse Med **49**(2): 104026.

Lee, B. H., Y. Lu, M. A. Prado, Y. Shi, G. Tian, S. Sun, S. Elsasser, S. P. Gygi, R. W. King and D. Finley (2016). "USP14 deubiquitinates proteasome-bound substrates that are ubiquitinated at multiple sites." Nature **532**(7599): 398-401.

Leggett, D. S., J. Hanna, A. Borodovsky, B. Crosas, M. Schmidt, R. T. Baker, T. Walz, H. Ploegh and D. Finley (2002). "Multiple associated proteins regulate proteasome structure and function." Mol Cell **10**(3): 495-507.

Lettieri, C. J., S. D. Nathan, S. D. Barnett, S. Ahmad and A. F. Shorr (2006). "Prevalence and outcomes of pulmonary arterial hypertension in advanced idiopathic pulmonary fibrosis." Chest **129**(3): 746-752.

Li, N., C. L. Kuo, G. Paniagua, H. van den Elst, M. Verdoes, L. I. Willems, W. A. van der Linden, M. Ruben, E. van Genderen, J. Gubbens, G. P. van Wezel, H. S. Overkleeft and B. I. Florea (2013). "Relative quantification of proteasome activity by activity-based protein profiling and LC-MS/MS." Nat Protoc **8**(6): 1155-1168.

Li, S., J. Shi and H. Tang (2021). "Animal models of drug-induced pulmonary fibrosis: an overview of molecular mechanisms and characteristics." Cell Biol Toxicol.

Lilienbaum, A. (2013). "Relationship between the proteasomal system and autophagy." Int J Biochem Mol Biol **4**(1): 1-26.

Lin, G., D. Li, L. P. de Carvalho, H. Deng, H. Tao, G. Vogt, K. Wu, J. Schneider, T. Chidawanyika, J. D. Warren, H. Li and C. Nathan (2009). "Inhibitors selective for mycobacterial versus human proteasomes." Nature **461**(7264): 621-626.

Liu, F., J. Liu, D. Weng, Y. Chen, L. Song, Q. He and J. Chen (2010). "CD4+CD25+Foxp3+ regulatory T cells depletion may attenuate the development of silica-induced lung fibrosis in mice." PLoS One **5**(11): e15404.

Liu, Q., H. Y. Wang and X. J. He (2019). "Induction of immunoproteasomes in porcine kidney (PK)-15 cells by interferon-gamma and tumor necrosis factor-alpha." J Vet Med Sci.

Liu, X., A. M. Das, J. Seideman, D. Griswold, C. N. Afuh, T. Kobayashi, S. Abe, Q. Fang, M. Hashimoto, H. Kim, X. Wang, L. Shen, S. Kawasaki and S. I. Rennard (2007). "The CC chemokine ligand 2 (CCL2) mediates fibroblast survival through IL-6." Am J Respir Cell Mol Biol **37**(1): 121-128.

Lopez-Ramirez, C., L. Suarez Valdivia and J. A. Rodriguez Portal (2018). "Causes of Pulmonary Fibrosis in the Elderly." Med Sci (Basel) **6**(3).

Maher, T. M., E. Bendstrup, L. Dron, J. Langley, G. Smith, J. M. Khalid, H. Patel and M. Kreuter (2021). "Global incidence and prevalence of idiopathic pulmonary fibrosis." Respir Res **22**(1): 197.

Martin, P. (1997). "Wound healing--aiming for perfect skin regeneration." Science **276**(5309): 75-81.

Mauviel, A. (2005). "Transforming growth factor-beta: a key mediator of fibrosis." Methods Mol Med **117**: 69-80.

Meiners, S. and O. Eickelberg (2012). "What shall we do with the damaged proteins in lung disease? Ask the proteasome!" Eur Respir J **40**(5): 1260-1268.

Meiners, S., I. E. Keller, N. Semren and A. Caniard (2014). "Regulation of the proteasome: evaluating the lung proteasome as a new therapeutic target." Antioxid Redox Signal **21**(17): 2364-2382.

Meiners, S., A. Ludwig, V. Stangl and K. Stangl (2008). "Proteasome inhibitors: poisons and remedies." Med Res Rev **28**(2): 309-327.

Mellett, M., B. Meier, D. Mohanan, R. Schairer, P. Cheng, T. K. Satoh, B. Kiefer, C. Ospelt, S. Nobbe, M. Thome, E. Contassot and L. E. French (2018). "CARD14 Gain-of-Function Mutation Alone Is Sufficient to

Drive IL-23/IL-17-Mediated Psoriasiform Skin Inflammation In Vivo." J Invest Dermatol **138**(9): 2010-2023.

Mi, S., Z. Li, H. Z. Yang, H. Liu, J. P. Wang, Y. G. Ma, X. X. Wang, H. Z. Liu, W. Sun and Z. W. Hu (2011). "Blocking IL-17A promotes the resolution of pulmonary inflammation and fibrosis via TGF-beta1-dependent and -independent mechanisms." J Immunol **187**(6): 3003-3014.

Midwood, K. S. and G. Orend (2009). "The role of tenascin-C in tissue injury and tumorigenesis." J Cell Commun Signal **3**(3-4): 287-310.

Moeller, A., K. Ask, D. Warburton, J. Gauldie and M. Kolb (2008). "The bleomycin animal model: a useful tool to investigate treatment options for idiopathic pulmonary fibrosis?" Int J Biochem Cell Biol **40**(3): 362-382.

Muchamuel, T., M. Basler, M. A. Aujay, E. Suzuki, K. W. Kalim, C. Lauer, C. Sylvain, E. R. Ring, J. Shields, J. Jiang, P. Shwonek, F. Parlati, S. D. Demo, M. K. Bennett, C. J. Kirk and M. Groettrup (2009). "A selective inhibitor of the immunoproteasome subunit LMP7 blocks cytokine production and attenuates progression of experimental arthritis." Nat Med **15**(7): 781-787.

Murata, S., H. Yashiroda and K. Tanaka (2009). "Molecular mechanisms of proteasome assembly." Nat Rev Mol Cell Biol **10**(2): 104-115.

Muro, A. F., F. A. Moretti, B. B. Moore, M. Yan, R. G. Atrasz, C. A. Wilke, K. R. Flaherty, F. J. Martinez, J. L. Tsui, D. Sheppard, F. E. Baralle, G. B. Toews and E. S. White (2008). "An essential role for fibronectin extra type III domain A in pulmonary fibrosis." Am J Respir Crit Care Med **177**(6): 638-645.

Mutlu, G. M., G. R. Budinger, M. Wu, A. P. Lam, A. Zirk, S. Rivera, D. Urich, S. E. Chiarella, L. H. Go, A. K. Ghosh, M. Selman, A. Pardo, J. Varga, D. W. Kamp, N. S. Chandel, J. I. Sznajder and M. Jain (2012). "Proteasomal inhibition after injury prevents fibrosis by modulating TGF-beta(1) signalling." Thorax **67**(2): 139-146.

Nalysnyk, L., J. Cid-Ruzafa, P. Rotella and D. Esser (2012). "Incidence and prevalence of idiopathic pulmonary fibrosis: review of the literature." Eur Respir Rev **21**(126): 355-361.

Oldham, J. M. and H. R. Collard (2017). "Comorbid Conditions in Idiopathic Pulmonary Fibrosis: Recognition and Management." Front Med (Lausanne) **4**: 123.

Oliveri, F., M. Basler, T. N. Rao, H. J. Fehling and M. Groettrup (2022). "Immunoproteasome Inhibition Reduces the T Helper 2 Response in Mouse Models of Allergic Airway Inflammation." Front Immunol **13**: 870720.

Pathare, G. R., I. Nagy, S. Bohn, P. Unverdorben, A. Hubert, R. Korner, S. Nickell, K. Lasker, A. Sali, T. Tamura, T. Nishioka, F. Forster, W. Baumeister and A. Bracher (2012). "The proteasomal subunit Rpn6 is a molecular clamp holding the core and regulatory subcomplexes together." Proc Natl Acad Sci U S A **109**(1): 149-154.

Pechkovsky, D. V., A. Prasse, F. Kollert, K. M. Engel, J. Dentler, W. Luttmann, K. Friedrich, J. Muller-Quernheim and G. Zissel (2010). "Alternatively activated alveolar macrophages in pulmonary fibrosis-mediator production and intracellular signal transduction." Clin Immunol **137**(1): 89-101.

Penke, L. R. K., J. Speth, S. Wettlaufer, C. Draijer and M. Peters-Golden (2022). "Bortezomib Inhibits Lung Fibrosis and Fibroblast Activation without Proteasome Inhibition." Am J Respir Cell Mol Biol **66**(1): 23-37.

Piguet, P. F. (1990). "Is "tumor necrosis factor" the major effector of pulmonary fibrosis?" Eur Cytokine Netw **1**(4): 257-258.

Piguet, P. F., C. Ribaux, V. Karpuz, G. E. Grau and Y. Kapanci (1993). "Expression and localization of tumor necrosis factor-alpha and its mRNA in idiopathic pulmonary fibrosis." Am J Pathol **143**(3): 651-655.

Piguet, P. F. and C. Vesin (1994). "Treatment by human recombinant soluble TNF receptor of pulmonary fibrosis induced by bleomycin or silica in mice." Eur Respir J **7**(3): 515-518.

Pletinckx, K., S. Vassen, I. Schlusche, S. Nordhoff, G. Bahrenberg and T. R. Dunkern (2019). "Inhibiting the immunoproteasome's beta5i catalytic activity affects human peripheral blood-derived immune cell viability." Pharmacol Res Perspect **7**(4): e00482.

Polke, M., Y. Kondoh, M. Wijsenbeek, V. Cottin, S. L. F. Walsh, H. R. Collard, N. Chaudhuri, S. Avdeev, J. Behr, G. Calligaro, T. J. Corte, K. Flaherty, M. Funke-Chambour, M. Kolb, J. Krisam, T. M. Maher, M. Molina Molina, A. Morais, C. C. Moor, J. Morisset, C. Pereira, S. Quadrelli, M. Selman, A. Tzouvelekis, C. Valenzuela, C. Vancheri, V. Vicens-Zygmunt, J. Walscher, W. Wuyts, E. Bendstrup and M. Kreuter (2021). "Management of Acute Exacerbation of Idiopathic Pulmonary Fibrosis in Specialised and Non-specialised ILD Centres Around the World." Front Med (Lausanne) **8**: 699644.

Prasse, A., D. V. Pechkovsky, G. B. Toews, W. Jungraithmayr, F. Kollert, T. Goldmann, E. Vollmer, J. Muller-Quernheim and G. Zissel (2006). "A vicious circle of alveolar macrophages and fibroblasts perpetuates pulmonary fibrosis via CCL18." Am J Respir Crit Care Med **173**(7): 781-792.

Raghu, G., H. R. Collard, J. J. Egan, F. J. Martinez, J. Behr, K. K. Brown, T. V. Colby, J. F. Cordier, K. R. Flaherty, J. A. Lasky, D. A. Lynch, J. H. Ryu, J. J. Swigris, A. U. Wells, J. Ancochea, D. Bouros, C. Carvalho, U. Costabel, M. Ebina, D. M. Hansell, T. Johkoh, D. S. Kim, T. E. King, Jr., Y. Kondoh, J. Myers, N. L. Muller, A. G. Nicholson, L. Richeldi, M. Selman, R. F. Dudden, B. S. Griss, S. L. Protzko, H. J. Schunemann and A. E. J. A. C. o. I. P. Fibrosis (2011). "An official ATS/ERS/JRS/ALAT statement: idiopathic pulmonary fibrosis: evidence-based guidelines for diagnosis and management." Am J Respir Crit Care Med **183**(6): 788-824.

Raghu, G., T. D. Freudenberger, S. Yang, J. R. Curtis, C. Spada, J. Hayes, J. K. Sillery, C. E. Pope, 2nd and C. A. Pellegrini (2006). "High prevalence of abnormal acid gastro-oesophageal reflux in idiopathic pulmonary fibrosis." Eur Respir J **27**(1): 136-142.

Raninga, P. V., A. Lee, D. Sinha, L. F. Dong, K. K. Datta, X. Lu, P. Kalita-de Croft, M. Dutt, M. Hill, N. Pouliot, H. Gowda, M. Kalimutho, J. Neuzil and K. K. Khanna (2020). "Marizomib suppresses triple-negative breast cancer via proteasome and oxidative phosphorylation inhibition." Theranostics **10**(12): 5259-5275.

Rath, M., I. Muller, P. Kropf, E. I. Closs and M. Munder (2014). "Metabolism via Arginase or Nitric Oxide Synthase: Two Competing Arginine Pathways in Macrophages." Front Immunol **5**: 532.

Redente, E. F., R. C. Keith, W. Janssen, P. M. Henson, L. A. Ortiz, G. P. Downey, D. L. Bratton and D. W. Riches (2014). "Tumor necrosis factor-alpha accelerates the resolution of established pulmonary fibrosis in mice by targeting profibrotic lung macrophages." Am J Respir Cell Mol Biol **50**(4): 825-837.

Reyfman, P. A., J. M. Walter, N. Joshi, K. R. Anekalla, A. C. McQuattie-Pimentel, S. Chiu, R. Fernandez, M. Akbarpour, C. I. Chen, Z. Ren, R. Verma, H. Abdala-Valencia, K. Nam, M. Chi, S. Han, F. J. Gonzalez-Gonzalez, S. Soberanes, S. Watanabe, K. J. N. Williams, A. S. Flozak, T. T. Nicholson, V. K. Morgan, D. R. Winter, M. Hinchcliff, C. L. Hrusch, R. D. Guzy, C. A. Bonham, A. I. Sperling, R. Bag, R. B. Hamanaka, G. M. Mutlu, A. V. Yeldandi, S. A. Marshall, A. Shilatifard, L. A. N. Amaral, H. Perlman, J. I. Sznajder, A. C. Argento, C. T. Gillespie, J. Dematte, M. Jain, B. D. Singer, K. M. Ridge, A. P. Lam, A. Bharat, S. M. Bhorade, C. J. Gottardi, G. R. S. Budinger and A. V. Misharin (2019). "Single-Cell Transcriptomic Analysis of Human Lung Provides Insights into the Pathobiology of Pulmonary Fibrosis." Am J Respir Crit Care Med **199**(12): 1517-1536.

Rezaei, R., S. Aslani, N. Dashti, A. Jamshidi, F. Gharibdoost and M. Mahmoudi (2018). "Genetic implications in the pathogenesis of systemic sclerosis." Int J Rheum Dis **21**(8): 1478-1486.

Rock, K. L., C. Gramm, L. Rothstein, K. Clark, R. Stein, L. Dick, D. Hwang and A. L. Goldberg (1994). "Inhibitors of the proteasome block the degradation of most cell proteins and the generation of peptides presented on MHC class I molecules." Cell **78**(5): 761-771.

Rockey, D. C., P. D. Bell and J. A. Hill (2015). "Fibrosis--A Common Pathway to Organ Injury and Failure." N Engl J Med **373**(1): 96.

Roszer, T. (2015). "Understanding the Mysterious M2 Macrophage through Activation Markers and Effector Mechanisms." Mediators Inflamm **2015**: 816460.

Santiago, J. J., A. L. Dangerfield, S. G. Rattan, K. L. Bathe, R. H. Cunnington, J. E. Raizman, K. M. Bedosky, D. H. Freed, E. Kardami and I. M. Dixon (2010). "Cardiac fibroblast to myofibroblast differentiation in vivo and in vitro: expression of focal adhesion components in neonatal and adult rat ventricular myofibroblasts." Dev Dyn **239**(6): 1573-1584.

Schiller, H. B., I. E. Fernandez, G. Burgstaller, C. Schaab, R. A. Scheltema, T. Schwarzmayr, T. M. Strom, O. Eickelberg and M. Mann (2015). "Time- and compartment-resolved proteome profiling of the extracellular niche in lung injury and repair." Mol Syst Biol **11**(7): 819.

Schiller, M., D. Javelaud and A. Mauviel (2004). "TGF-beta-induced SMAD signaling and gene regulation: consequences for extracellular matrix remodeling and wound healing." J Dermatol Sci **35**(2): 83-92.

Schmidt, N., E. Gonzalez, A. Visekruna, A. A. Kuhl, C. Loddenkemper, H. Mollenkopf, S. H. Kaufmann, U. Steinhoff and T. Joeris (2010). "Targeting the proteasome: partial inhibition of the proteasome by bortezomib or deletion of the immunosubunit LMP7 attenuates experimental colitis." Gut **59**(7): 896-906.

Schoenfeld, S. R. and F. V. Castelino (2017). "Evaluation and management approaches for scleroderma lung disease." Ther Adv Respir Dis **11**(8): 327-340.

Schwaiblmair, M., W. Behr, T. Haeckel, B. Markl, W. Foerg and T. Berghaus (2012). "Drug induced interstitial lung disease." Open Respir Med J **6**: 63-74.

Seibold, M. A., A. L. Wise, M. C. Speer, M. P. Steele, K. K. Brown, J. E. Loyd, T. E. Fingerlin, W. Zhang, G. Gudmundsson, S. D. Groshong, C. M. Evans, S. Garantziotis, K. B. Adler, B. F. Dickey, R. M. du Bois, I. V. Yang, A. Herron, D. Kervitsky, J. L. Talbert, C. Markin, J. Park, A. L. Crews, S. H. Slifer, S. Auerbach, M. G.

Roy, J. Lin, C. E. Hennessy, M. I. Schwarz and D. A. Schwartz (2011). "A common MUC5B promoter polymorphism and pulmonary fibrosis." N Engl J Med **364**(16): 1503-1512.

Seifert, U., L. P. Bialy, F. Ebstein, D. Bech-Otschir, A. Voigt, F. Schroter, T. Prozorovski, N. Lange, J. Steffen, M. Rieger, U. Kuckelkorn, O. Aktas, P. M. Kloetzel and E. Kruger (2010). "Immunoproteasomes preserve protein homeostasis upon interferon-induced oxidative stress." Cell **142**(4): 613-624.

Selman, M. and A. Pardo (2014). "Revealing the pathogenic and aging-related mechanisms of the enigmatic idiopathic pulmonary fibrosis. an integral model." Am J Respir Crit Care Med **189**(10): 1161-1172.

Semren, N., N. C. Habel-Ungewitter, I. E. Fernandez, M. Konigshoff, O. Eickelberg, T. Stoger and S. Meiners (2015). "Validation of the 2nd Generation Proteasome Inhibitor Oprozomib for Local Therapy of Pulmonary Fibrosis." PLoS One **10**(9): e0136188.

Semren, N., V. Welk, M. Korfei, I. E. Keller, I. E. Fernandez, H. Adler, A. Gunther, O. Eickelberg and S. Meiners (2015). "Regulation of 26S Proteasome Activity in Pulmonary Fibrosis." Am J Respir Crit Care Med **192**(9): 1089-1101.

Sijts, E. J. and P. M. Kloetzel (2011). "The role of the proteasome in the generation of MHC class I ligands and immune responses." Cell Mol Life Sci **68**(9): 1491-1502.

Silman, A. J. (1991). "Epidemiology of scleroderma." Ann Rheum Dis **50 Suppl 4**: 846-853.

Simonian, P. L., C. L. Roark, F. Wehrmann, A. K. Lanham, F. Diaz del Valle, W. K. Born, R. L. O'Brien and A. P. Fontenot (2009). "Th17-polarized immune response in a murine model of hypersensitivity pneumonitis and lung fibrosis." J Immunol **182**(1): 657-665.

Singh, P., C. Carraher and J. E. Schwarzbauer (2010). "Assembly of fibronectin extracellular matrix." Annu Rev Cell Dev Biol **26**: 397-419.

Siwik, D. A., D. L. Chang and W. S. Colucci (2000). "Interleukin-1beta and tumor necrosis factor-alpha decrease collagen synthesis and increase matrix metalloproteinase activity in cardiac fibroblasts in vitro." Circ Res **86**(12): 1259-1265.

Skeoch, S., N. Weatherley, A. J. Swift, A. Oldroyd, C. Johns, C. Hayton, A. Giollo, J. M. Wild, J. C. Waterton, M. Buch, K. Linton, I. N. Bruce, C. Leonard, S. Bianchi and N. Chaudhuri (2018). "Drug-Induced Interstitial Lung Disease: A Systematic Review." J Clin Med **7**(10).

Snyder, J. C., A. C. Zemke and B. R. Stripp (2009). "Reparative capacity of airway epithelium impacts deposition and remodeling of extracellular matrix." Am J Respir Cell Mol Biol **40**(6): 633-642.

Solomon, J. J., A. L. Olson, A. Fischer, T. Bull, K. K. Brown and G. Raghu (2013). "Scleroderma lung disease." Eur Respir Rev **22**(127): 6-19.

Solon, J., I. Levental, K. Sengupta, P. C. Georges and P. A. Janmey (2007). "Fibroblast adaptation and stiffness matching to soft elastic substrates." Biophys J **93**(12): 4453-4461.

Somogyi, V., N. Chaudhuri, S. E. Torrisi, N. Kahn, V. Muller and M. Kreuter (2019). "The therapy of idiopathic pulmonary fibrosis: what is next?" Eur Respir Rev **28**(153).

Song, J. W., S. B. Hong, C. M. Lim, Y. Koh and D. S. Kim (2011). "Acute exacerbation of idiopathic pulmonary fibrosis: incidence, risk factors and outcome." Eur Respir J **37**(2): 356-363.

Soti, C. and P. Csermely (2007). "Protein stress and stress proteins: implications in aging and disease." J Biosci **32**(3): 511-515.

Sottile, P. D., D. Iturbe, T. R. Katsumoto, M. K. Connolly, H. R. Collard, L. A. Leard, S. Hays, J. A. Golden, C. Hoopes, J. Kukreja and J. P. Singer (2013). "Outcomes in systemic sclerosis-related lung disease after lung transplantation." Transplantation **95**(7): 975-980.

Spira, A., J. Beane, V. Shah, G. Liu, F. Schembri, X. Yang, J. Palma and J. S. Brody (2004). "Effects of cigarette smoke on the human airway epithelial cell transcriptome." Proc Natl Acad Sci U S A **101**(27): 10143-10148.

Stadtmueller, B. M. and C. P. Hill (2011). "Proteasome activators." Mol Cell **41**(1): 8-19.

Straub, J. M., J. New, C. D. Hamilton, C. Lominska, Y. Shnayder and S. M. Thomas (2015). "Radiation-induced fibrosis: mechanisms and implications for therapy." J Cancer Res Clin Oncol **141**(11): 1985-1994.

Sula Karreci, E., H. Fan, M. Uehara, A. B. Mihali, P. K. Singh, A. T. Kurdi, Z. Solhjou, L. V. Riella, I. Ghobrial, T. Laragione, S. Routray, J. P. Assaker, R. Wang, G. Sukenick, L. Shi, F. J. Barrat, C. F. Nathan, G. Lin and J. Azzi (2016). "Brief treatment with a highly selective immunoproteasome inhibitor promotes long-term cardiac allograft acceptance in mice." Proc Natl Acad Sci U S A **113**(52): E8425-E8432.

Taskar, V. and D. Coultas (2008). "Exposures and idiopathic lung disease." Semin Respir Crit Care Med **29**(6): 670-679.

Thibaudeau, T. A. and D. M. Smith (2019). "A Practical Review of Proteasome Pharmacology." Pharmacol Rev **71**(2): 170-197.

Thomas, A. Q., K. Lane, J. Phillips, 3rd, M. Prince, C. Markin, M. Speer, D. A. Schwartz, R. Gaddipati, A. Marney, J. Johnson, R. Roberts, J. Haines, M. Stahlman and J. E. Loyd (2002). "Heterozygosity for a surfactant protein C gene mutation associated with usual interstitial pneumonitis and cellular nonspecific interstitial pneumonitis in one kindred." Am J Respir Crit Care Med **165**(9): 1322-1328.

Toes, R. E., A. K. Nussbaum, S. Degermann, M. Schirle, N. P. Emmerich, M. Kraft, C. Laplace, A. Zwinderman, T. P. Dick, J. Muller, B. Schonfisch, C. Schmid, H. J. Fehling, S. Stevanovic, H. G. Rammensee and H. Schild (2001). "Discrete cleavage motifs of constitutive and immunoproteasomes revealed by quantitative analysis of cleavage products." J Exp Med **194**(1): 1-12.

Tomko, R. J., Jr. and M. Hochstrasser (2013). "Molecular architecture and assembly of the eukaryotic proteasome." Annu Rev Biochem **82**: 415-445.

Trebaul, A., E. K. Chan and K. S. Midwood (2007). "Regulation of fibroblast migration by tenascin-C." Biochem Soc Trans **35**(Pt 4): 695-697.

Tsakiri, K. D., J. T. Cronkhite, P. J. Kuan, C. Xing, G. Raghu, J. C. Weissler, R. L. Rosenblatt, J. W. Shay and C. K. Garcia (2007). "Adult-onset pulmonary fibrosis caused by mutations in telomerase." Proc Natl Acad Sci U S A **104**(18): 7552-7557.

Tyndall, A. J., B. Bannert, M. Vonk, P. Airo, F. Cozzi, P. E. Carreira, D. F. Bancel, Y. Allanore, U. Muller-Ladner, O. Distler, F. Iannone, R. Pellerito, M. Pileckyte, I. Miniati, L. Ananieva, A. B. Gurman, N. Damjanov, A. Mueller, G. Valentini, G. Riemekasten, M. Tikly, L. Hummers, M. J. Henriques, P. Caramaschi, A. Scheja, B. Rozman, E. Ton, G. Kumanovics, B. Coleiro, E. Feierl, G. Szucs, C. A. Von Muhlen, V. Riccieri, S. Novak, C. Chizzolini, A. Kotulska, C. Denton, P. C. Coelho, I. Kotter, I. Simsek, P. G. de la Pena Lefebvre, E. Hachulla, J. R. Seibold, S. Rednic, J. Stork, J. Morovic-Vergles and U. A. Walker (2010). "Causes and risk factors for death in systemic sclerosis: a study from the EULAR Scleroderma Trials and Research (EUSTAR) database." Ann Rheum Dis **69**(10): 1809-1815.

Vachharajani, N., T. Joeris, M. Luu, S. Hartmann, S. Pautz, E. Jenike, G. Pantazis, I. Prinz, M. J. Hofer, U. Steinhoff and A. Visekruna (2017). "Prevention of colitis-associated cancer by selective targeting of immunoproteasome subunit LMP7." Oncotarget **8**(31): 50447-50459.

van der Fits, L., S. Mourits, J. S. Voerman, M. Kant, L. Boon, J. D. Laman, F. Cornelissen, A. M. Mus, E. Florencia, E. P. Prens and E. Lubberts (2009). "Imiquimod-induced psoriasis-like skin inflammation in mice is mediated via the IL-23/IL-17 axis." J Immunol **182**(9): 5836-5845.

Van Kaer, L., P. G. Ashton-Rickardt, M. Eichelberger, M. Gaczynska, K. Nagashima, K. L. Rock, A. L. Goldberg, P. C. Doherty and S. Tonegawa (1994). "Altered peptidase and viral-specific T cell response in LMP2 mutant mice." Immunity **1**(7): 533-541.

VanderLinden, R. T., C. W. Hemmis, B. Schmitt, A. Ndoja, F. G. Whitby, H. Robinson, R. E. Cohen, T. Yao and C. P. Hill (2016). "Structural Basis for the Activation and Inhibition of the UCH37 Deubiquitylase." Mol Cell **61**(3): 487.

Verrecchia, F. and A. Mauviel (2007). "Transforming growth factor-beta and fibrosis." World J Gastroenterol **13**(22): 3056-3062.

Volkov, A., S. Hagner, S. Loser, S. Alnahas, H. Raifer, A. Hellhund, H. Garn and U. Steinhoff (2013). "beta5i subunit deficiency of the immunoproteasome leads to reduced Th2 response in OVA induced acute asthma." PLoS One **8**(4): e60565.

Vu, T. N., X. Chen, H. D. Foda, G. C. Smaldone and N. A. Hasaneen (2019). "Interferon-gamma enhances the antifibrotic effects of pirfenidone by attenuating IPF lung fibroblast activation and differentiation." Respir Res **20**(1): 206.

Walters, D. M. and S. R. Kleeberger (2008). "Mouse models of bleomycin-induced pulmonary fibrosis." Curr Protoc Pharmacol **Chapter 5**: Unit 5 46.

Wang, S. Y., Y. H. Shih, T. M. Shieh and Y. H. Tseng (2021). "Proteasome Inhibitors Interrupt the Activation of Non-Canonical NF-kappaB Signaling Pathway and Induce Cell Apoptosis in Cytarabine-Resistant HL60 Cells." Int J Mol Sci **23**(1).

Wang, X., T. Meul and S. Meiners (2020). "Exploring the proteasome system: A novel concept of proteasome inhibition and regulation." Pharmacol Ther **211**: 107526.

Wang, X., H. Zhang, Y. Wang, L. Bramasole, K. Guo, F. Mourtada, T. Meul, Q. Hu, V. Viteri, I. Kammerl, M. Konigshoff, M. Lehmann, T. Magg, F. Hauck, I. E. Fernandez and S. Meiners (2023). "DNA sensing via the cGAS/STING pathway activates the immunoproteasome and adaptive T-cell immunity." EMBO J **42**(8): e110597.

Wang, Y., P. J. Kuan, C. Xing, J. T. Cronkhite, F. Torres, R. L. Rosenblatt, J. M. DiMaio, L. N. Kinch, N. V. Grishin and C. K. Garcia (2009). "Genetic defects in surfactant protein A2 are associated with pulmonary fibrosis and lung cancer." Am J Hum Genet **84**(1): 52-59.

Welk, V., T. Meul, C. Lukas, I. E. Kammerl, S. R. Mulay, A. C. Schamberger, N. Semren, I. E. Fernandez, H. J. Anders, A. Gunther, J. Behr, O. Eickelberg, M. Korfei and S. Meiners (2019). "Proteasome activator PA200 regulates myofibroblast differentiation." Sci Rep **9**(1): 15224.

Wickner, S., M. R. Maurizi and S. Gottesman (1999). "Posttranslational quality control: folding, refolding, and degrading proteins." Science **286**(5446): 1888-1893.

Wietecha, M. S., W. L. Cerny and L. A. DiPietro (2013). "Mechanisms of vessel regression: toward an understanding of the resolution of angiogenesis." Curr Top Microbiol Immunol **367**: 3-32.

Wilson, E. C., L. Shulgina, A. P. Cahn, E. R. Chilvers, H. Parfrey, A. B. Clark, O. P. Twentyman and A. M. Wilson (2014). "Treating idiopathic pulmonary fibrosis with the addition of co-trimoxazole: an economic evaluation alongside a randomised controlled trial." Pharmacoeconomics **32**(1): 87-99.

Wilson, M. S., S. K. Madala, T. R. Ramalingam, B. R. Gochuico, I. O. Rosas, A. W. Cheever and T. A. Wynn (2010). "Bleomycin and IL-1beta-mediated pulmonary fibrosis is IL-17A dependent." J Exp Med **207**(3): 535-552.

Wynn, T. A. (2008). "Cellular and molecular mechanisms of fibrosis." J Pathol **214**(2): 199-210.

Wynn, T. A. (2011). "Integrating mechanisms of pulmonary fibrosis." J Exp Med **208**(7): 1339-1350.

Wynn, T. A. and L. Barron (2010). "Macrophages: master regulators of inflammation and fibrosis." Semin Liver Dis **30**(3): 245-257.

Wynn, T. A. and T. R. Ramalingam (2012). "Mechanisms of fibrosis: therapeutic translation for fibrotic disease." Nat Med **18**(7): 1028-1040.

Yan, W., H. L. Bi, L. X. Liu, N. N. Li, Y. Liu, J. Du, H. X. Wang and H. H. Li (2017). "Knockout of immunoproteasome subunit beta2i ameliorates cardiac fibrosis and inflammation in DOCA/Salt hypertensive mice." Biochem Biophys Res Commun **490**(2): 84-90.

Yang, L., J. Herrera, A. Gilbertsen, H. Xia, K. Smith, A. Benyumov, P. B. Bitterman and C. A. Henke (2018). "IL-8 mediates idiopathic pulmonary fibrosis mesenchymal progenitor cell fibrogenicity." Am J Physiol Lung Cell Mol Physiol **314**(1): L127-L136.

Zaiss, D. M., C. P. Bekker, A. Grone, B. A. Lie and A. J. Sijts (2011). "Proteasome immunosubunits protect against the development of CD8 T cell-mediated autoimmune diseases." J Immunol **187**(5): 2302-2309.

Zhang, M. and S. Zhang (2020). "T Cells in Fibrosis and Fibrotic Diseases." Front Immunol **11**: 1142.

Zhang, Y., T. C. Lee, B. Guillemin, M. C. Yu and W. N. Rom (1993). "Enhanced IL-1 beta and tumor necrosis factor-alpha release and messenger RNA expression in macrophages from idiopathic pulmonary fibrosis or after asbestos exposure." J Immunol **150**(9): 4188-4196.

# 12 Acknowledgements

During and after my time at the Comprehensive Pneumology Center in Munich many people contributed to this thesis, either by scientific input or by practical help which I appreciate beyond measure. In the first place I want to sincerely thank my supervisor Silke Meiners for the overall surveillance.

Within my stay at the lung institute, I got insights into science in general and the proteasome in specific. I greatly appreciated the encouraging discussions with you, Silke and I am deeply impressed not only by your countless research ideas, but even more by the way you appreciate people in your kind and open and respectful way. I was fascinated by your scientific and personal approach to research partners, always aiming to enlarge your network of proteasome and lung specialists and potentially fruitful collaborations. Your lab belonged to the most internationally mixed and for sure to the nicest research groups and I always felt well integrated as medical student. At the end of my time, I was able to perform very accurately in basic lab work such as Western Blotting and DNA or RNA methods, as well as surgical procedures in mice, such as tracheal cannulation and the generation of precision cut lung slices which was very amazing and which I will never forget. I cannot be grateful enough for all the effort that has been invested in me in terms of theoretical input and practical instruction. The latter, such as bench work or animal experiments were instructed and supported by Dr. Ilona Kammerl, my lab supervisor. You were extremely helpful in the animal house and the mouse work in general. Ilona, your precise accuracy was sometimes exhausting to me but still fascinates me in retrospect, as I wish, I was as much as you on the cutting edge of research and, as technically accurate as you were. I will always remember your kindness and your patience with me.

Thank you, Dr. Vanessa Neiens (formerly Welk) and Dr. Thomas Meul, who also took some valuable time during their PhD theses to support, to give hints or assist in technical questions or took care of my cells sometimes. Thank you, Christina Lukas for your companionship especially in the early morning hours when we were the first two people in the entire institute and thank you, Silvia Weidner for your great support with

the mice and RNA works. Thank you, Dr. Jie Chen for your help with the precision cut lung slices and many thanks to Dr. Xinyuan Wang for trying to teach me some Chinese. I am very grateful for having also met Dr. Claudia Staab-Weijnitz who lead the research school of the CPC and took care of the Journal Club. Your cheerfulness and your sympathetic ear will never be forgotten. You joined us students so many times outside in front of the institute or outreach activities and your approachability was fascinating and inspiring to all of us. Dear Dr. Gabriel Stoleriu, thank you for introducing me to the CPC institute and Silke´s group. The entire story started after having met you in my internship in the thoracic surgery department in the Asklepios hospital in Gauting. And finally, I want to express my special thanks to my family and my girlfriend for supporting me throughout my medical studies and this thesis. I could not have done it without your support.